

LHC detectors

A close-up, low-angle view of the interior of an LHC detector. The image shows a complex arrangement of copper and silicon components, with a bright light source illuminating the central area. The detector's structure is highly detailed, with various wires, cables, and mechanical parts visible. The background is dark, emphasizing the metallic and illuminated components.

P. Ferreira da Silva (CERN)

Course on Physics at the LHC

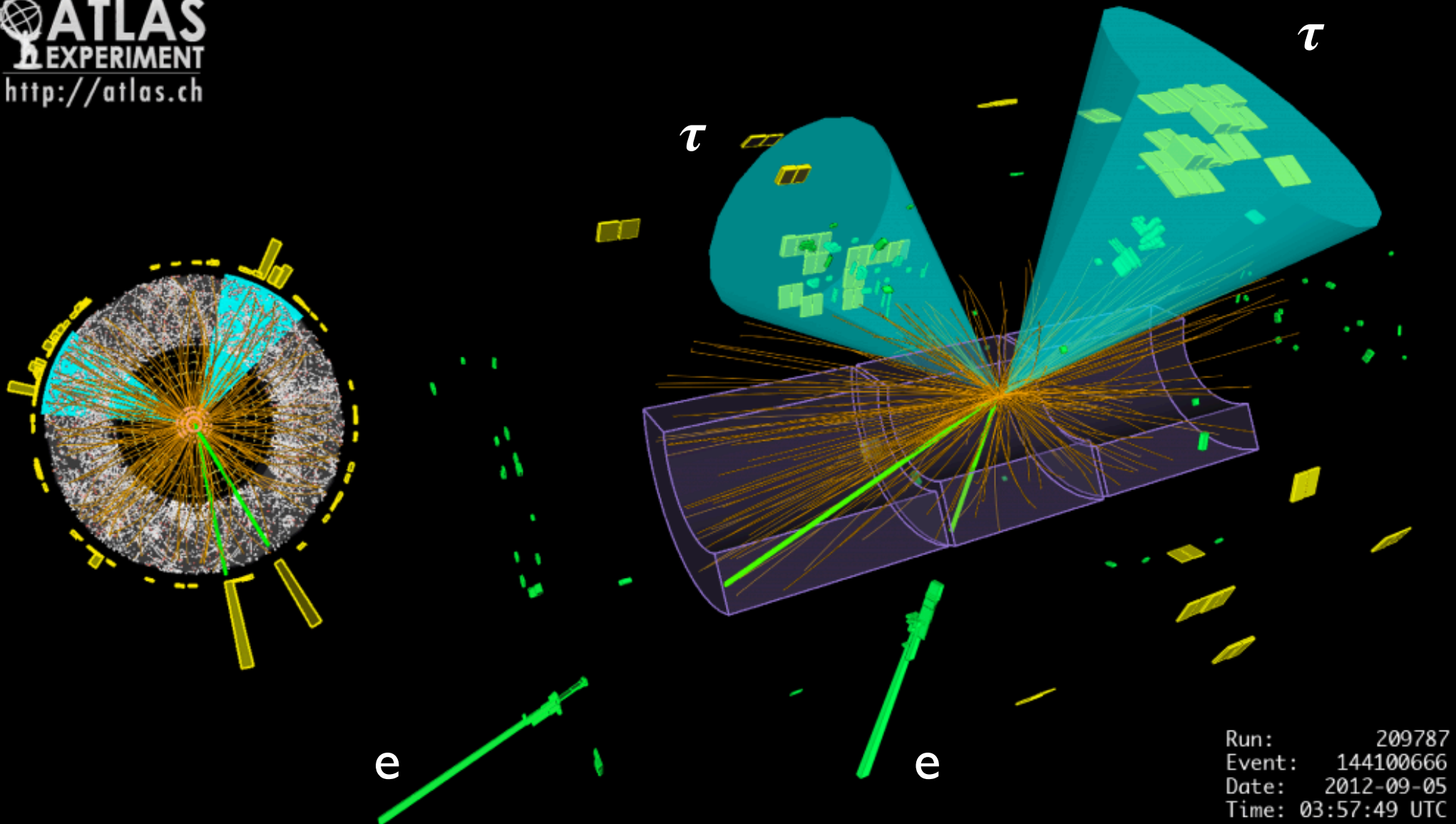
LIP, 14th March 2018

From collision remnants to physics

We hunt for new physics with exciting signatures

3

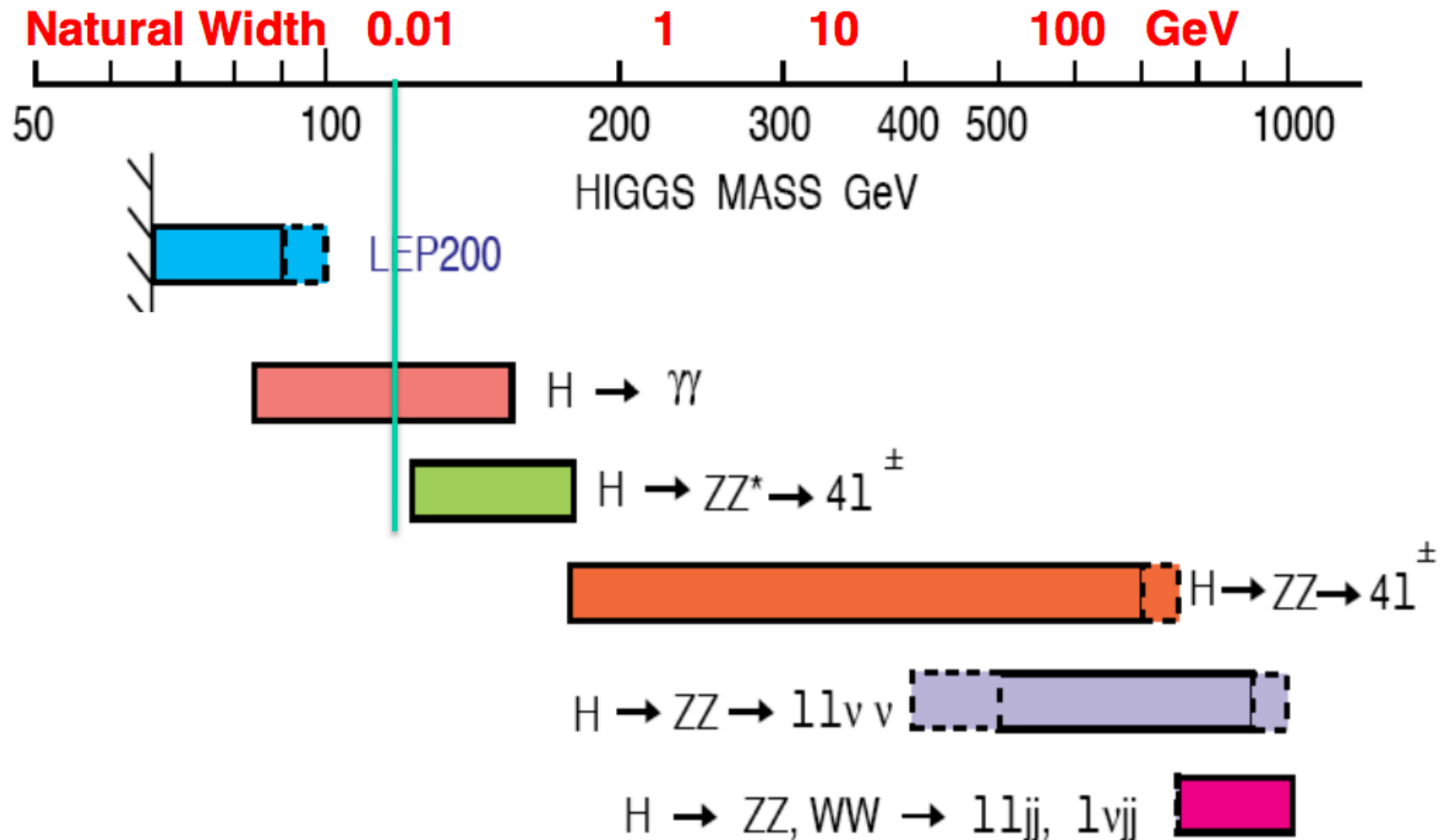
ATLAS
EXPERIMENT
<http://atlas.ch>



Discovery drives the LHC detectors concept

4

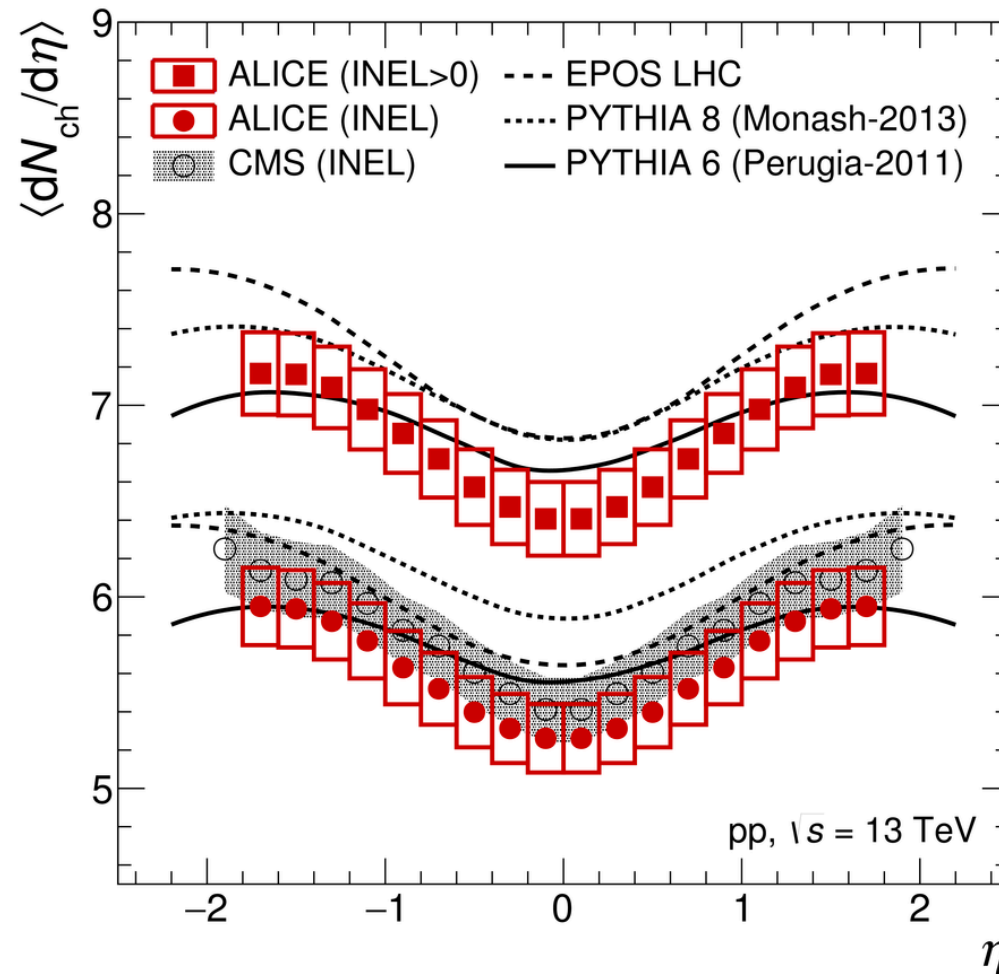
- Before discovery different signatures to be expected depending on the Higgs mass
- 4 π -hermetic general purpose detectors are needed covering: leptons, photons, jets, ...



Proton-remnants underly the hard processes

5

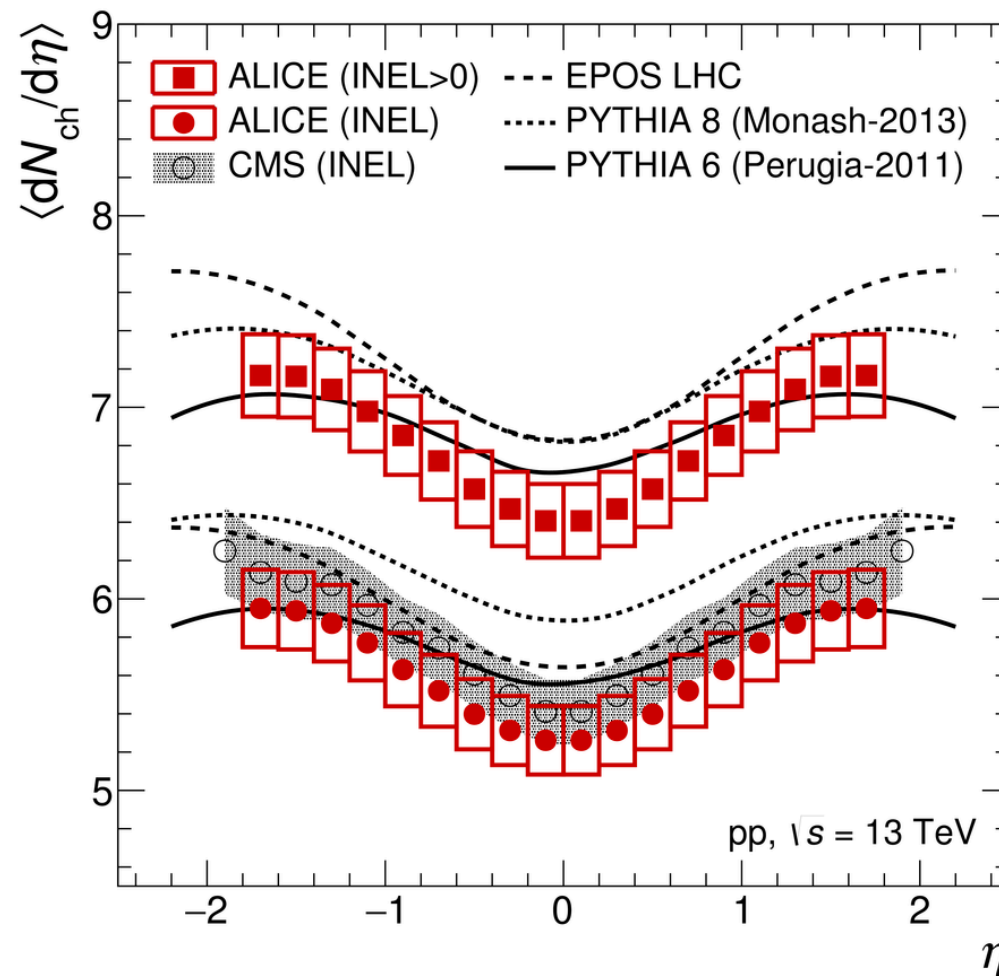
- Single proton collisions produce high multiplicity events



Proton-remnants underly the hard processes

6

- Single proton collisions produce high multiplicity events
- Distributions are approximately uniform in pseudo-rapidity

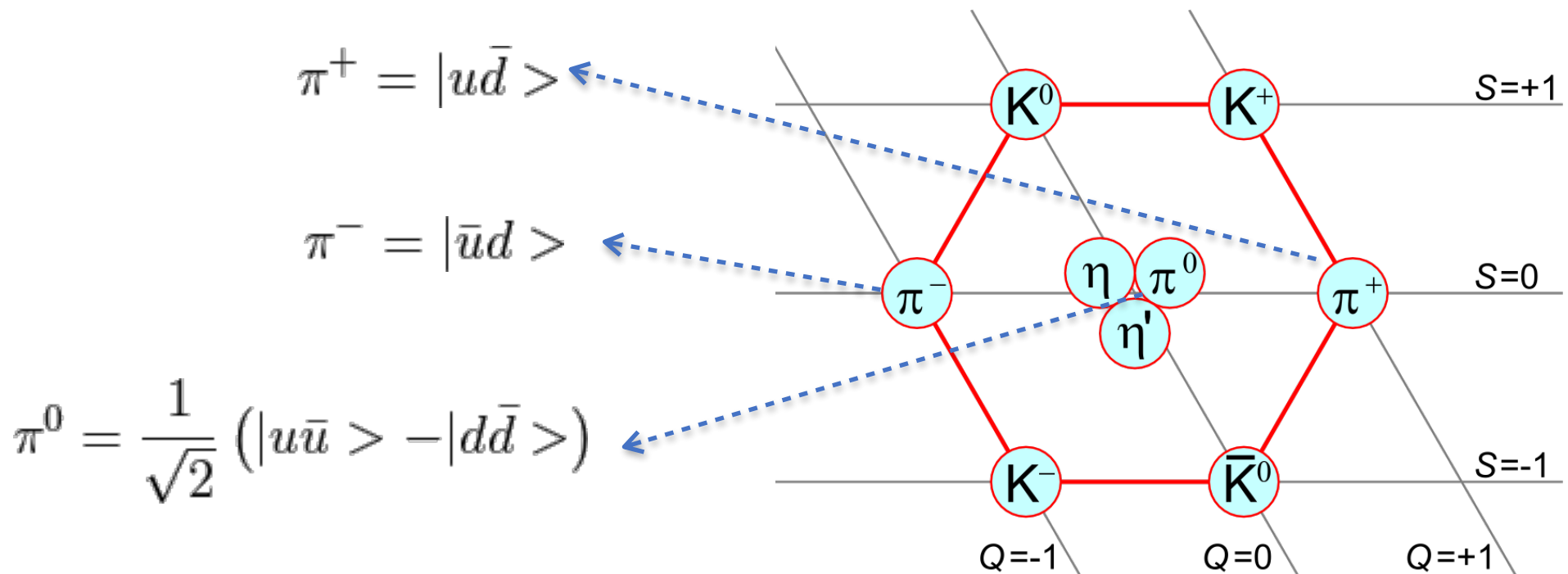


Average 15-20 charged particles per inelastic collision

Proton-remnants underly the hard processes

7

- Single proton collisions produce high multiplicity events
- Distributions are approximately uniform in pseudo-rapidity
- Most particles are pions with $N(\pi^0) \approx \frac{1}{2}N(\pi^\pm)$

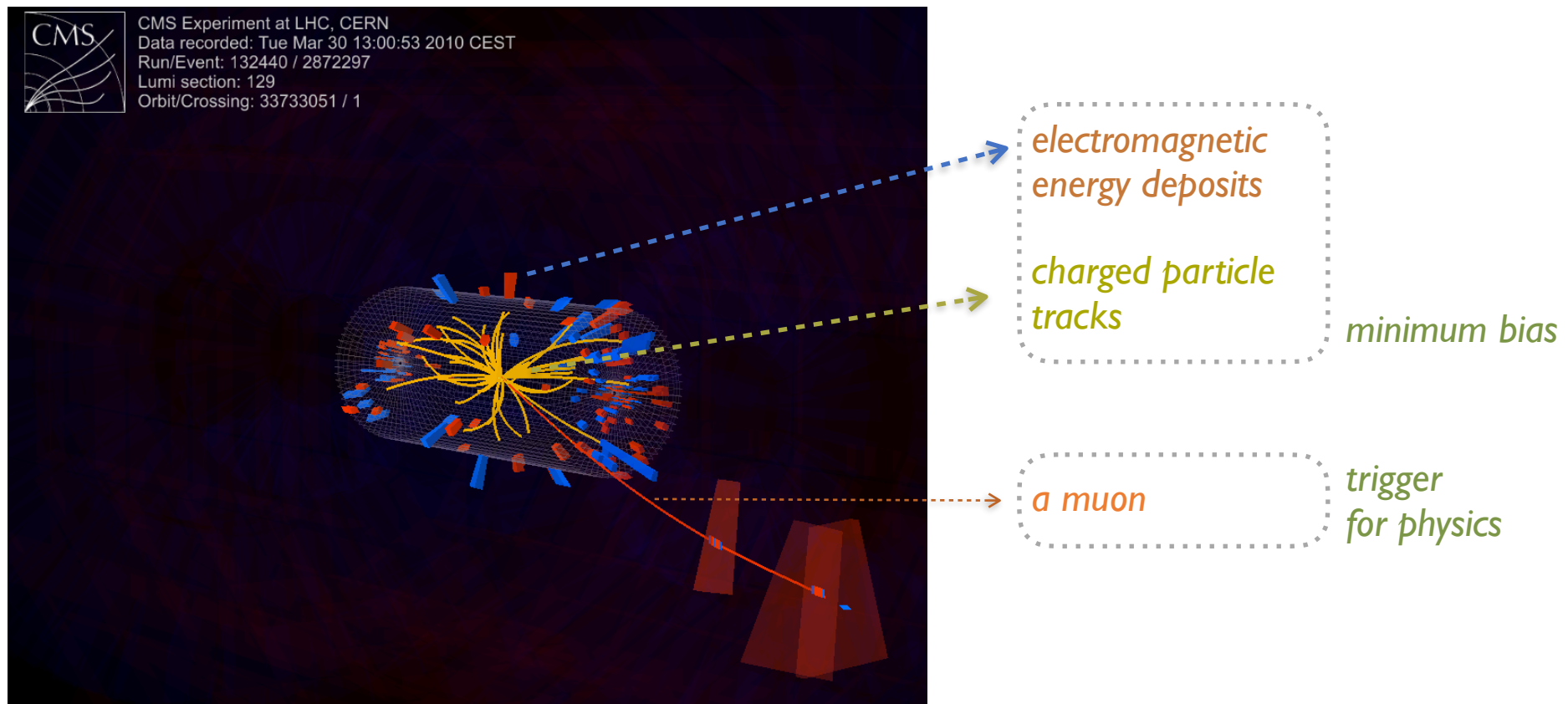


strong interactions preserve isospin

Proton-remnants underly the hard processes

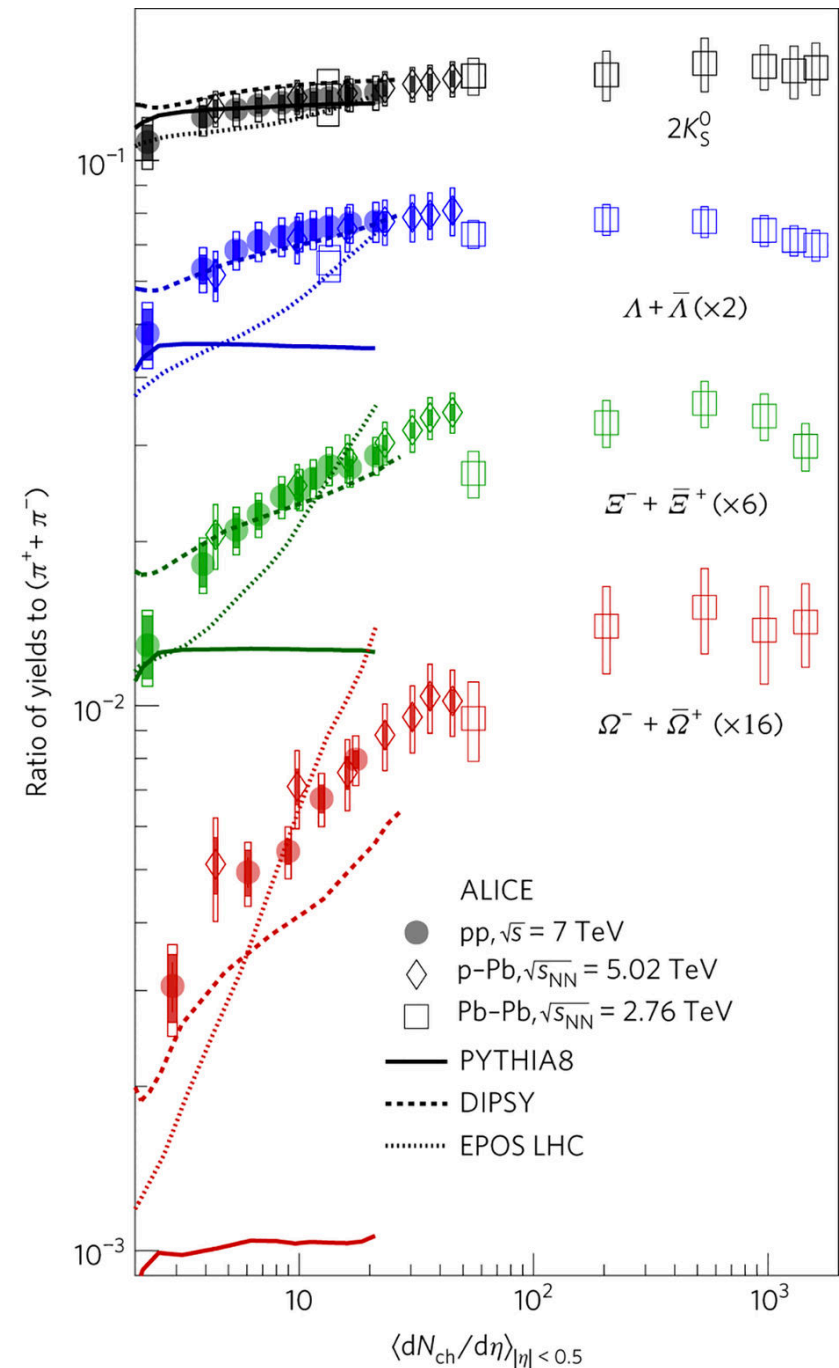
8

- Single proton collisions produce high multiplicity events
- Distributions are approximately uniform in pseudo-rapidity
- Most particles are pions with $N(\pi^0) \approx \frac{1}{2}N(\pi^\pm)$
- As $\pi^0 \rightarrow \gamma\gamma$ dominates $N(\gamma) \approx N(\pi^\pm)$ in the detector

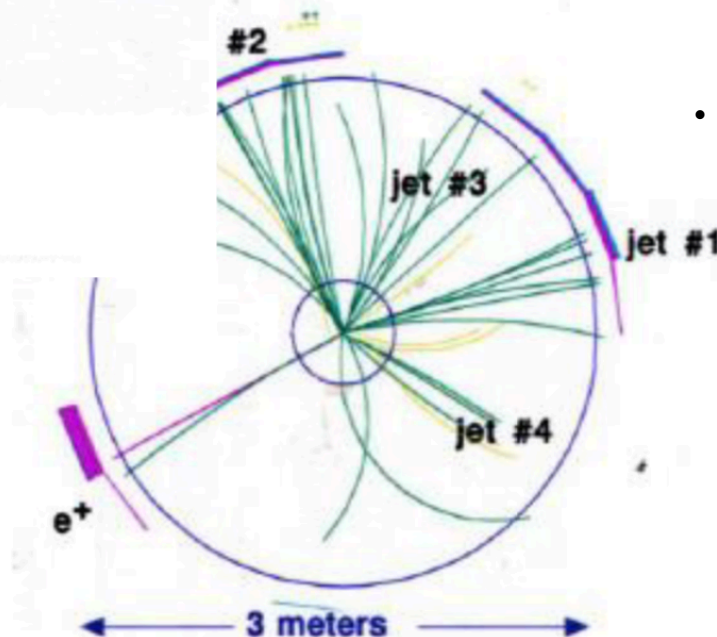
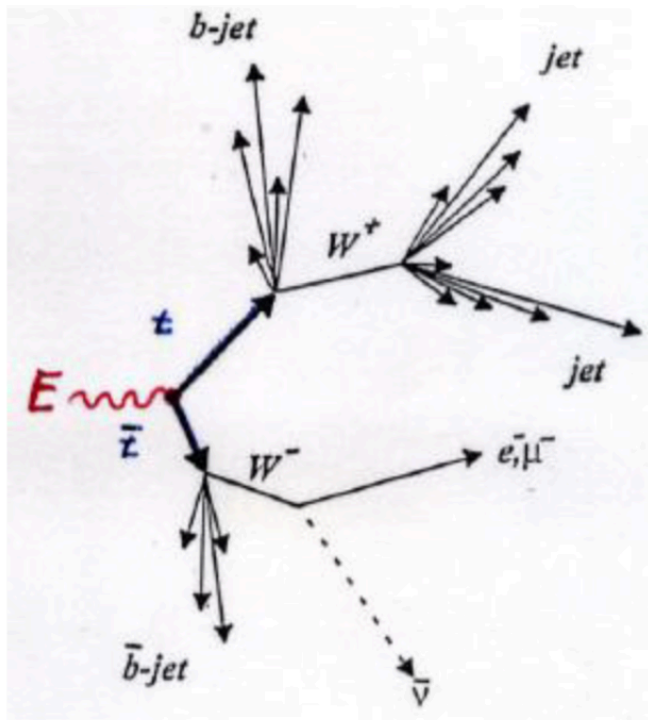


Beyond pions and photons

- Production of other particles suppressed by
 - content of the proton (PDFs)
 - mass ($m_s \sim 19 m_d$)
 - interactions



strange particles account for $O(10\%)$ of the multiplicities

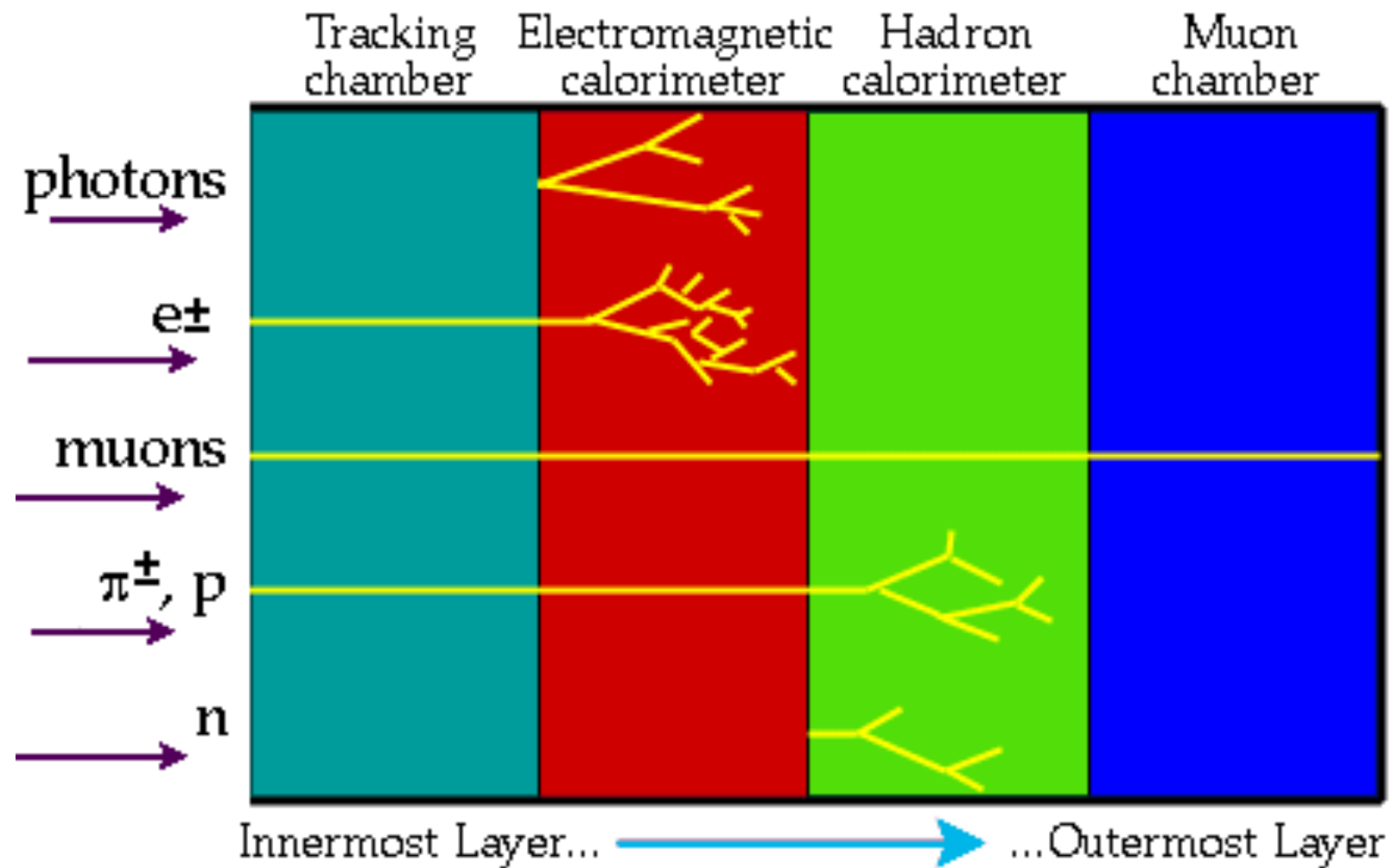


maximum information
needed to reconstruct
the hard process

- Final states
 - secondary vertices from long-lived decays only in rare cases
- Must interact within detector volume
 - electromagnetic or strong interactions
 - electrons, muons, photons
 - neutral or charged hadrons
- Long-lived weakly interacting particles
 - indirectly detected
 - missing transverse energy
 - good resolution when balancing energy

Particles and their interactions

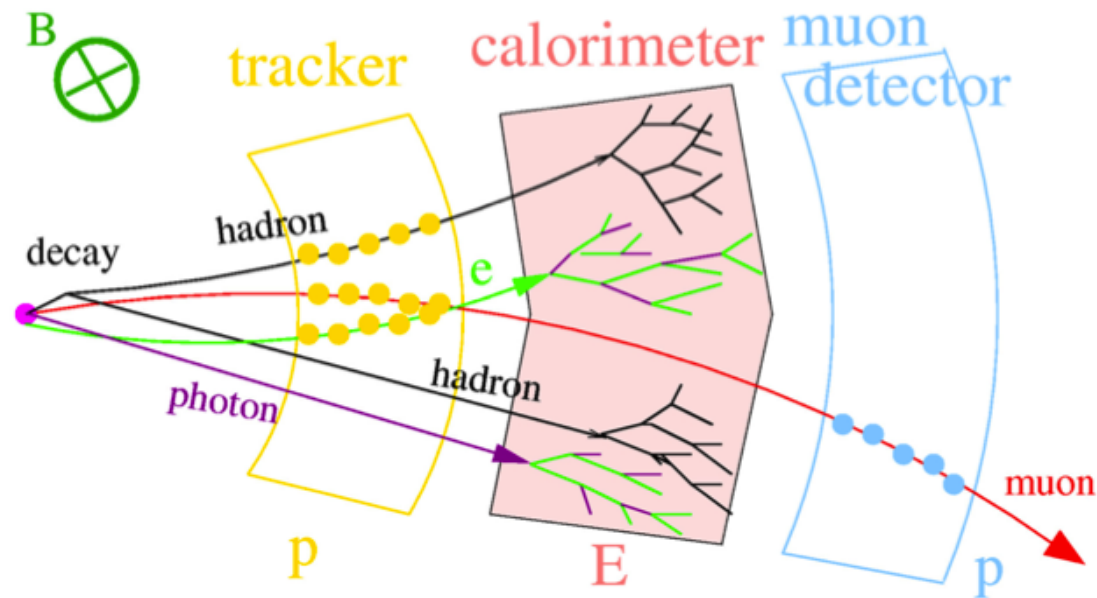
11



- Detectors register the passage of particle through matter
- Combine **absorbers** (start interactions) with **sensitive materials** (convert to optical/voltage)

Main concepts behind general purpose detectors

12



Magnetic field “ $F_c = qvB$ ”

- separate by charge
- measure p by curvature

Calorimetry

- measure E from deposits
- electromagnetic and hadronic

Inner tracking

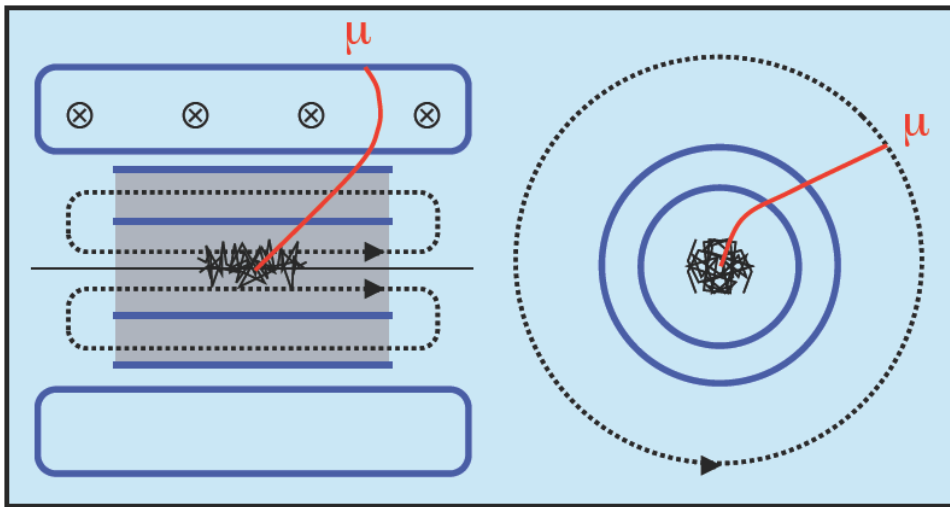
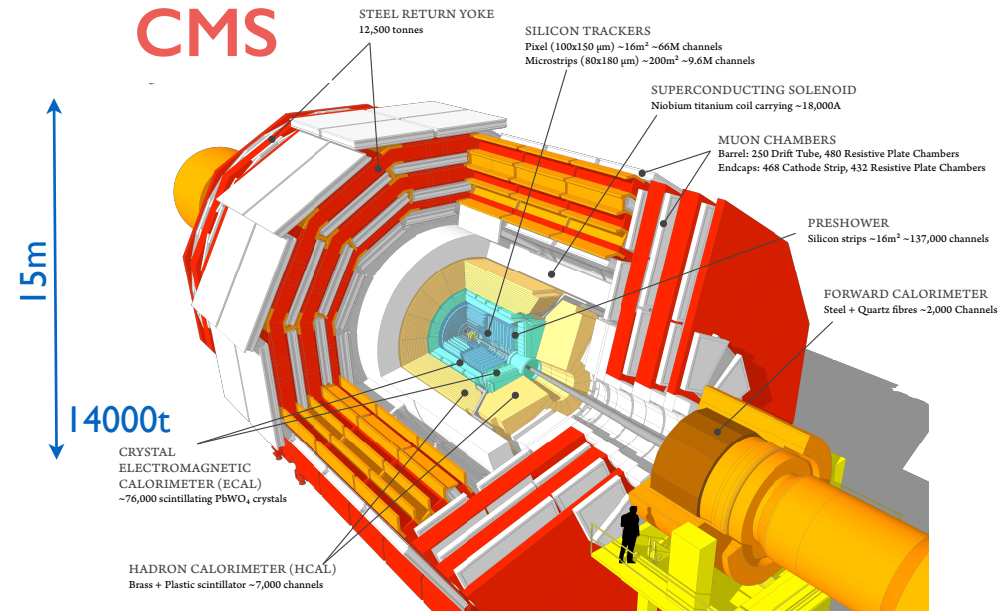
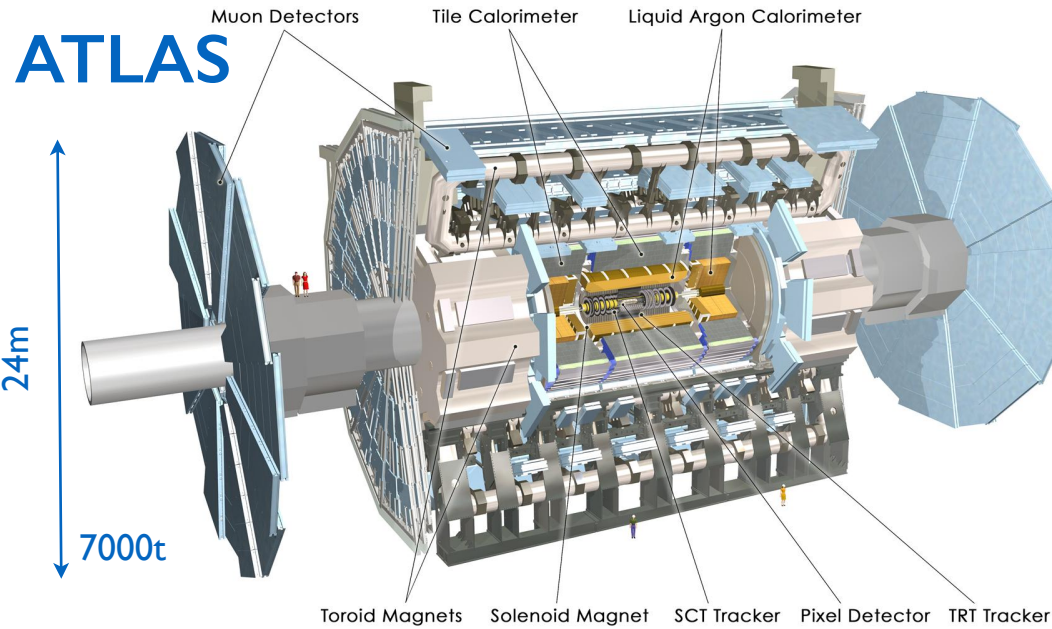
- minimal interference with event
- points to measure curved tracks
- particle identification

Outer tracking

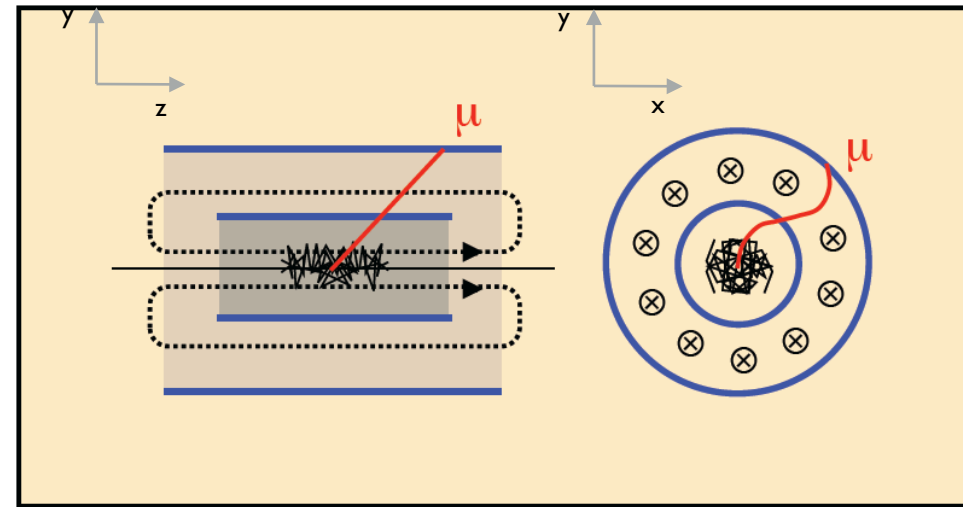
- muons (weakly interacting)

The two general purpose detectors

13



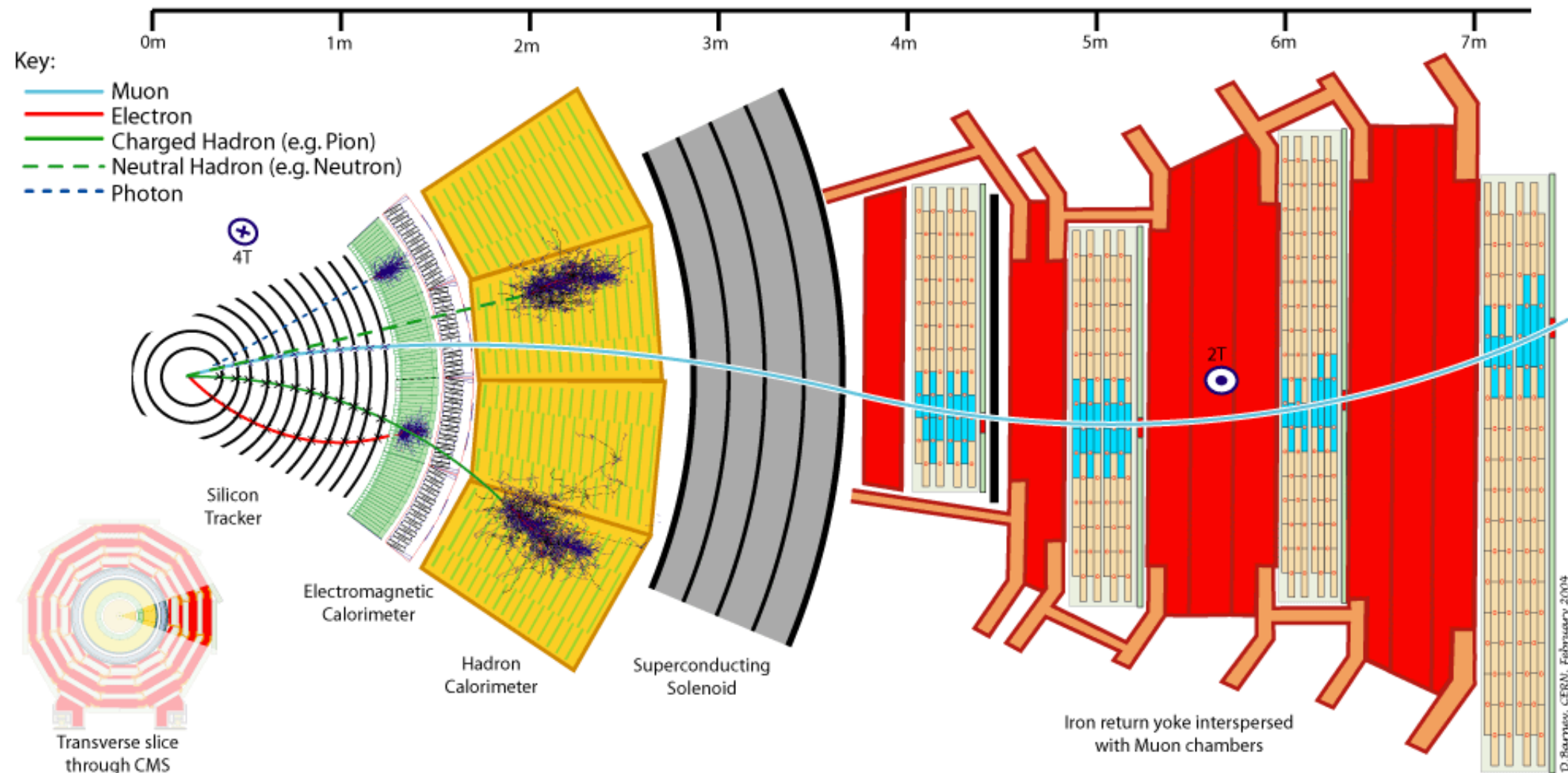
- Standalone measurement of $p(\mu)$
- Resolution is flat in η and independent of pileup



- Two complementary $p(\mu)$ measurements
- Tracks point to primary vertex

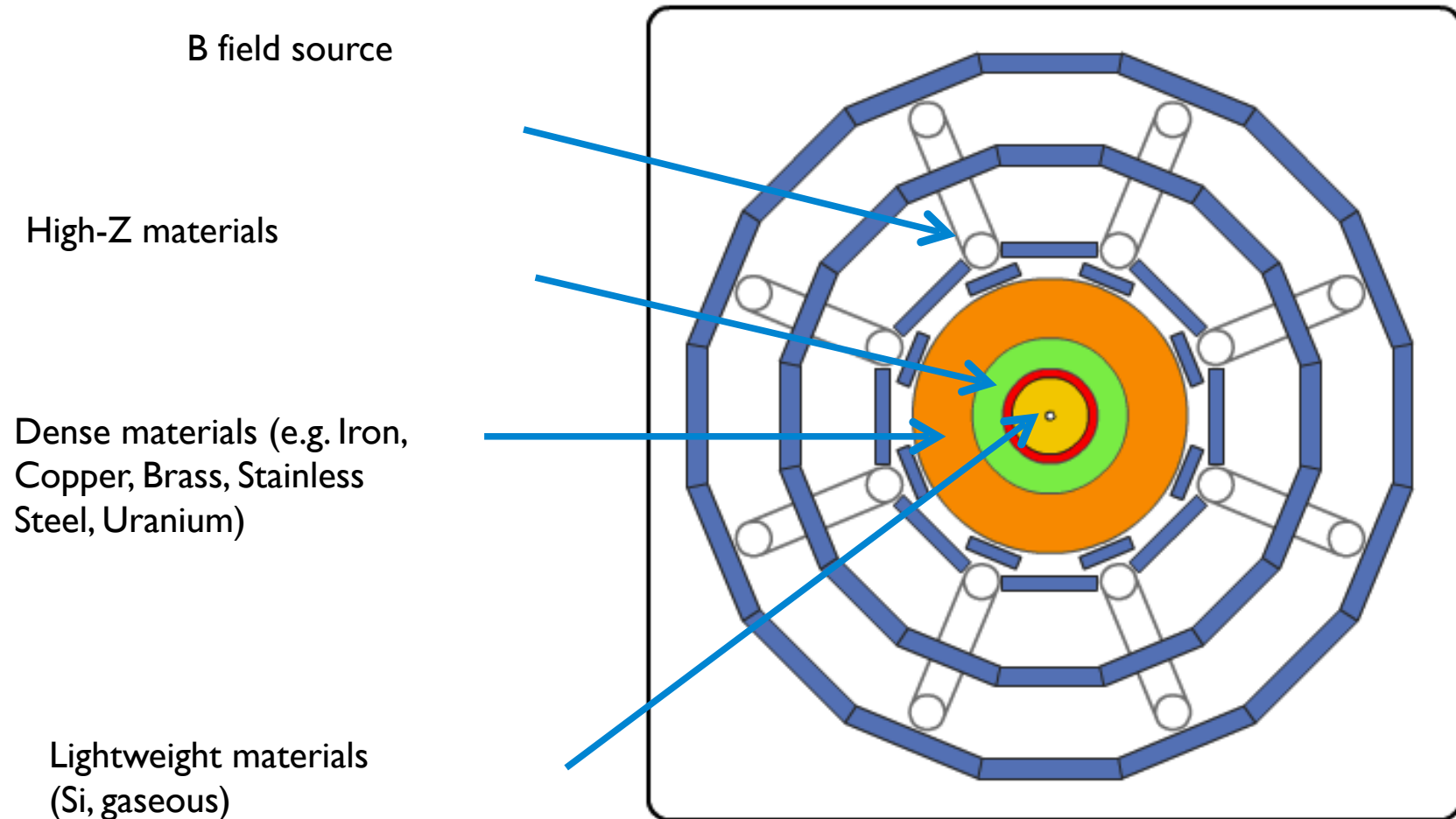
Particles and their interactions

14

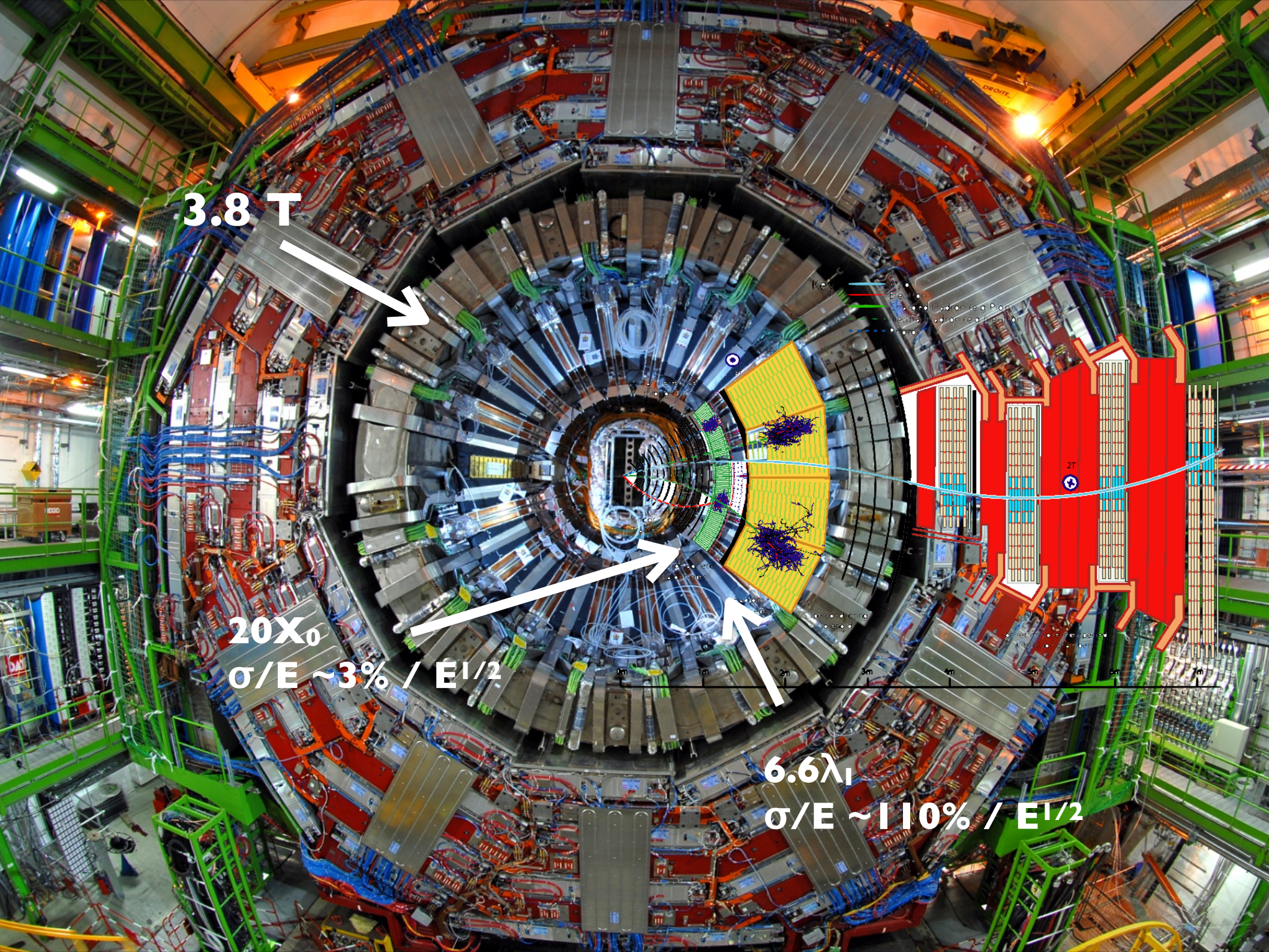


Material distribution in general purpose detectors

15

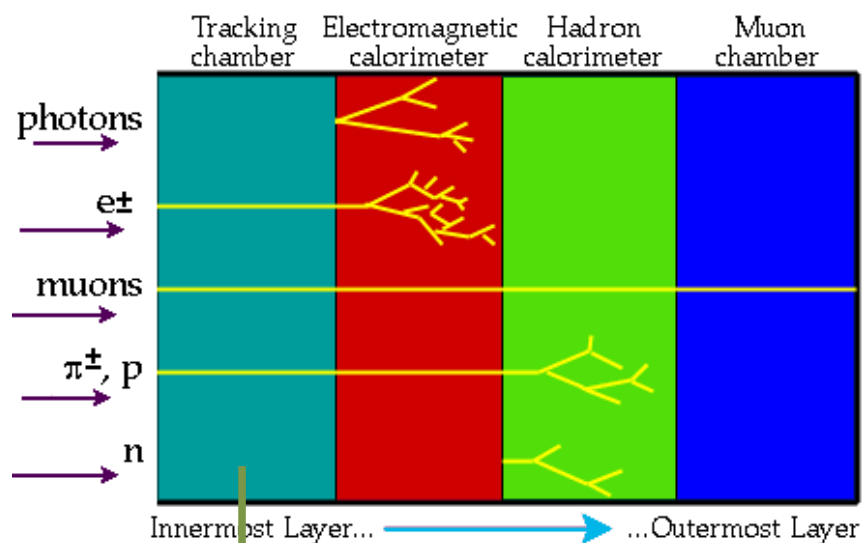


*it's a challenge to fit it all within volume
trade-off between best energy resolution and particle identification*

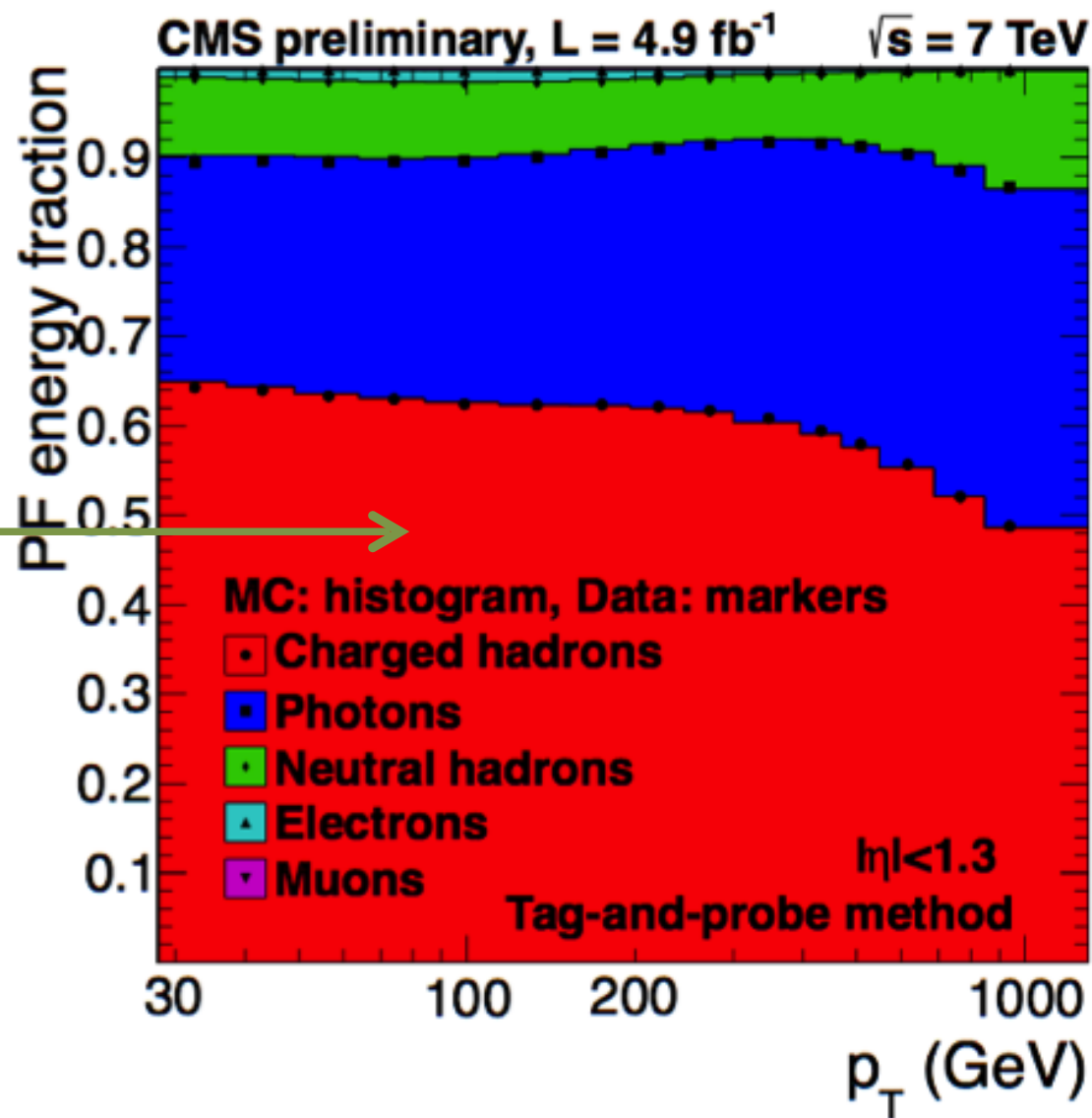


Particle flow

17



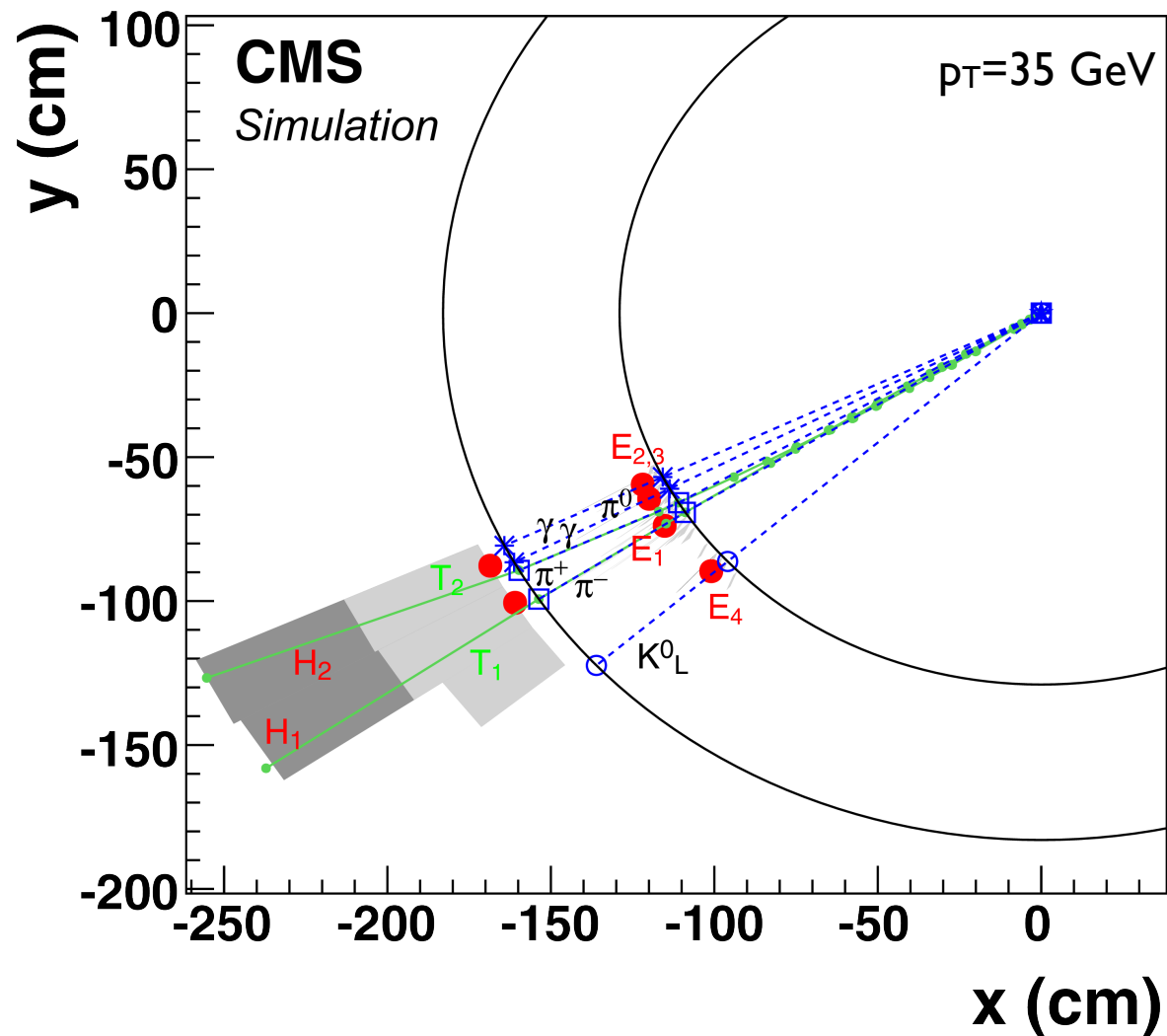
>60% of the energy of a jet may be reconstructed at the level of the tracker



Example: a jet of 5 particles

18

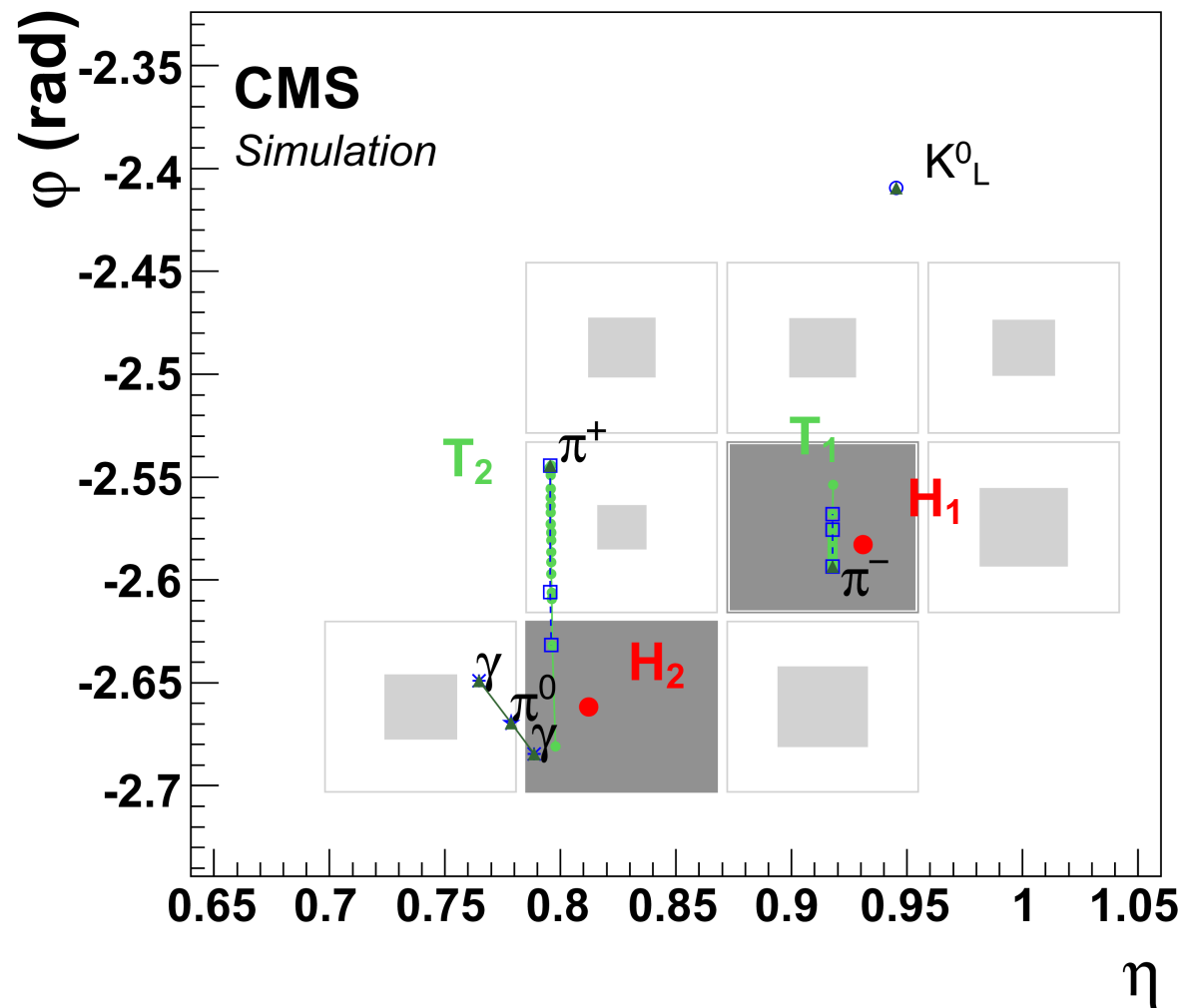
- Reconstruction starts in the tracker (start from easy tracks, use remaining hits for others)
 - but that does 2/3 particles in this jet



Example: a jet of 5 particles

19

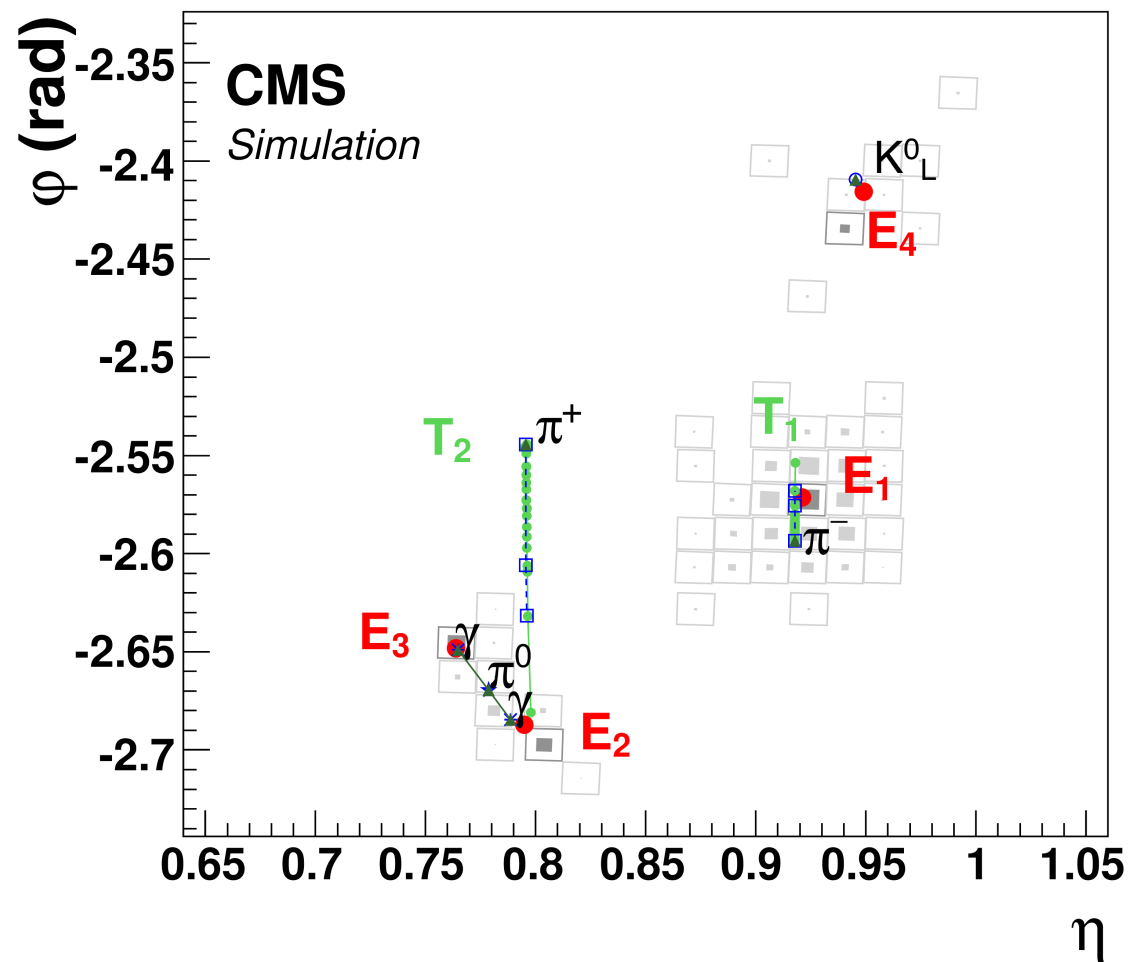
- Coarse granularity in the hadronic calorimeter
- See local energy maxima, connect neighbours
- Determine energy sharing iteratively



Example: a jet of 5 particles

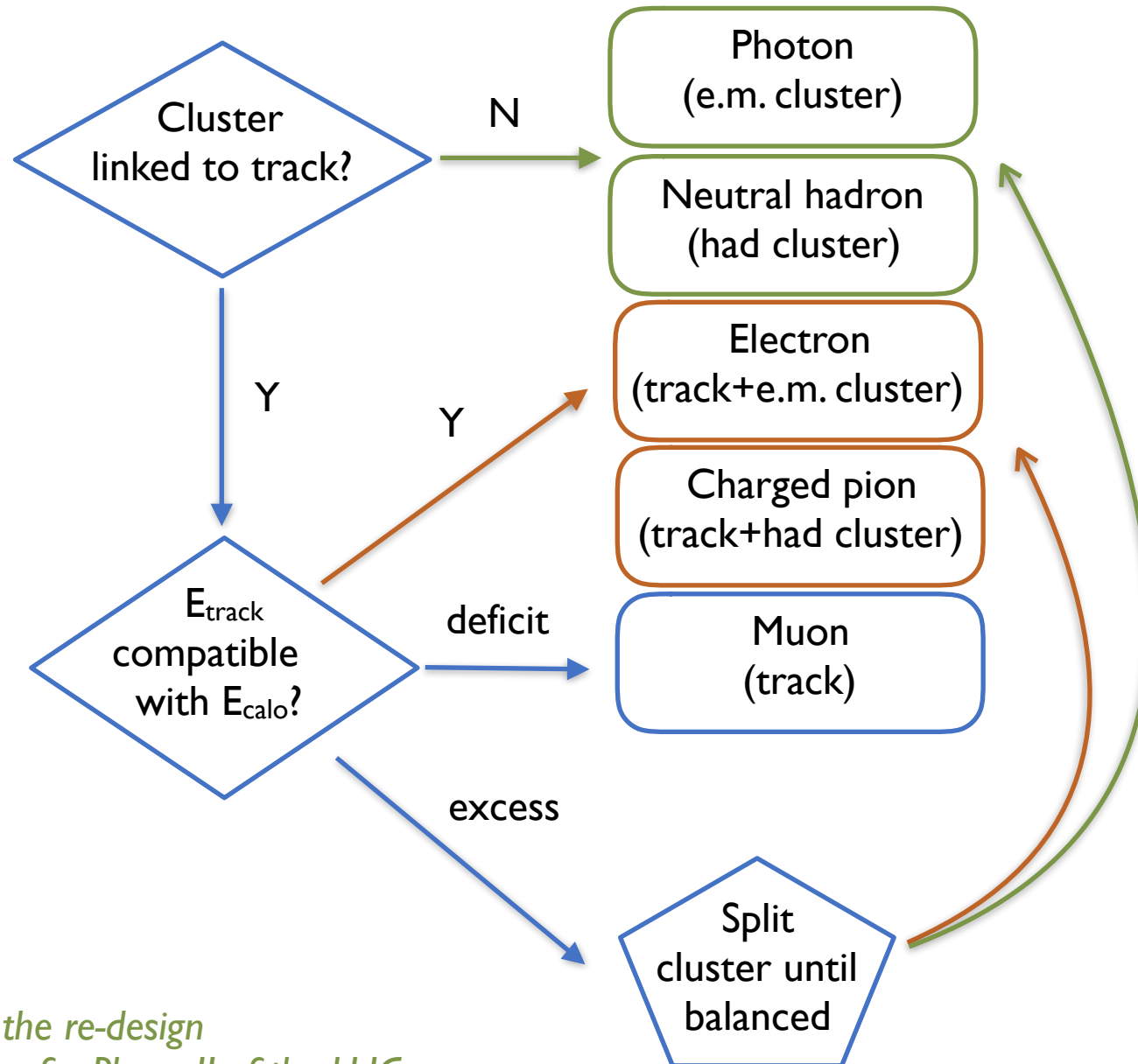
20

- The electromagnetic calorimeter sees things in coarser detail ($\Delta\phi, \Delta\eta \sim 0.02$)
- Use to refine entry point in calorimeter, link to tracks and balance energy
- Cluster energy unassociated to tracks: photons and neutral hadrons



Particle flow algorithm is a reconstruction paradigm

21

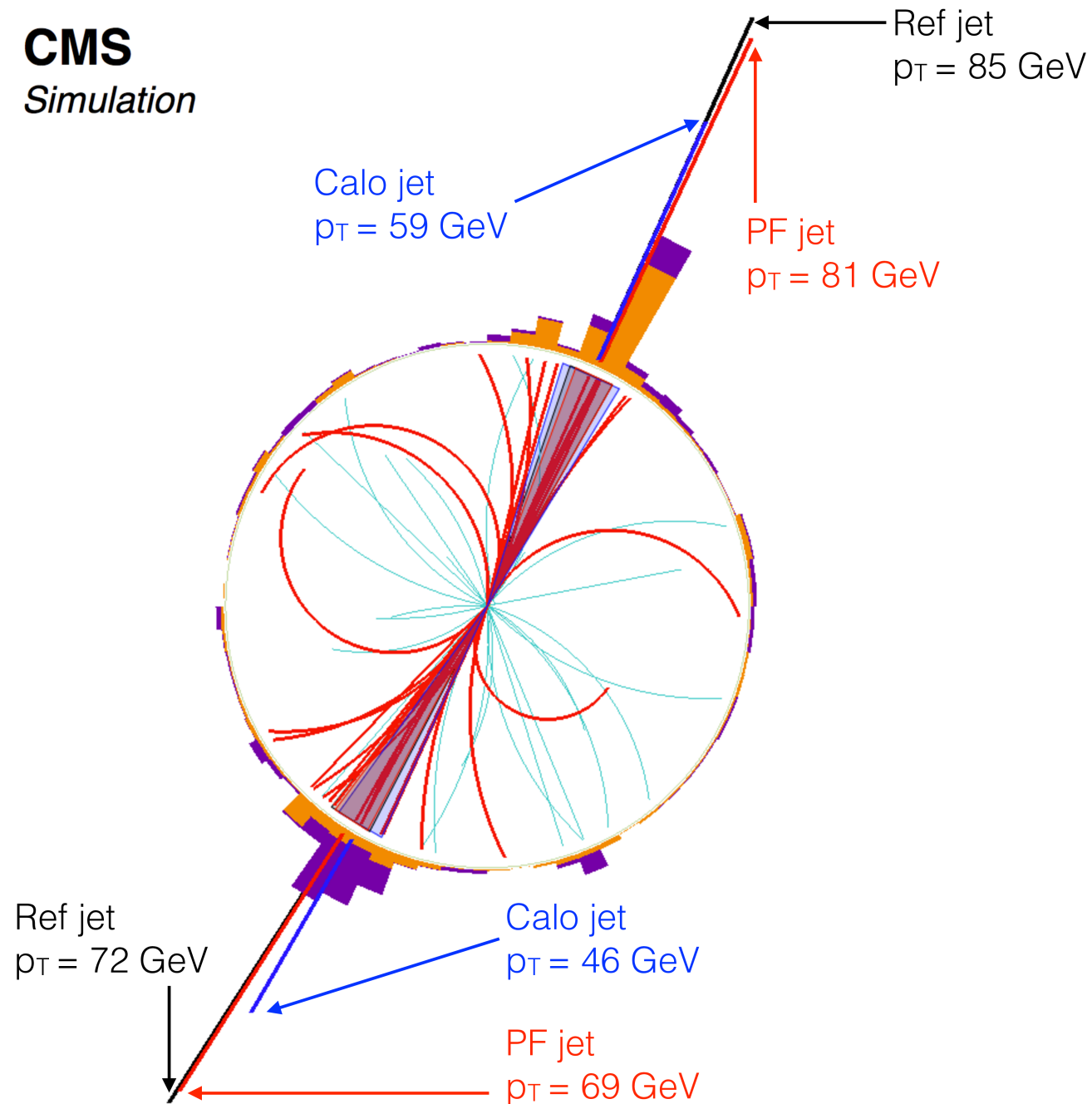


*it also shapes the re-design
of the detectors for Phase II of the LHC*

Particle flow algorithm is a reconstruction paradigm

22

CMS
Simulation

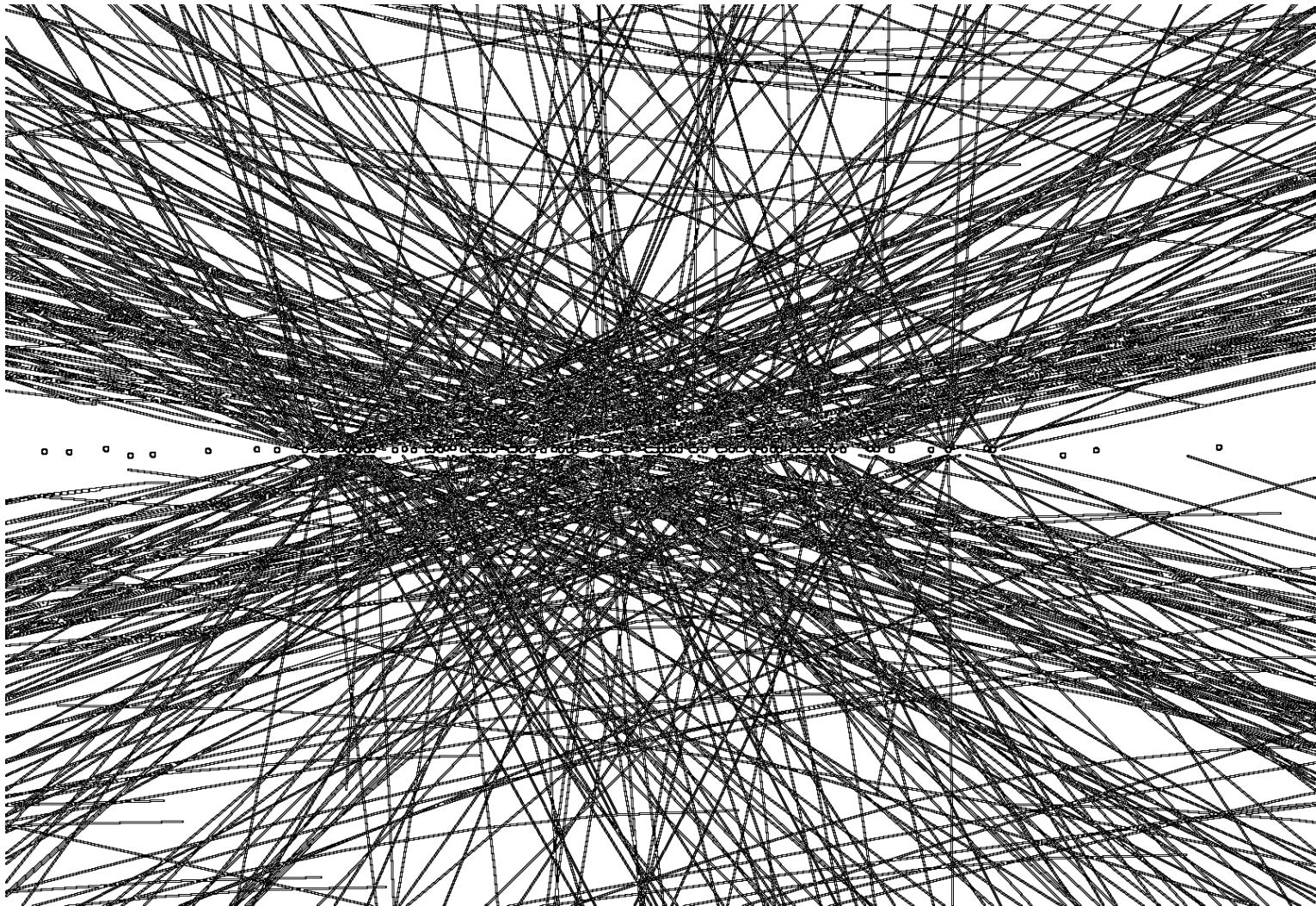


Connecting the dots with tracking

Why?

- Identify the **vertex** from the hard interaction

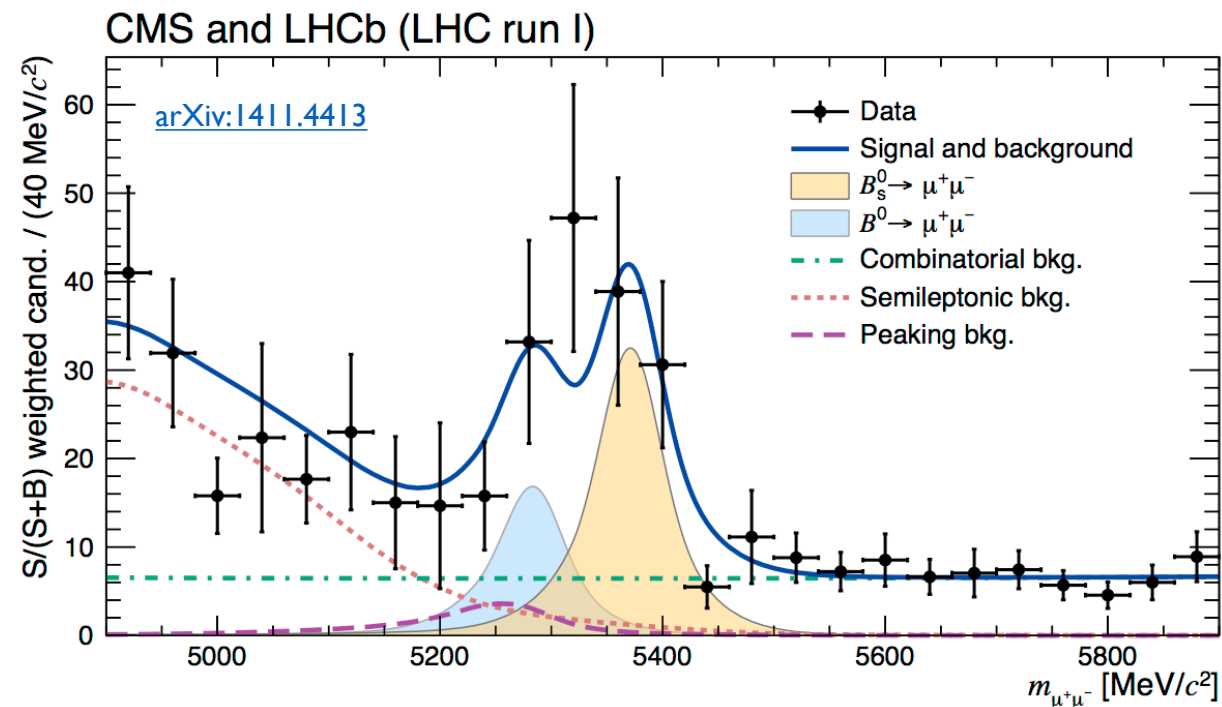
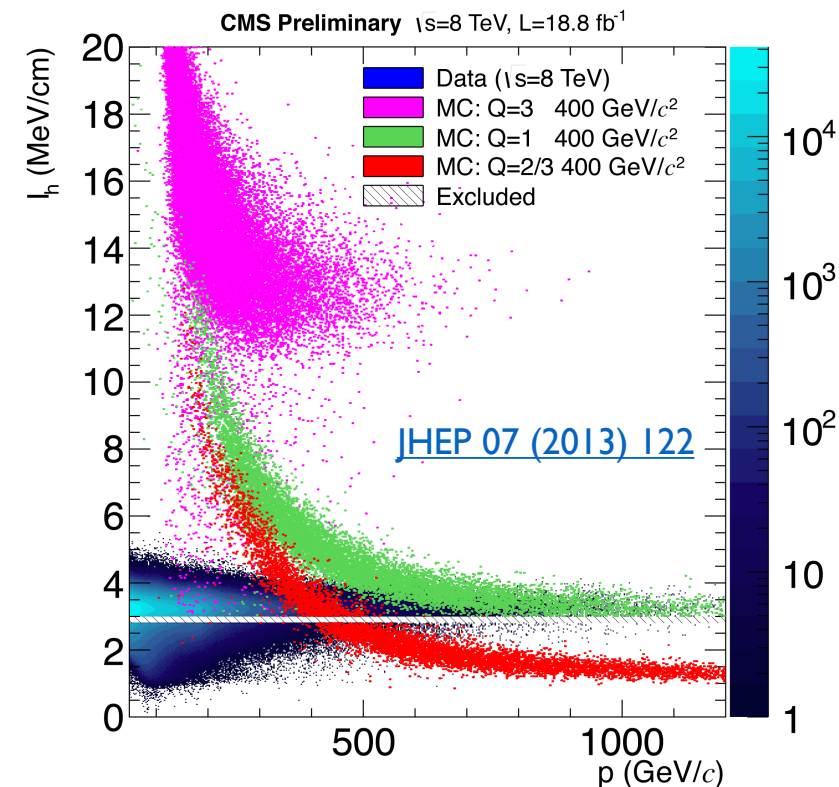
...but also secondary vertices from long lived particles



Why?

25

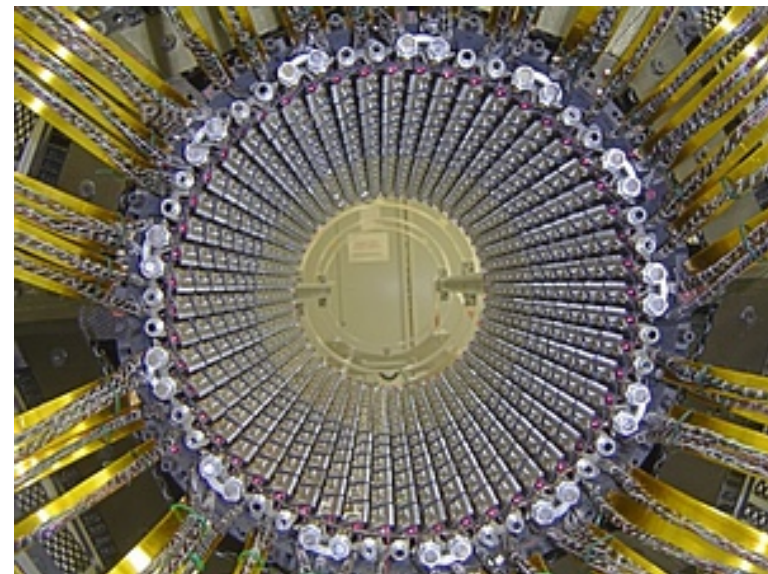
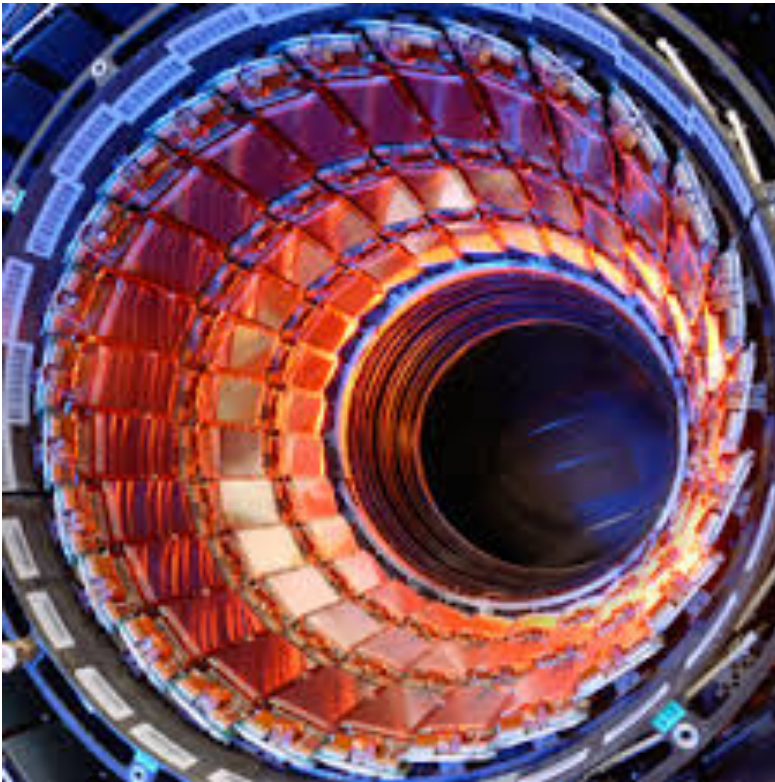
- Identify the **vertex** from the hard interaction
 - ...but also secondary vertices from long lived particles
- Measure **particle trajectories**
 - momentum (p), energy loss (dE/dx), link to coarser calorimeters and muon chambers



With what?

26

- Solid state detectors
 - Ge, Si, Diamond,...
 - pixels and strips

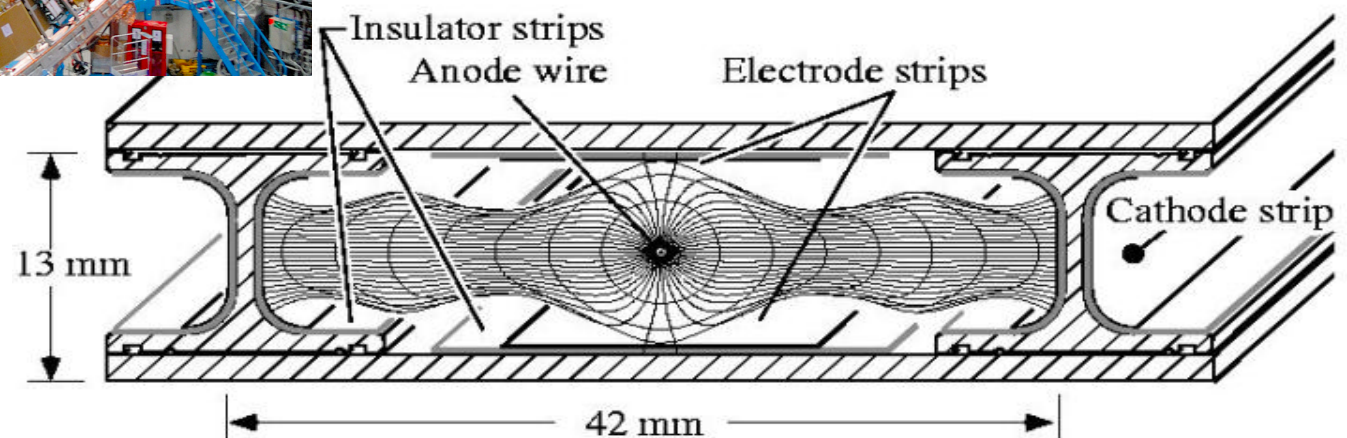
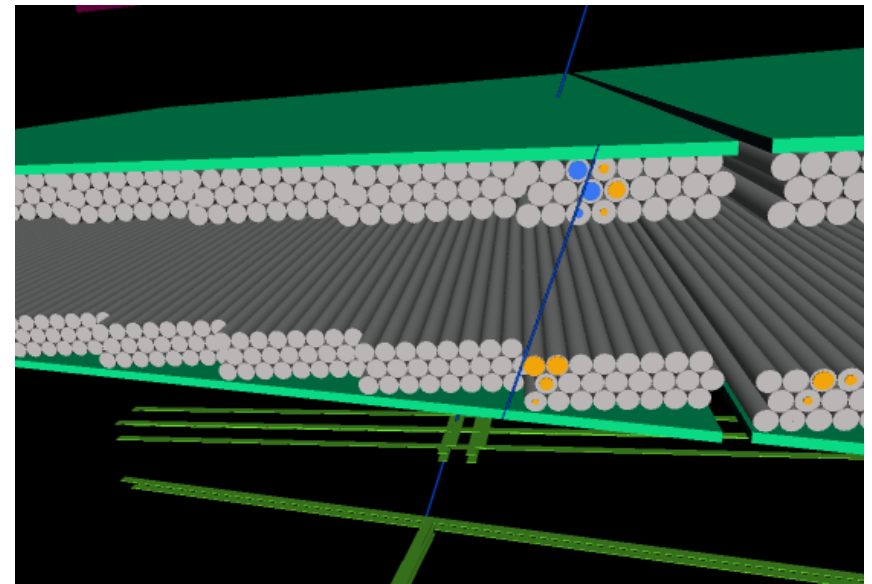
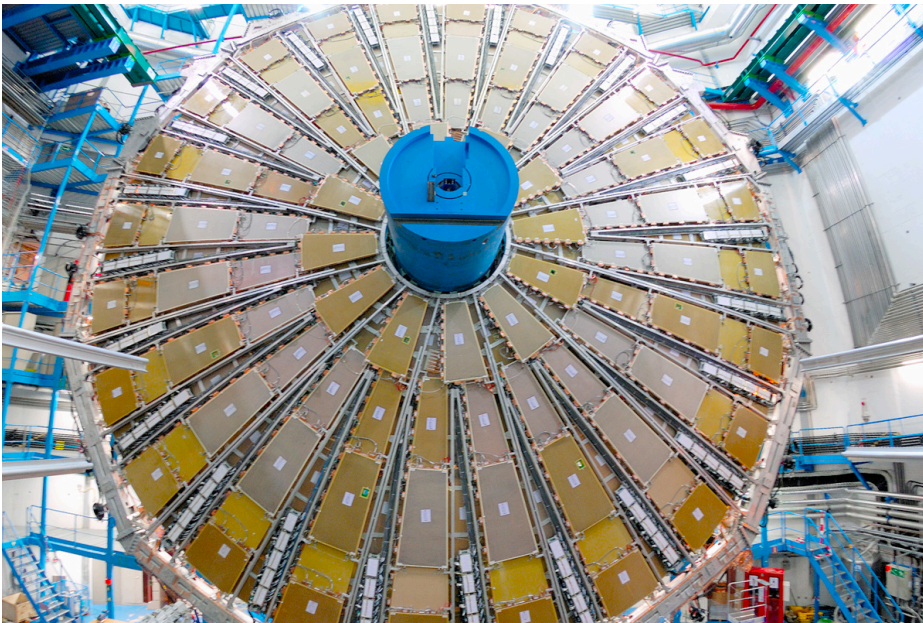


With what?

27

- Gaseous detectors

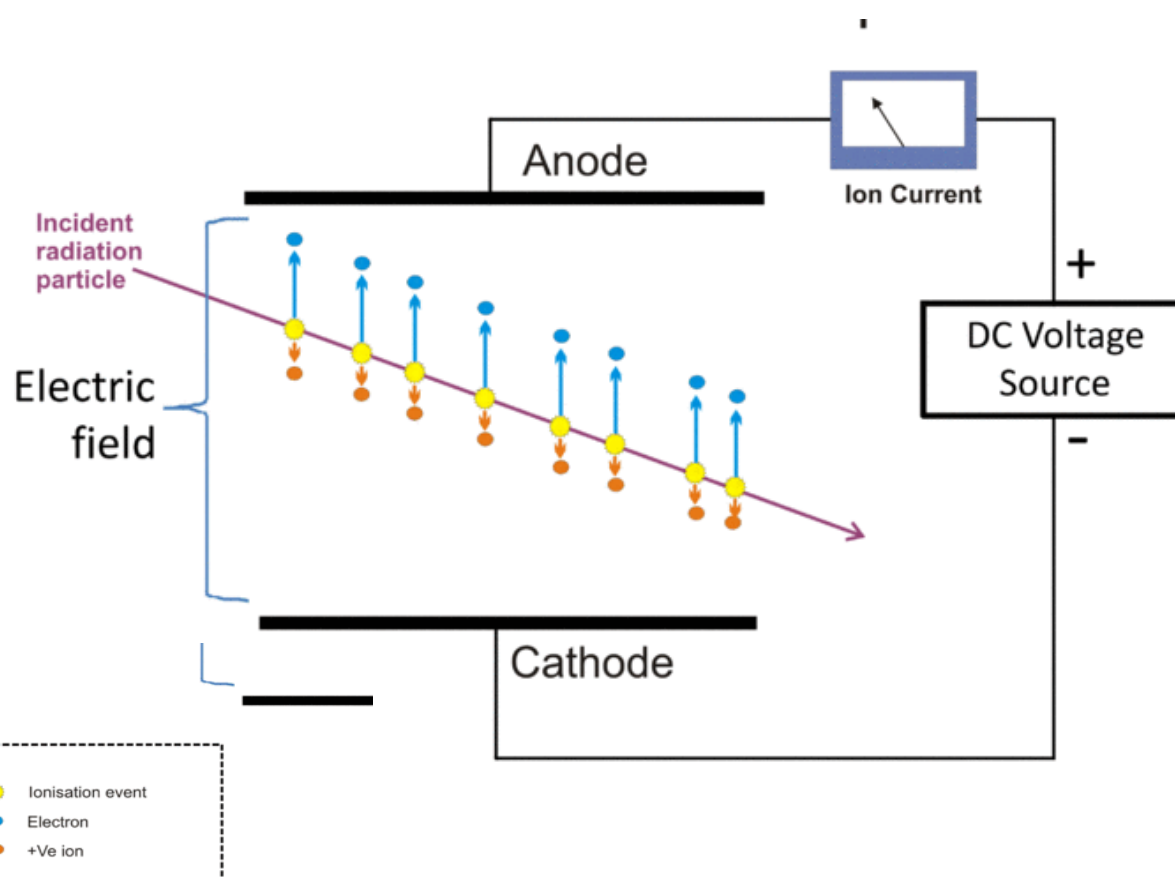
- drift tubes, resistive plate chambers, cathod strip chambers, gas electron multipliers, ...
- usually for outer tracking



How?

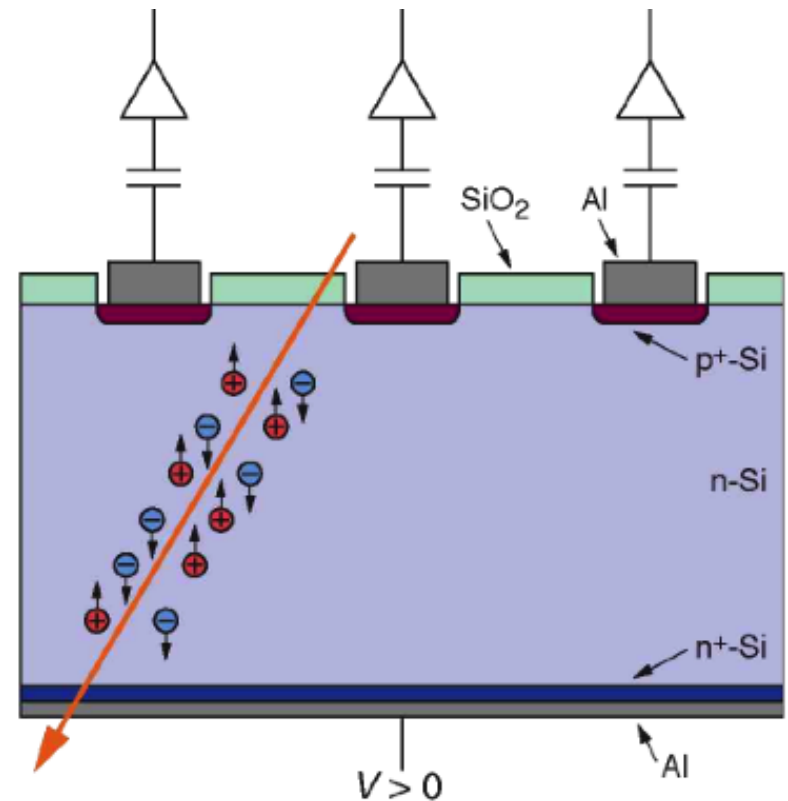
28

- While transversing a medium a **charged particle leaves an ionization trace**
 - create a depletion zone in between electrodes: gaseous, liquid or solid-state (semi-conductor)
 - ionization charges drift towards electrodes
 - amplify electric charge signal and deduce position from signals collected in individual strips



ionization chamber

≈



Si strip detector

Gaseous versus solid state

29

- In solid state detectors ionization energy converts in e-h pairs
 - 10 times smaller with respect to gaseous-based ionization
 - charge is increased → improved E resolution

	Gas		Solid state	
Density (g/cm ³)	Low	C ₂ H ₂ F ₄	High	Si
Atomic number (Z)	Low	(~95% for CMS RPC)	Moderate	
Ionization energy (ε _i)	Moderate	30eV	Low	3.6eV
Signal speed	Moderate	10ns-10μs	Fast	<20ns

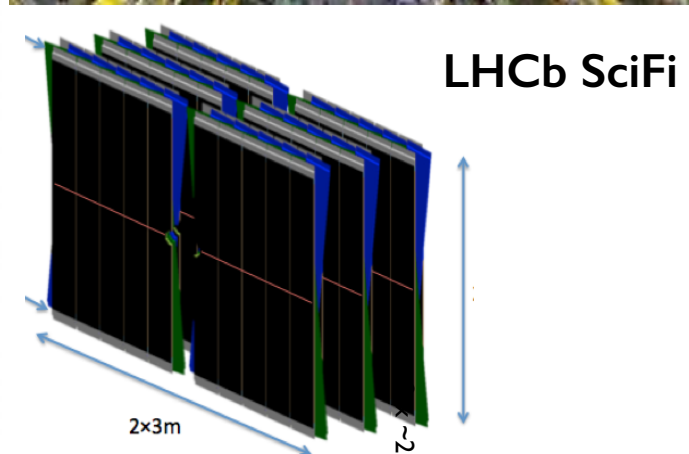
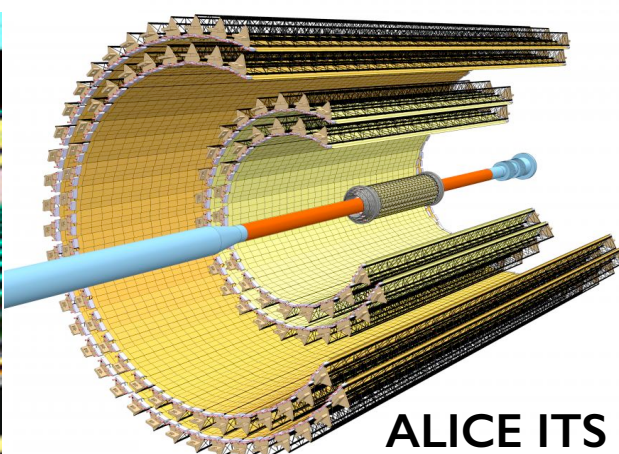
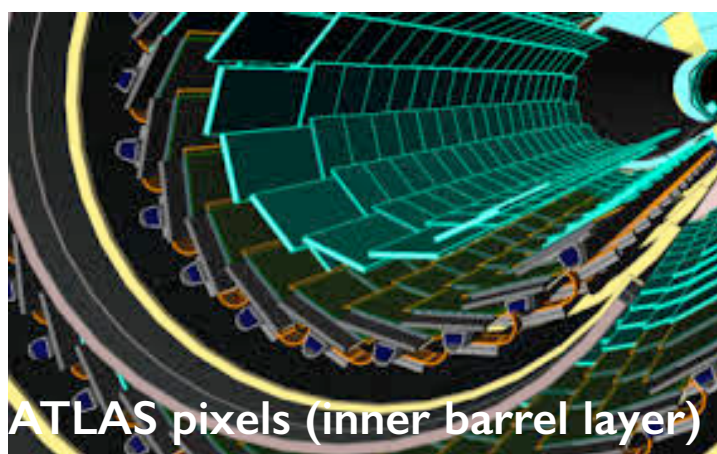
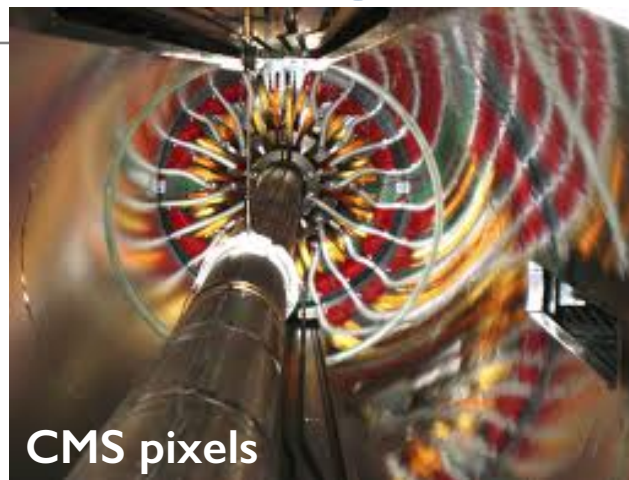
$$n = \frac{E_{loss}}{E_{eh}} \rightarrow \frac{\sigma_E}{E} \propto \frac{1}{\sqrt{n}} \propto \sqrt{\frac{E_{eh}}{E_{loss}}}$$

- Higher density materials are used in solid state detectors
 - charge collected is proportional to the thickness
 - most probable value for Silicon

$$\frac{\Delta_p}{x} \sim 0.74 \cdot 3.876 \text{ MeV/cm} \rightarrow N_{eh} \sim \frac{23 \cdot 10^3}{300 \mu m}$$

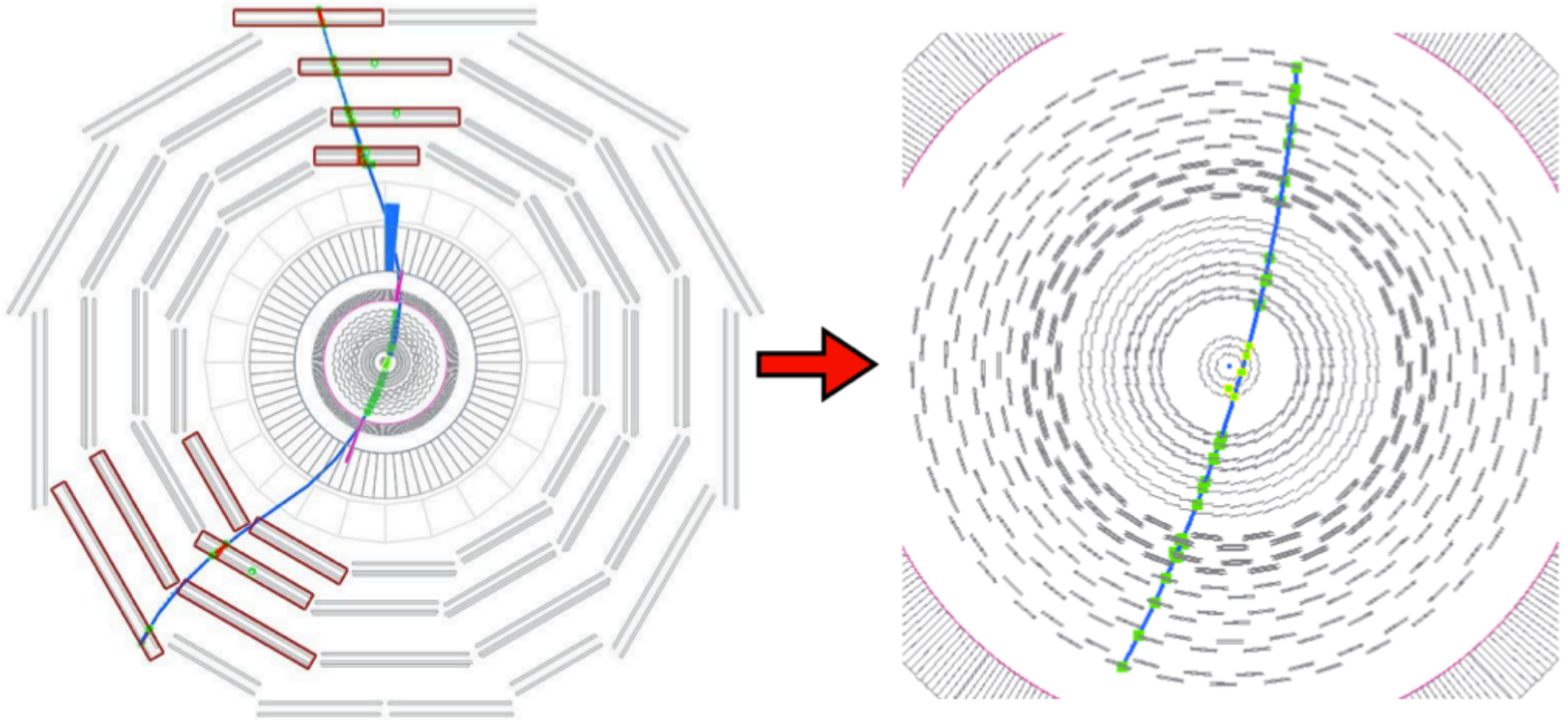
- excellent spatial resolution: short range for secondary electrons

Inner tracking at the LHC



Outer \longleftrightarrow inner tracking

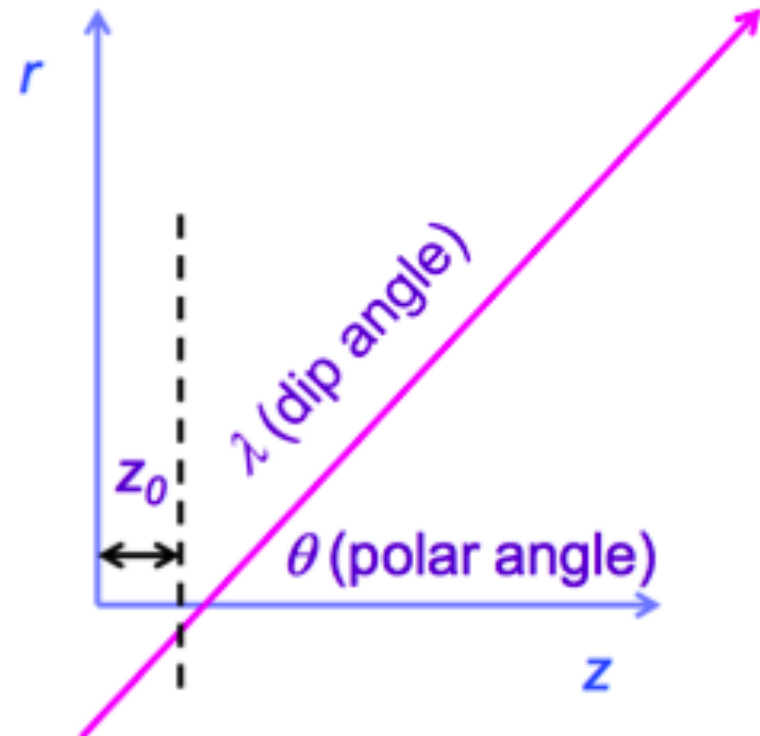
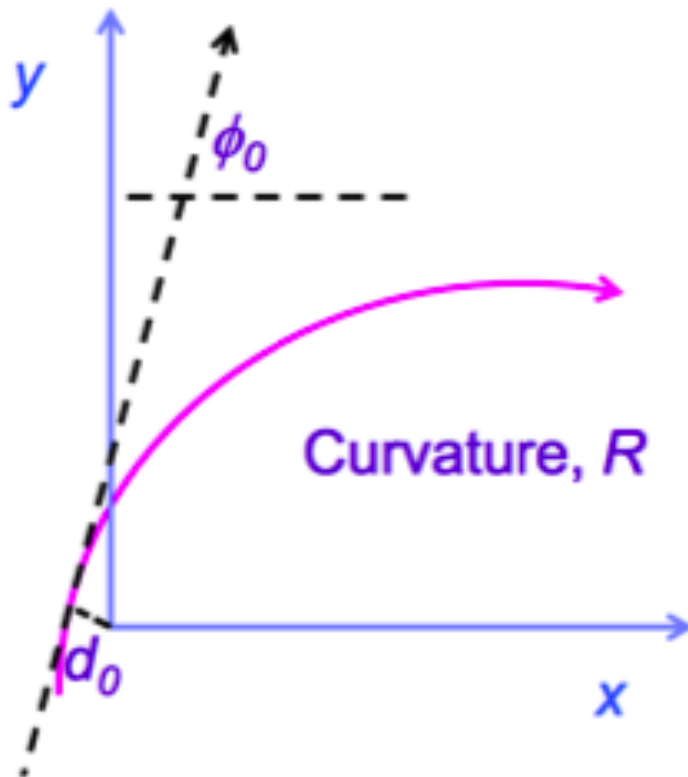
32



Coordinates for tracking

33

- The LHC experiments use a uniform B field along the beam line (z-axis)
 - trajectory of charged particles is an helix – radius R
 - use transverse (xy) and longitudinal (rz) projections
 - pseudo-rapidity: $\eta = -\ln \tan \frac{\theta}{2}$ transverse momentum: $p_T = p \sin \theta = p / \cosh \eta$
- **Impact parameter** is defined from distance of closest approach to primary vertex



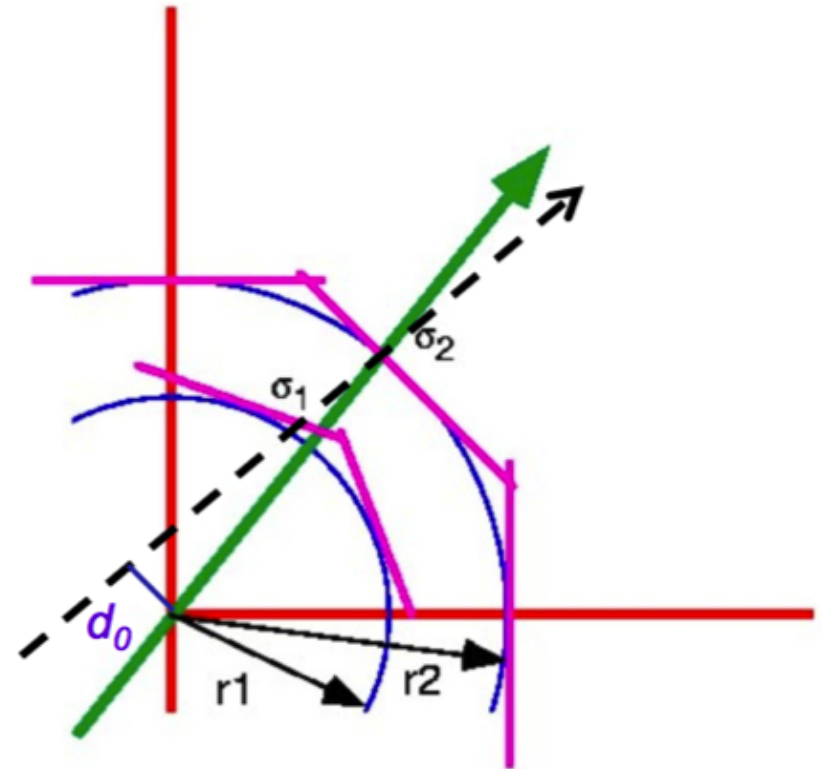
Resolution for the impact parameter

34

- Depends on radii+space point precisions
- For two layers we expect

$$\sigma_{d_0}^2 = \frac{r_2^2 \sigma_1^2 + r_1^2 \sigma_2^2}{(r_2 - r_1)^2}$$

- Improve with small r_1 , large r_2
- Improves with better σ_i



Resolution for the impact parameter

35

- Depends on radii+space point precisions

- For two layers we expect

$$\sigma_{d_0}^2 = \frac{r_2^2 \sigma_1^2 + r_1^2 \sigma_2^2}{(r_2 - r_1)^2}$$

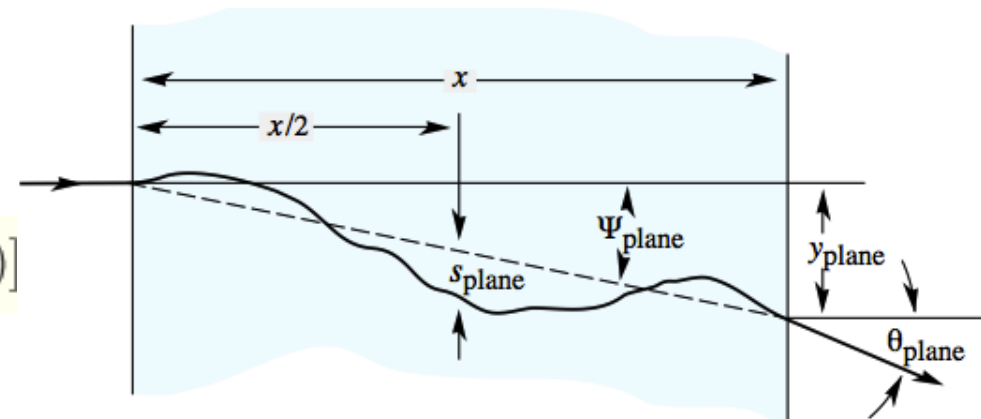
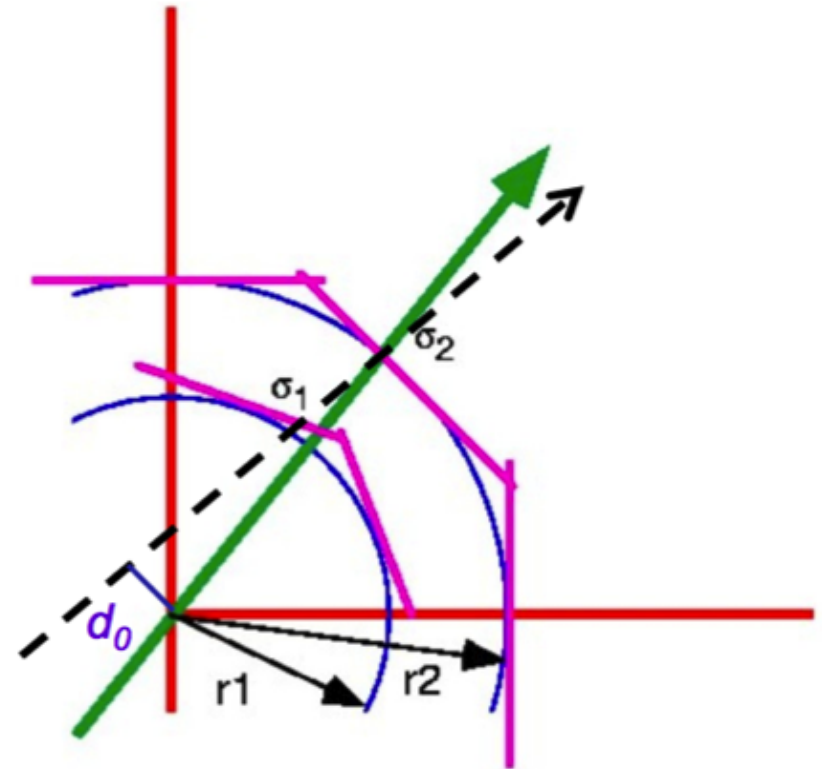
- Improve with small r_1 , large r_2
- Improves with better σ_i

- Precision is degraded by multiple scattering

- Gaussian approximation is valid
- Width given by

$$\theta_0 = \frac{13.6 \text{ MeV}}{\beta c p} z \sqrt{x / X_0} [1 + 0.038 \ln(x / X_0)]$$

- extra degradation term for d_0 $\sigma_{d_0} \sim \theta_0$



Resolution for the impact parameter

36

- For a track with $\theta \neq 90^\circ$ we can write $r \rightarrow r/\sin\theta$ and $x \rightarrow x/\sin\theta$
- By substitution in the formulas of the previous slide we have:

$$\sigma_{d0} \sim \sqrt{\frac{r_2^2 \sigma_1^2 + r_1^2 \sigma_2^2}{(r_2 - r_1)^2}} \oplus \frac{r}{p \sin^{3/2} \theta} \rightarrow a \oplus \frac{b}{p_T \sin^{1/2} \theta}$$

geometry-dependent

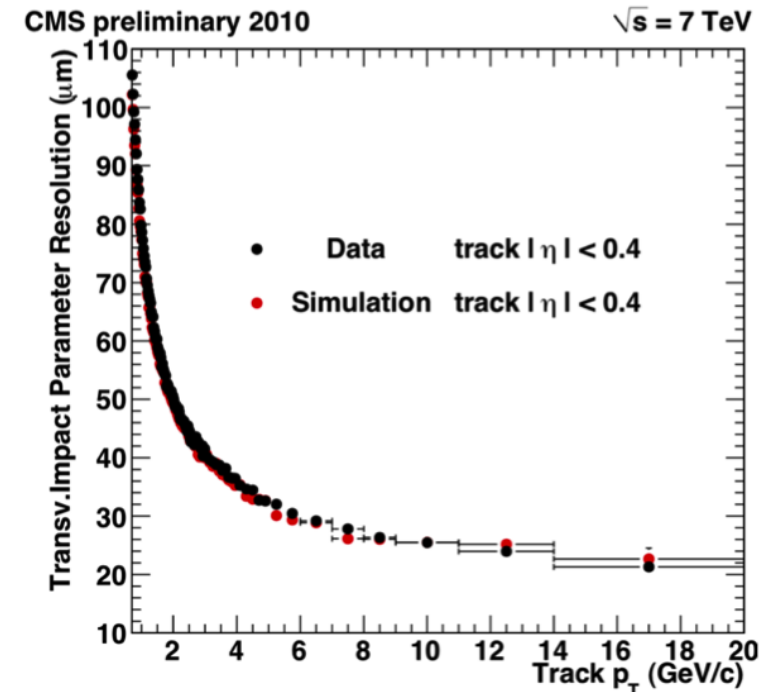
Material- and p_T -dependent

- Typical resolution expected/measured

- 100 μm @ 1 GeV 20 μm @ 20 GeV

- Typical lifetimes (rest frame)

- $B \sim 500 \mu\text{m}$ $D^0 \sim 120 \mu\text{m}$ $\tau \sim 87 \mu\text{m}$



Momentum measurement

37

- Circular motion under uniform B-field

$$R[m] = 0.3 \frac{B[T]}{p_T[GeV]}$$

- Typically measure the sagitta

- deviation to straight line relates to R by

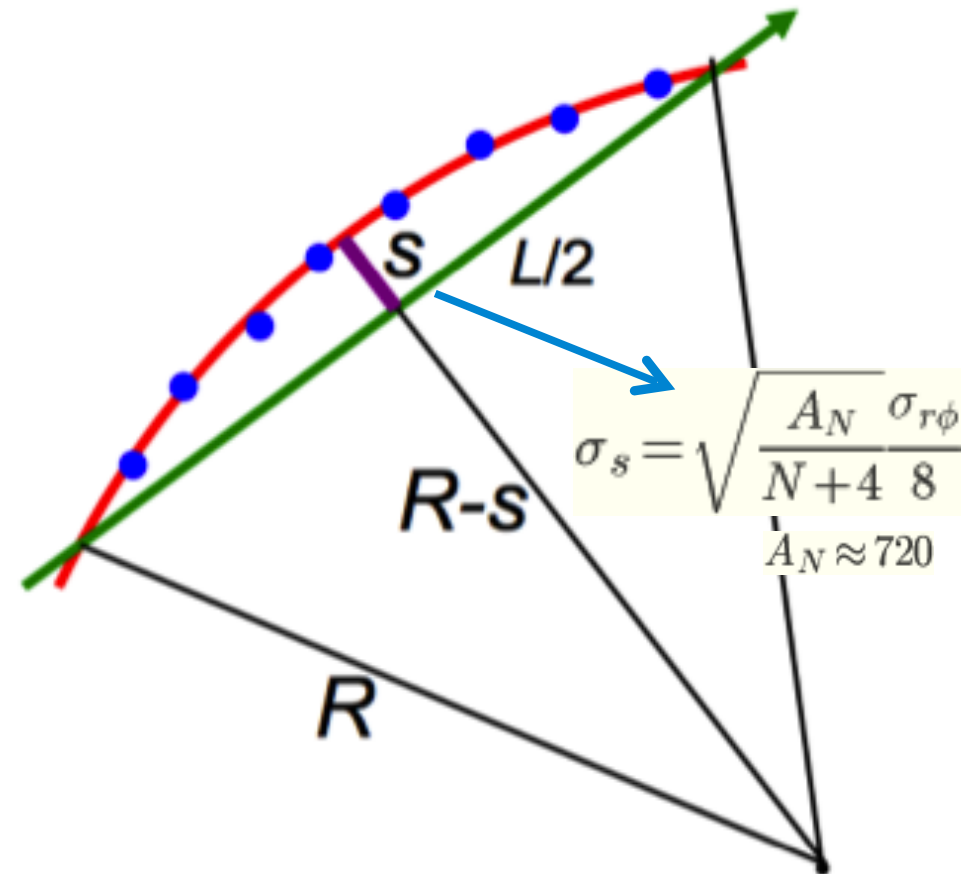
$$R = \frac{L^2}{2s} + \frac{s}{2} \approx \frac{L^2}{2s}$$

- Uncertainty in pT measurement improves with B, number of hits and path

$$\frac{\sigma_{p_T}}{p_T} = \frac{8p_T}{0.3BL^2} \sigma_s$$

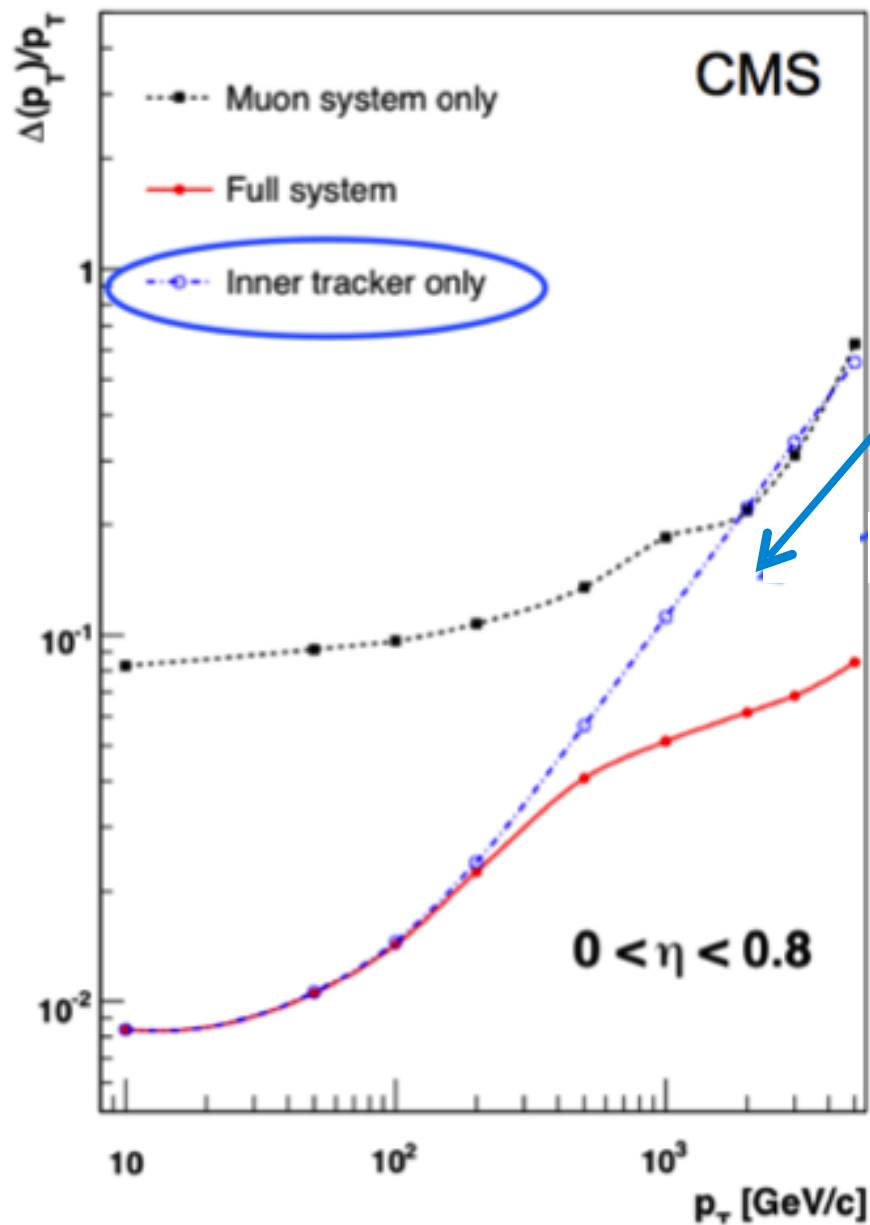
- Multiple scattering introduces, again extra degradation

$$\frac{\sigma_{p_T}}{p_T} \sim a p_T \oplus \frac{b}{\sin^{1/2}\theta}$$



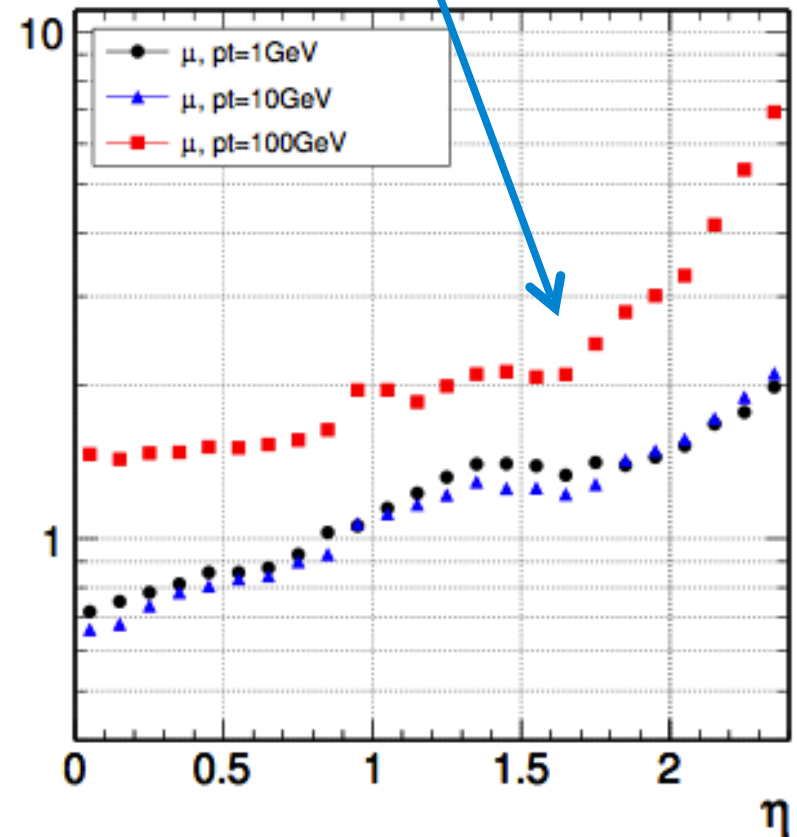
Momentum resolution

38



$$\frac{\sigma_{p_T}}{p_T} \sim a p_T \oplus \frac{b}{\sin^{1/2}\theta}$$

$\sigma(\delta p_T/p_T)$ [%]

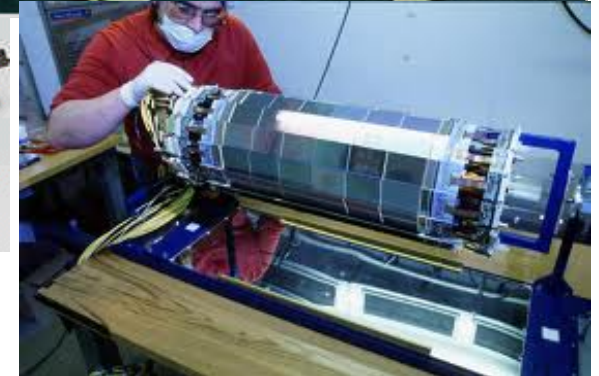
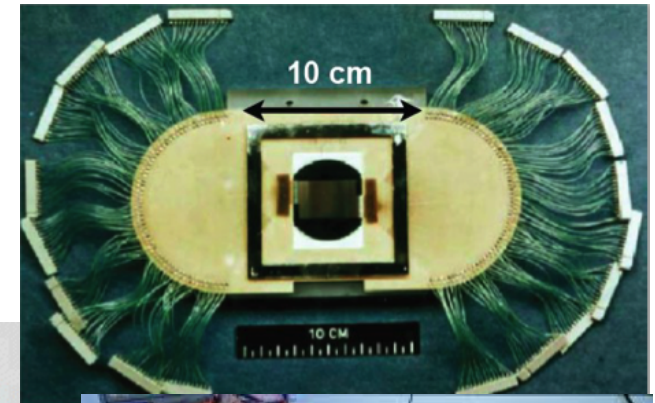
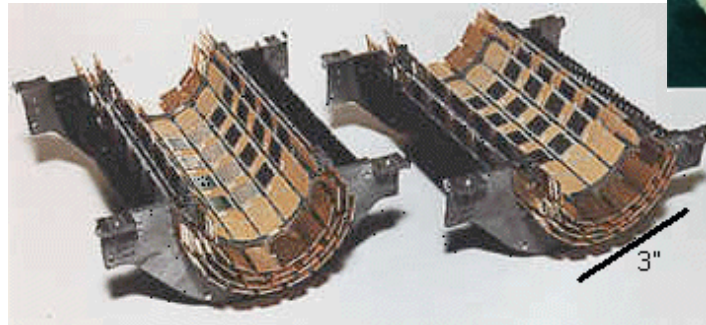


Si-based detectors

Usage of Si-based trackers for HEP

40

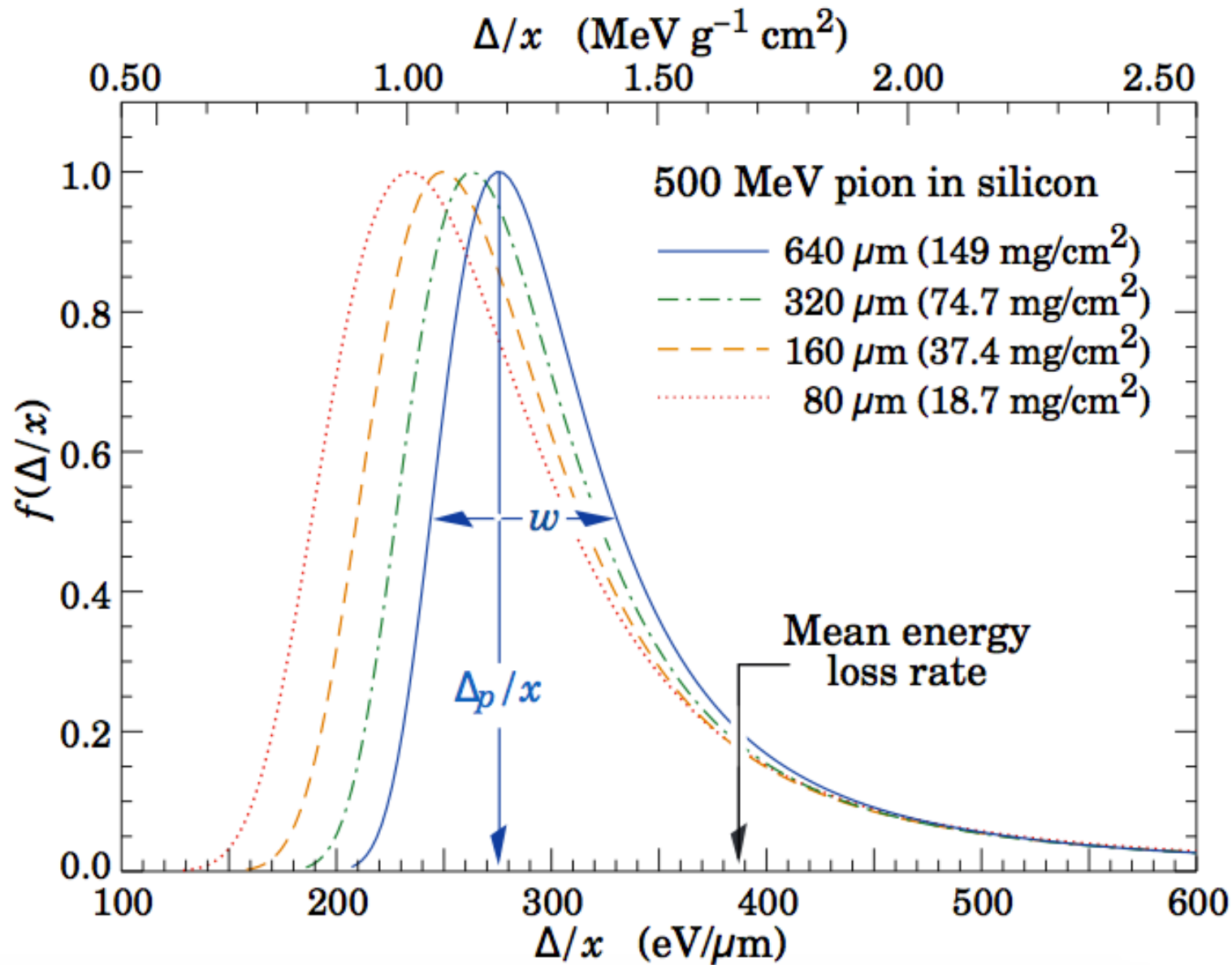
- **Kemmer, 1979** transferred Si-technology for electrons to detector - NIM 169(1980)499
- **NA1 I/32** spectrometer at CERN →
 - 6 planes Si-Strip, <2k channels
 - Resolution $\sim 4.5\mu\text{m}$
- **SLD** vertex detector at SLAC →
 - 120-307 M pixels: $0.4\%X_0$
 - Resolution $<4\mu\text{m}$, $d_0 \sim 11-9\mu\text{m}$
- **ALEPH** detector at LEP →
 - Enable precise measurements for B-physics (lifetime, b-tagging)



Experiment	Detectors	Channels (10^3)	Si area [m^2]
Aleph (LEP)	144	95	0.49
CDF II (TEV)	720	405	1.9
D0 II (TEV)	768	793	4.7
AMS II	2300	196	6.5
ATLAS (LHC)	4088	6300	61
CMS (LHC)	15148	10000	200

Ionization energy loss in the Si

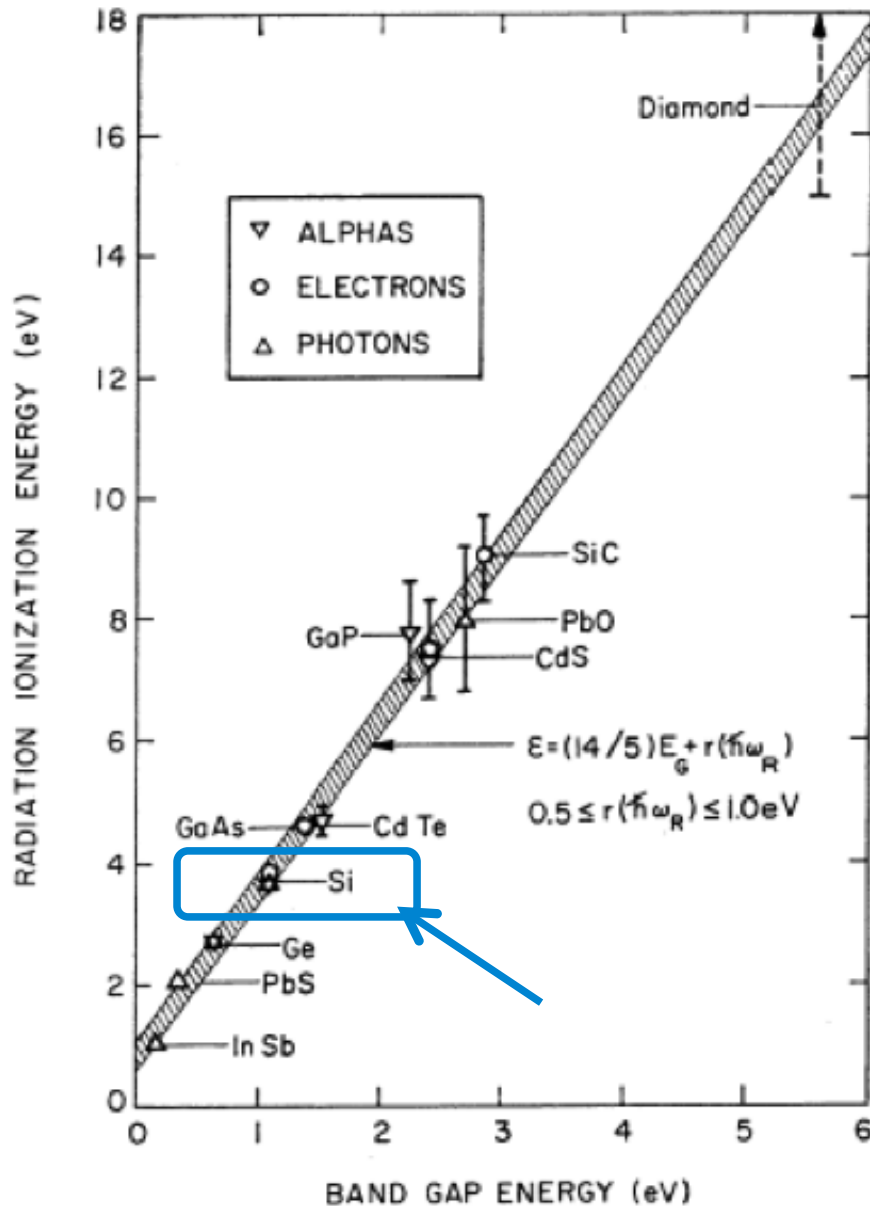
41



Most probable value of the Landau distribution for energy loss defines the minimum ionizing particle

Si properties

42

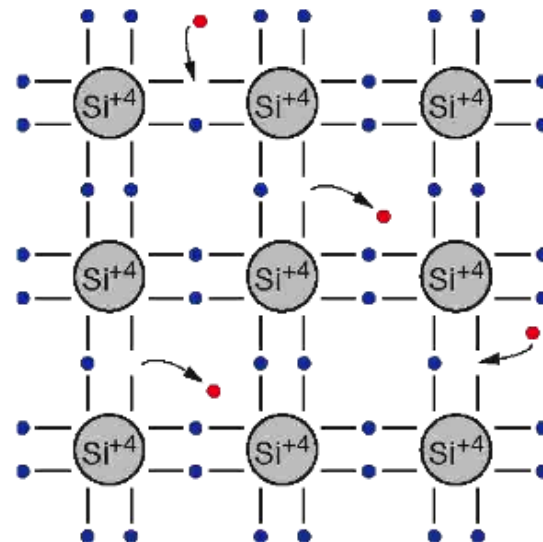
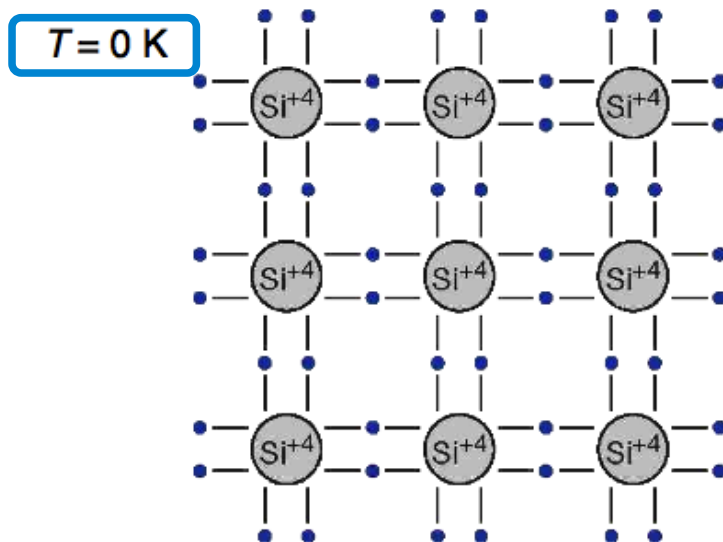
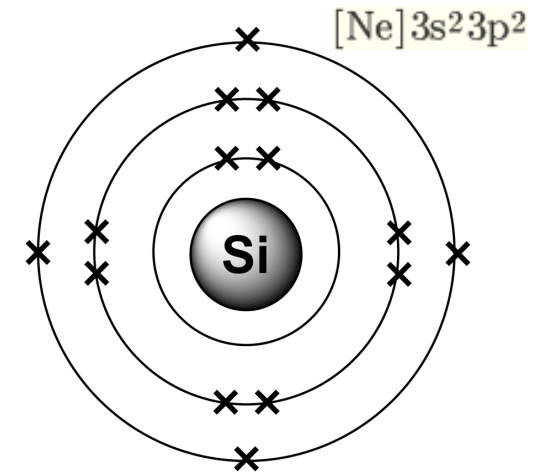


- Widely used in high energy physics and industry
- Low ionization energy
 - Band gap is 1.12 eV
 - Takes 3.6 eV to ionize atom → remaining yields phonon excitations
 - Long free mean path → good charge collection efficiency
 - High mobility → fast charge collection
 - Low Z → reduced multiple scattering
- Good electrical properties (SiO_2)
- Good mechanical properties
 - Easily patterned to small dimensions
 - Can be operated at room temperature
 - Crystalline → resilient against radiation

Bond model of semi-conductors

43

- Covalent bonds formed after sharing electrons in the outermost shell
- Thermal vibrations
 - break bonds and yield electron conduction (free e^-)
 - remaining open bonds attract free $e^- \rightarrow$ holes change position \rightarrow hole conduction

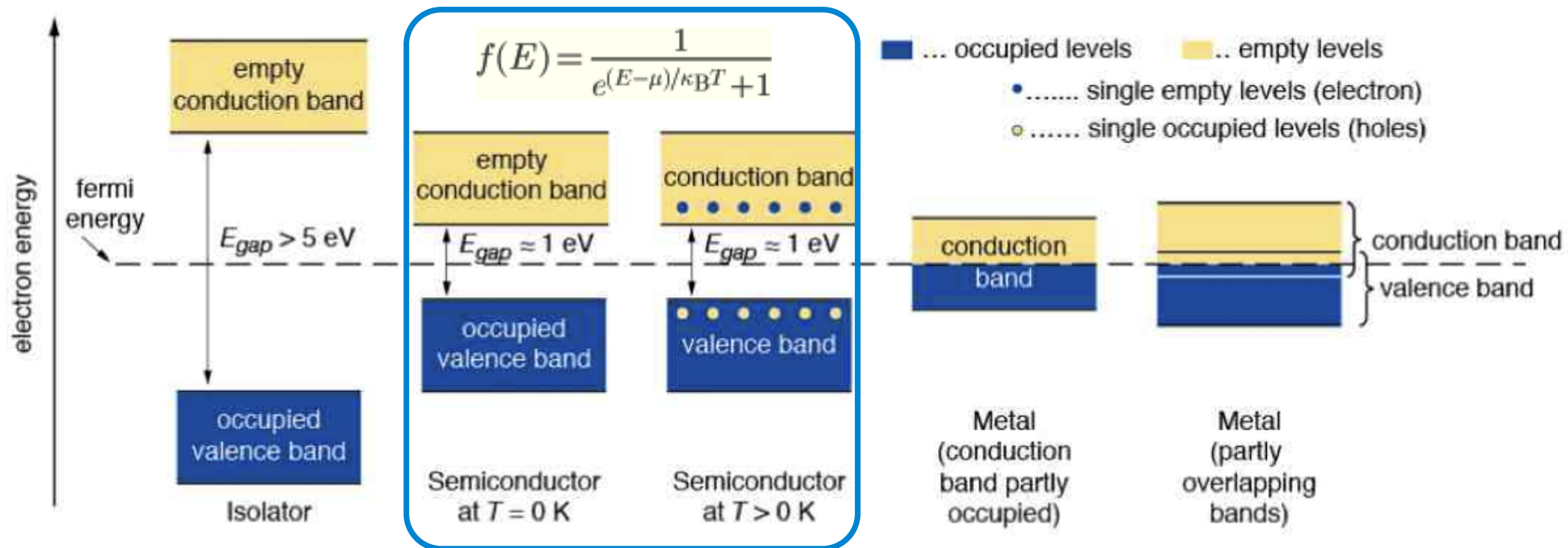


- ... Valence electron
- ... Conduction electron

Energy bands structure compared

44

- In solids, the quantized energy levels merge
 - Metals: conduction and valence band overlap
 - Insulators and semi-conductors: conduction and valence band separated by energy (band) gap
 - If μ (band gap) sufficiently low : electrons fill conduction band according to Fermi-Dirac statistics



Intrinsic carrier concentration

45

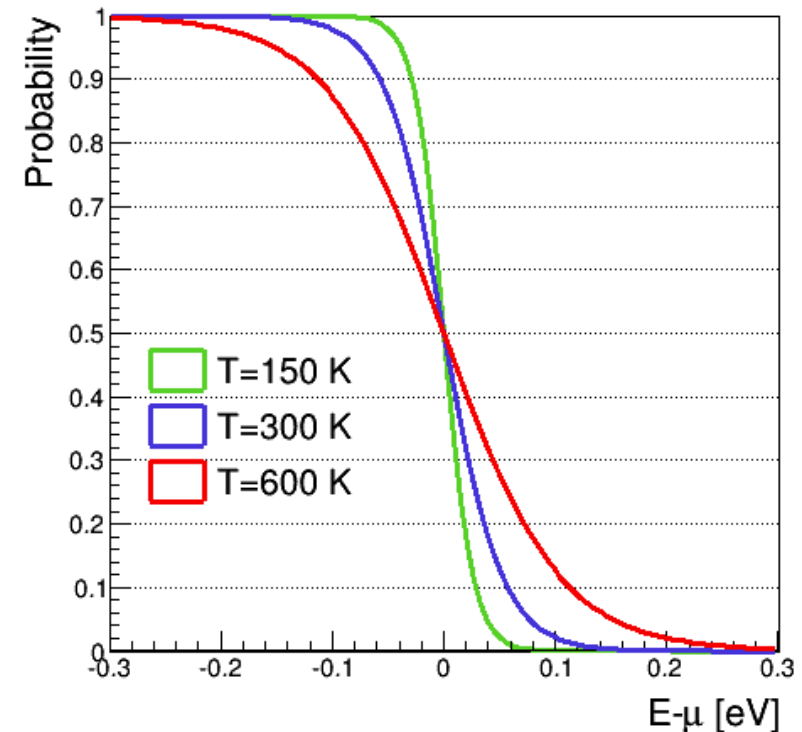
- Energy state occupation probability follows Fermi statistics distribution

$$f(E) = \frac{1}{e^{(E-\mu)/k_B T} + 1}$$

- Typical behaviour @ room temperature
 - excited electrons move to conduction band
 - electrons recombine with holes
- Excitation and recombination in thermal equilibrium
- Intrinsic carrier concentration given by

$$n_e = n_h = n_i = A \cdot T^{3/2} \cdot e^{-E_g/k_B T}$$

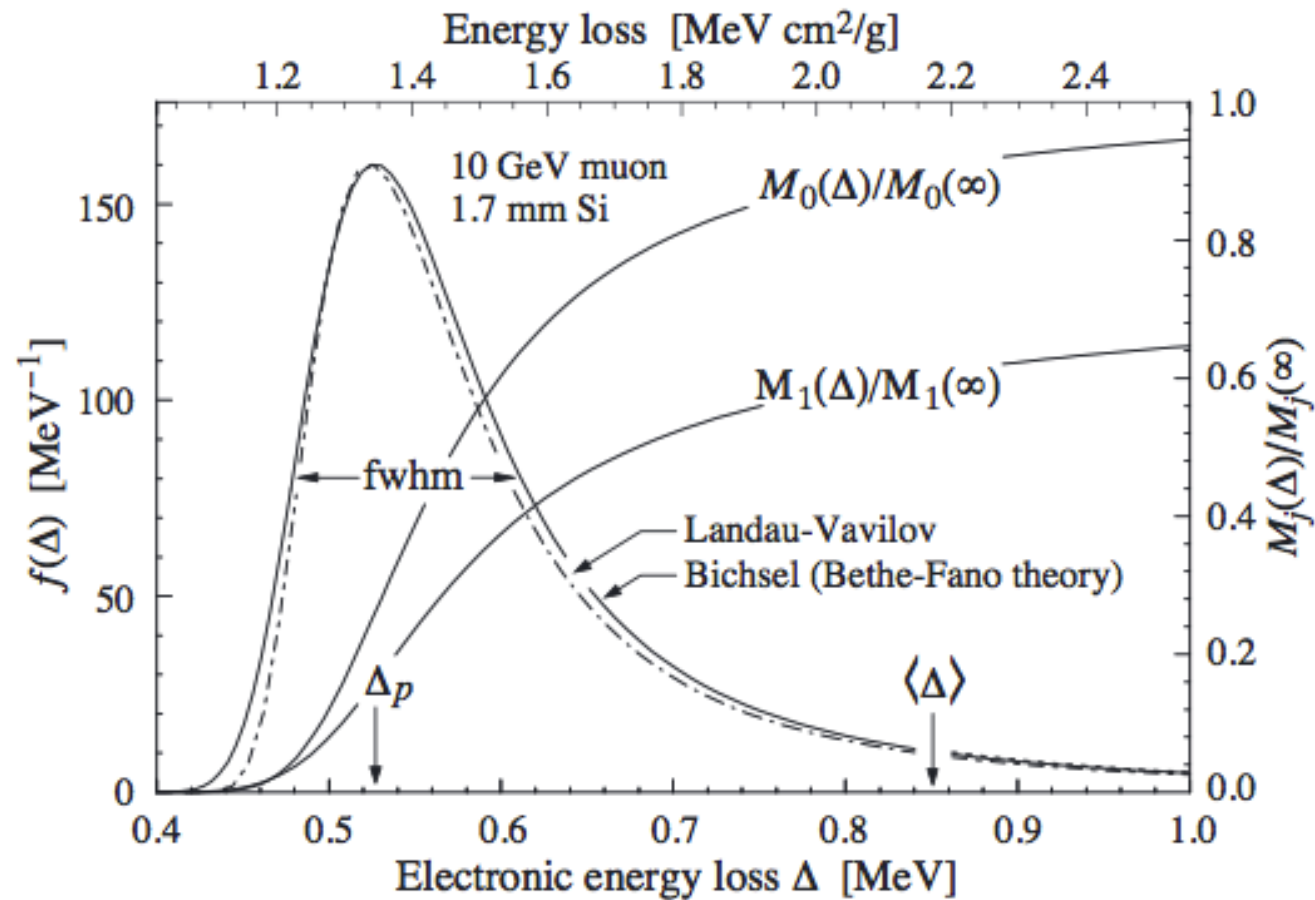
with $A = 3.1 \times 10^{16} \text{ K}^{-3/2} \text{ cm}^{-3}$ and $E_g/2k_B = 7 \times 10^3 \text{ K}$



$$n_i \sim 1.45 \times 10^{10} \text{ cm}^{-3}$$

$\Rightarrow 1/10^{12}$ Si atoms is ionized

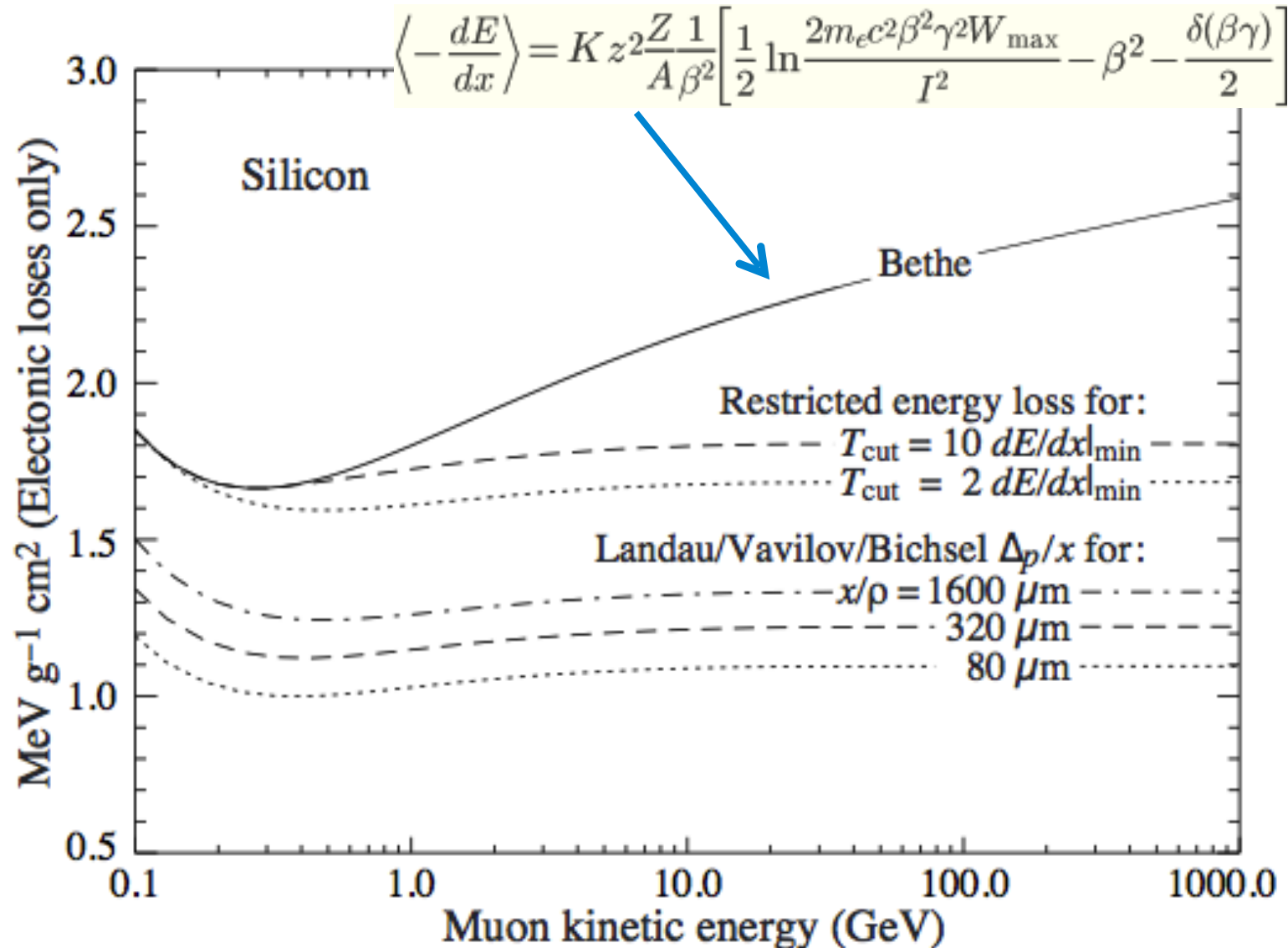
Intrinsic S/N in Si detectors



Intrinsic S/N in Si detectors

47

Example: Si detector with thickness $d=300\mu\text{m}$



S/N in intrinsic Si detector

48

For a 300μm thickness sensor

- Minimum ionizing particle (MIP) creates:

$$\frac{1}{E_{eh}} \frac{dE}{dx} \cdot d = \frac{3.87 \cdot 10^6 \text{ eV/cm}}{3.63 \text{ eV}} \cdot 0.03 \text{ cm} = 3.2 \cdot 10^4 \text{ eh pairs}$$

- Intrinsic charge carriers (recall slide 43):

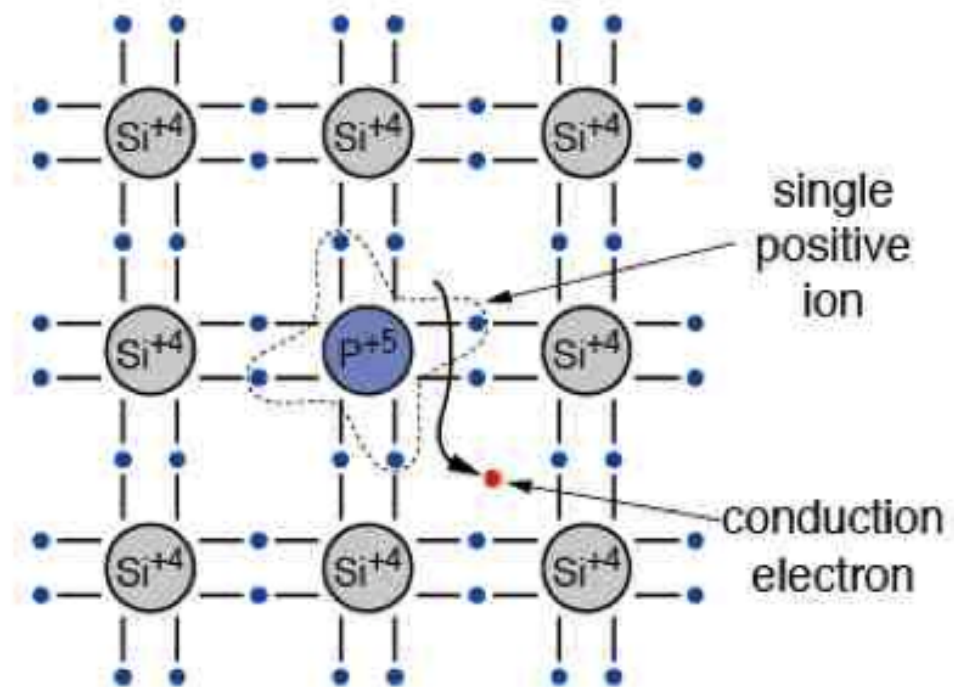
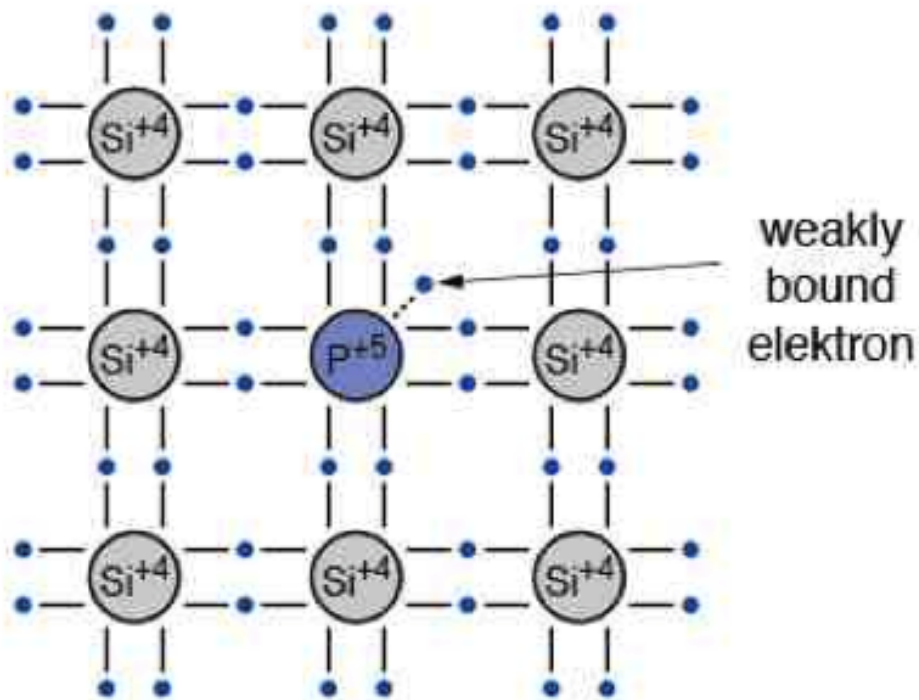
$$n_i \cdot d = 1.45 \cdot 10^{10} \text{ cm}^{-3} \cdot 0.03 \text{ cm} = 4.35 \cdot 10^8 \text{ eh pairs}$$

Number of thermally-created e-h pairs exceeds mip signal by factor 10!

Si doping: n-dope bond model

49

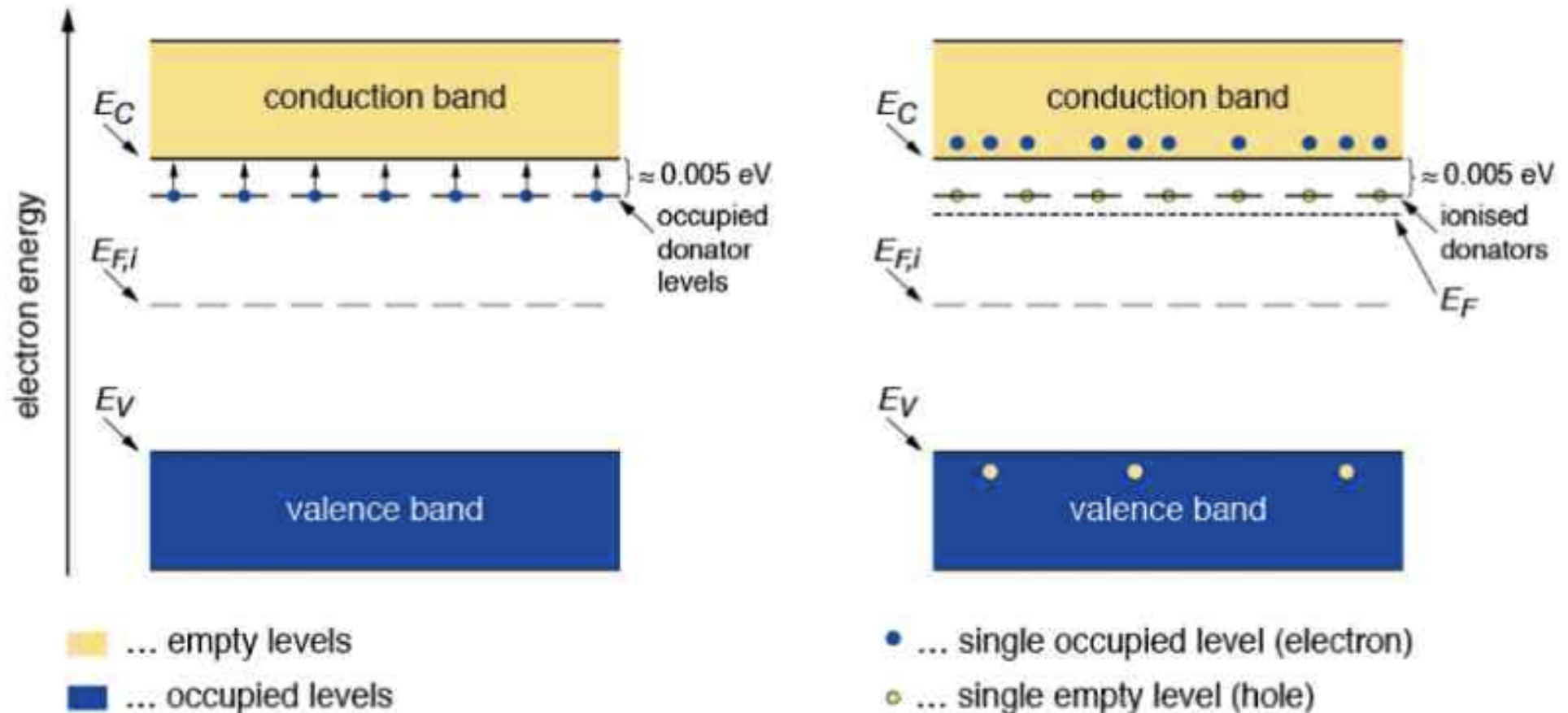
- Doping with a group 5 atom (e.g. P, As, Sb)
 - atom is an electron **donor/donator**
 - Weakly bound 5th valence electron
 - Positive ion is left after conduction electron is released



Si doping: n-dope bond model II

50

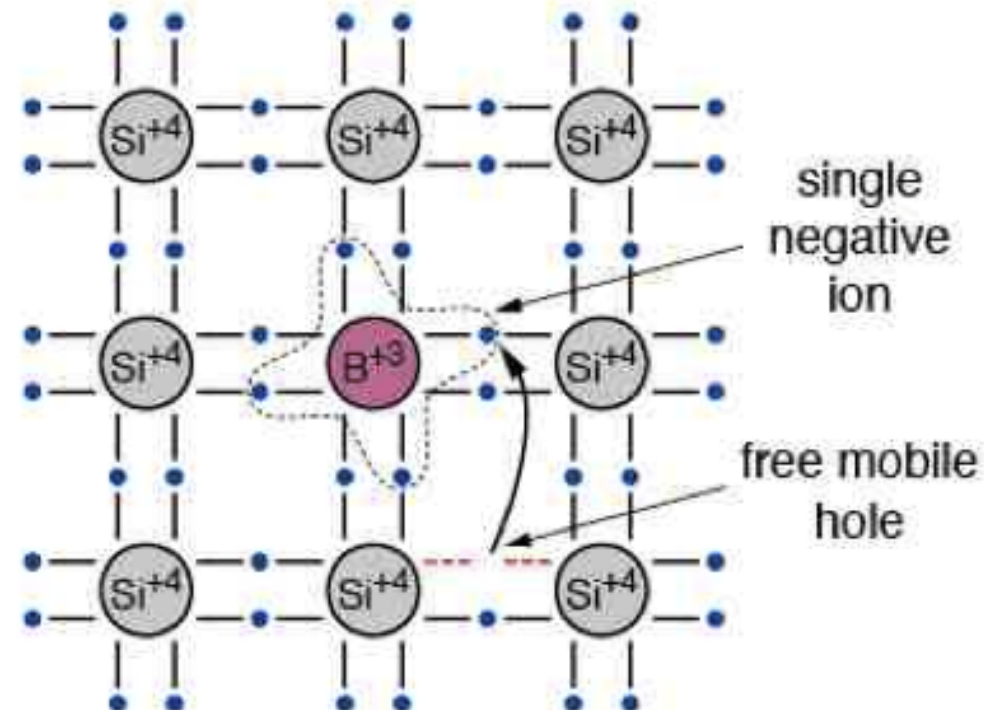
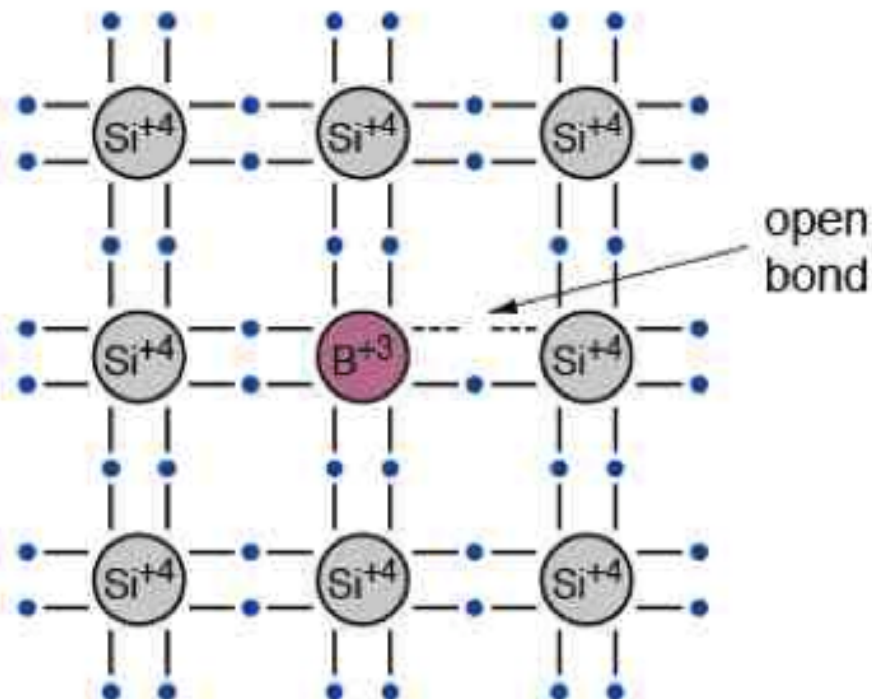
- Energy level of donor is below edge of conduction band
 - Most electrons enter conduction band at room temperature
 - Fermi level moves up with respect to pure Si



Si doping: p-dope bond model

51

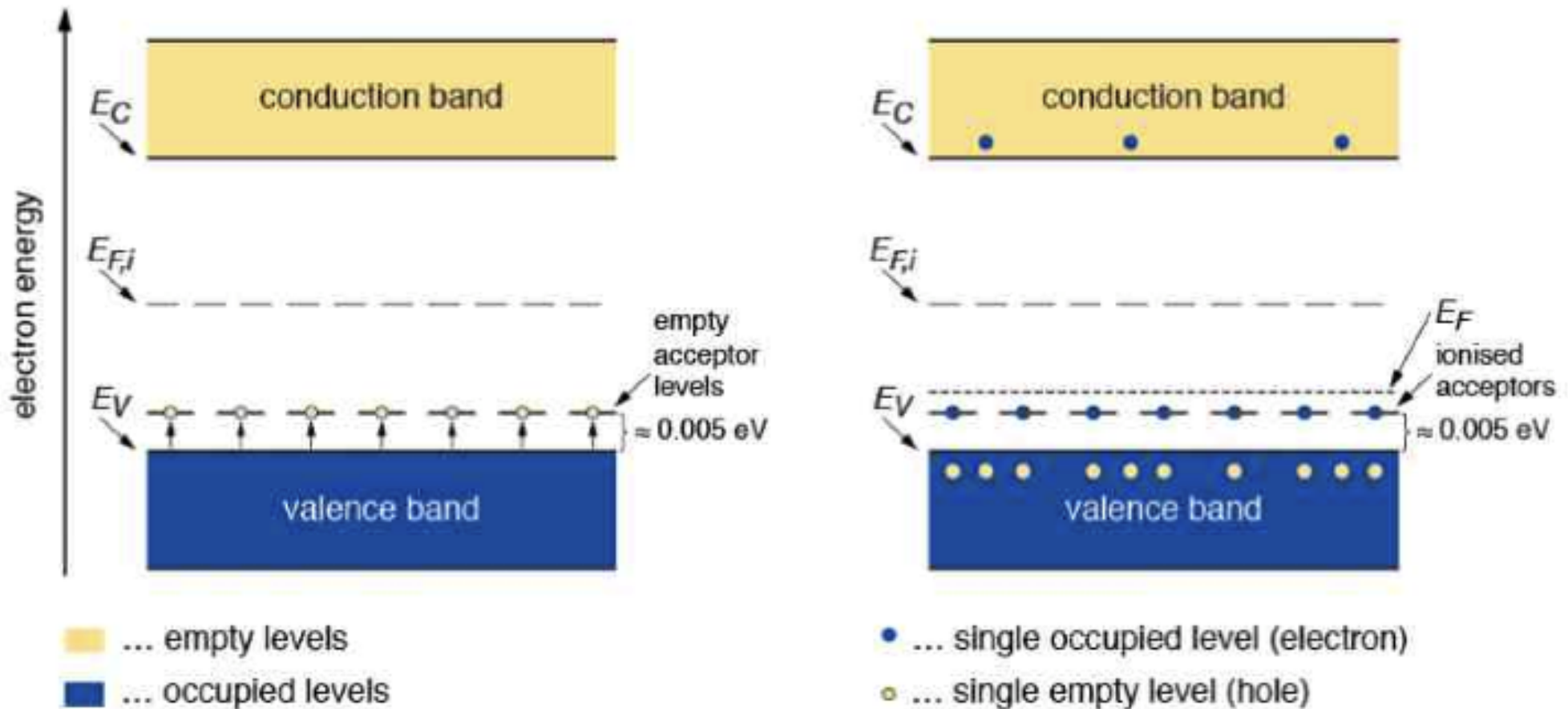
- Doping with a group 3 atom (e.g. B, Al, Ga, In)
 - atom is an electron **acceptor**
 - open bond attracts electrons from neighbouring atoms
 - acceptor atom in the lattice becomes negatively charged



Si doping: p-dope bond model - II

52

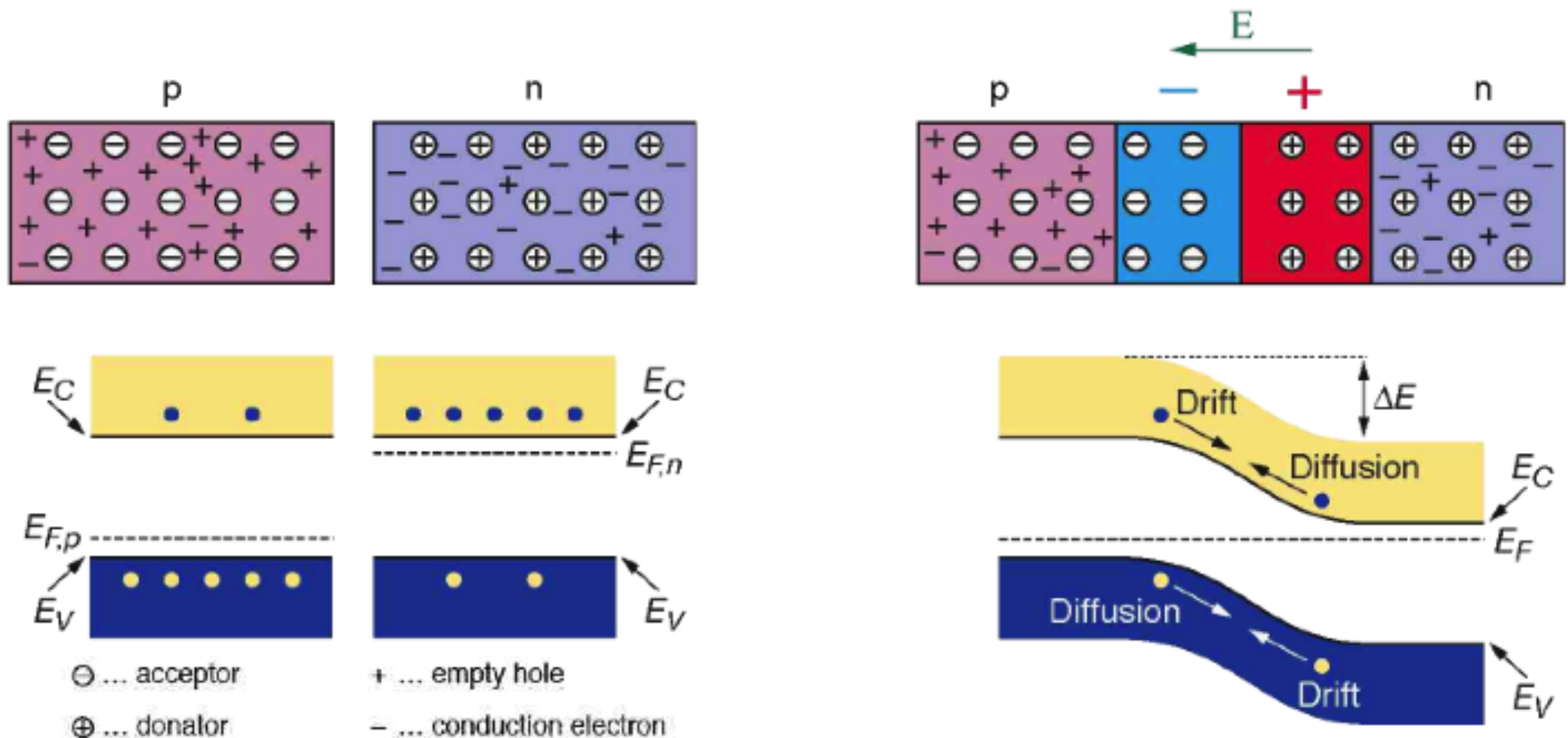
- Energy level of acceptor is above edge of conduction band
 - Most levels are occupied by electrons \rightarrow holes in the valence band
 - Fermi level moves down with respect to pure Si



p-n junctions

53

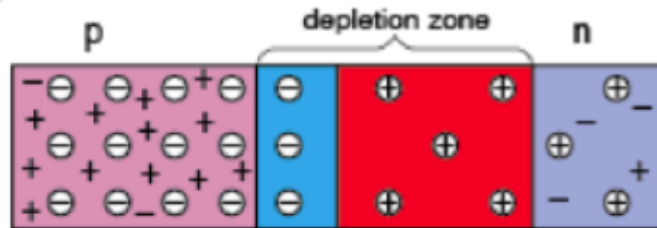
- Difference in Fermi levels at the interface of n-type or p-type
 - diffusion of excess of charge carriers until thermal equilibrium (or equal Fermi level)
 - remaining ions create a **depletion zone**: electric field prevents further the diffusion



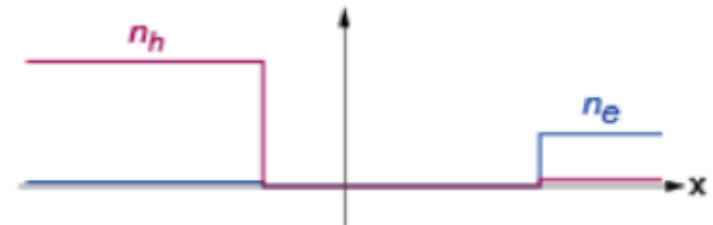
p-n junctions

54

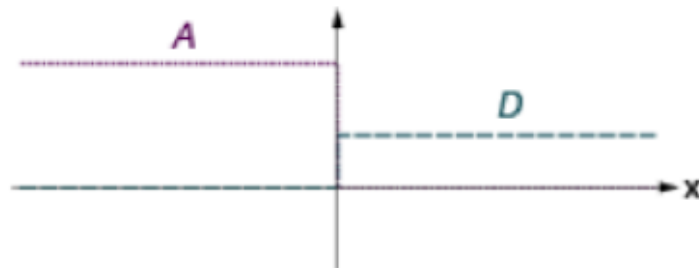
pn junction scheme



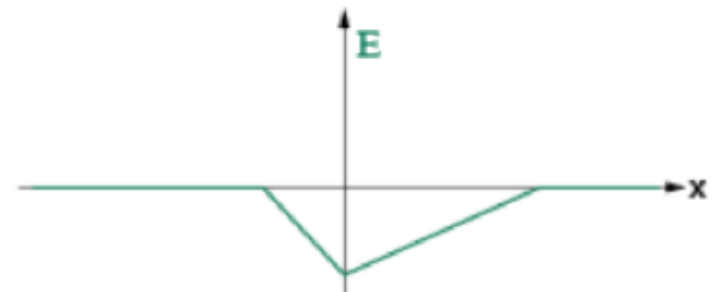
concentration of free charge carriers



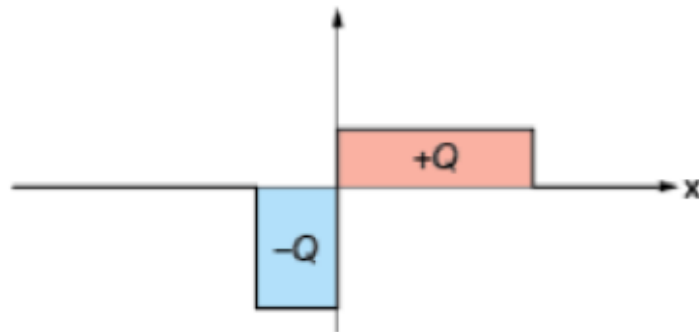
acceptor and donator concentration



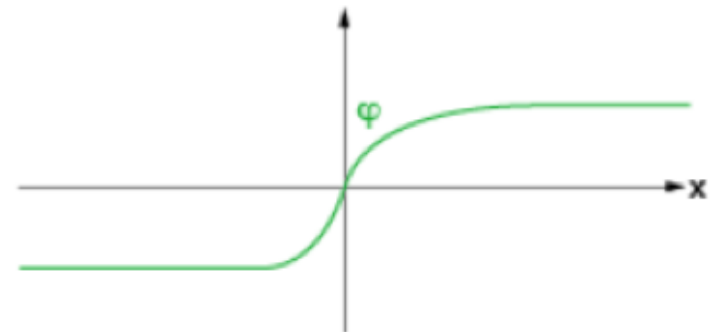
electric field



space charge density



electric potential

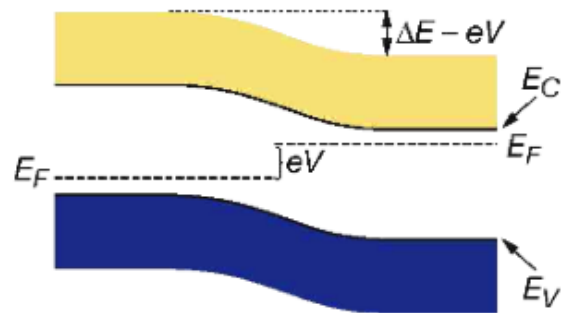
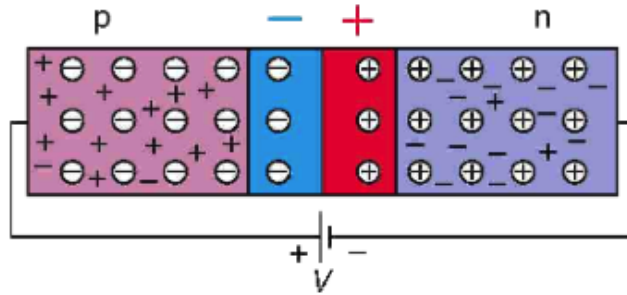


\ominus ... acceptor \oplus ... empty hole
 \oplus ... donator \ominus ... conduction electron

Biasing p-n junctions

55

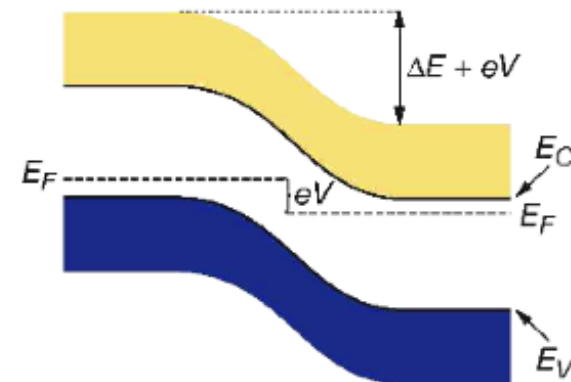
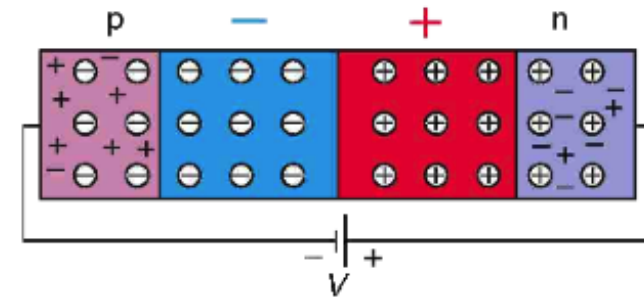
p-n junction with forward bias



Forward-biased junction

- Anode to p, cathode to n
- Depletion zone becomes narrower
- Smaller potential barrier facilitates diffusion
- Current across the junction tends to increase

p-n junction with reverse bias



Reverse-biased junction

- Anode to n, cathode to p
- e,h pulled out of the depletion zone
- Potential barrier is suppressed
- Only leakage current across junction

Depletion zone width and capacitance

56

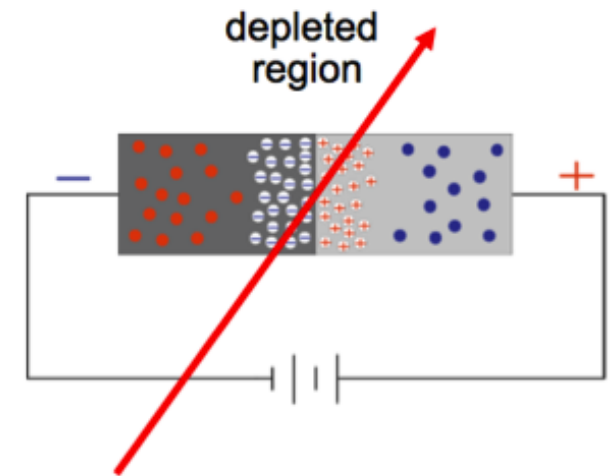
- Characterize depletion zone from Poisson equation with charge conservation:

$$\nabla^2 \phi = -\frac{\rho_f}{\epsilon}$$

- Typically: $N_a = 10^{15} \text{ cm}^{-3}$ (p+ region) $\gg N_d = 10^{12} \text{ cm}^{-3}$ (n bulk)

- **Width of depletion zone** (n bulk):

$$W \approx \sqrt{\frac{2\epsilon V_{\text{bias}}}{q} \cdot \frac{1}{N_d}}$$

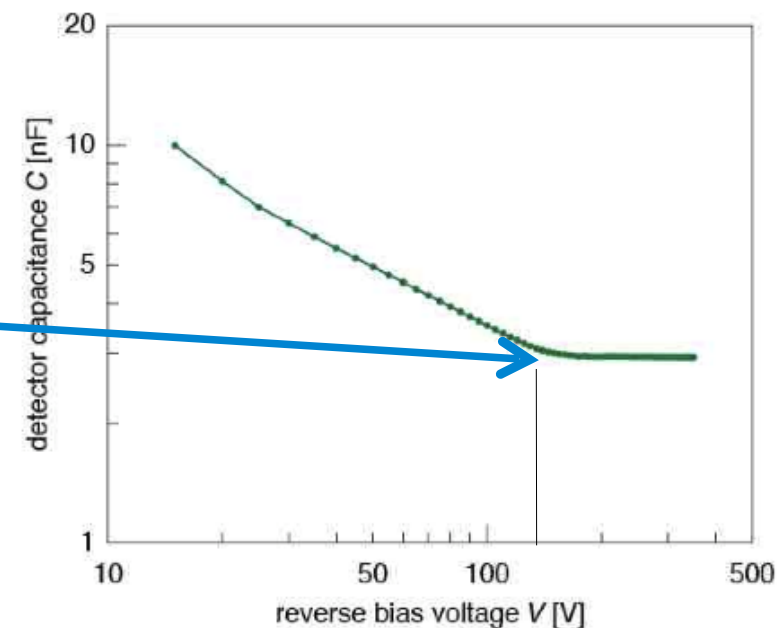


Reverse bias voltage (V)	W_p (μm)	W_n (μm)
0	0.02	23
100	0.4	363

- **Device is similar to a parallel-plate capacitor**

$$C = \frac{q}{V} = \frac{\epsilon A}{d} = A \sqrt{\frac{\epsilon q N_d}{2V_{\text{bias}}}}$$

- Depletion voltage saturates the capacitance
- Typical curve obtained for CMS strip detector

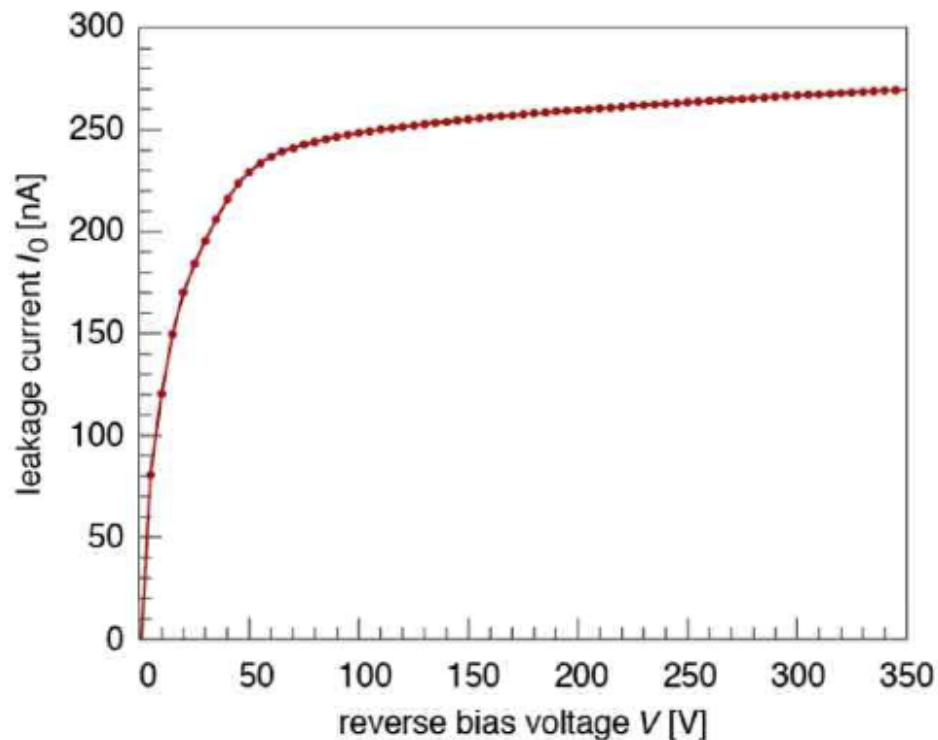


Leakage current

57

- Thermal excitation generates eh pairs
- Reverse bias applied separates pairs
- eh pairs do not recombine and drift

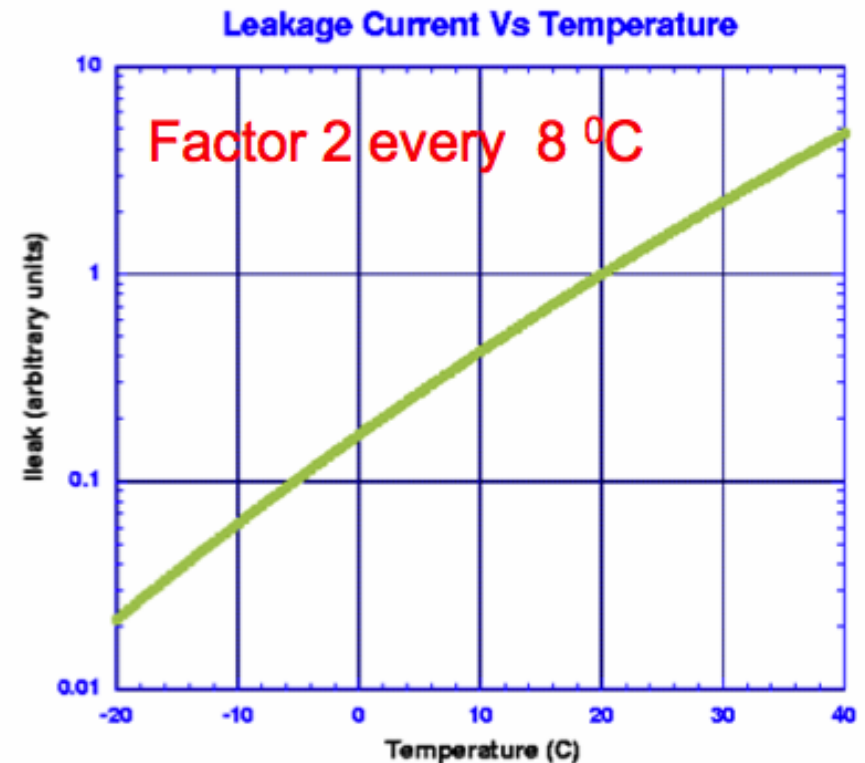
⇒ leakage current



- Depends on purity, defects and temperature

$$j_{\text{gen}} \propto T^{3/2} e^{\frac{1}{k_B T}}$$

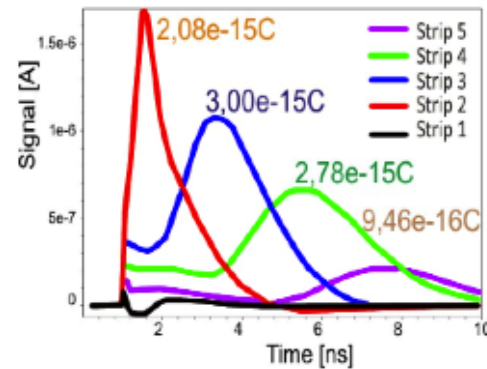
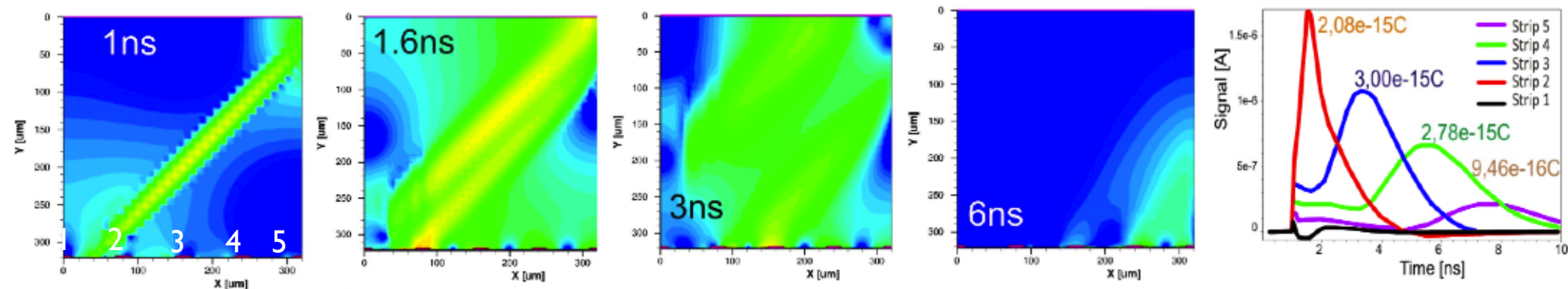
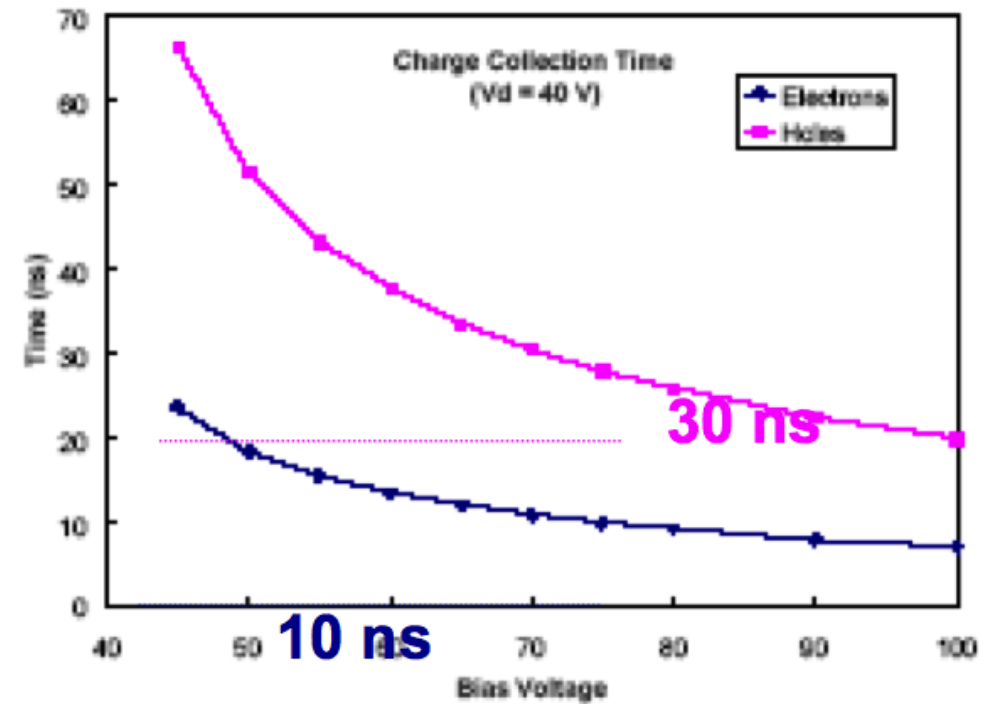
⇒ usually require detector cooling
for stable operation (-30°C-10°C)



Charge collection

58

- eh pairs move under the electric field
 - larger biases smaller collection times
 - typically smaller than LHC bunch crossing



Simulation by Thomas Eichhorn (KIT)

charge collection simulation for a 45° incident particle

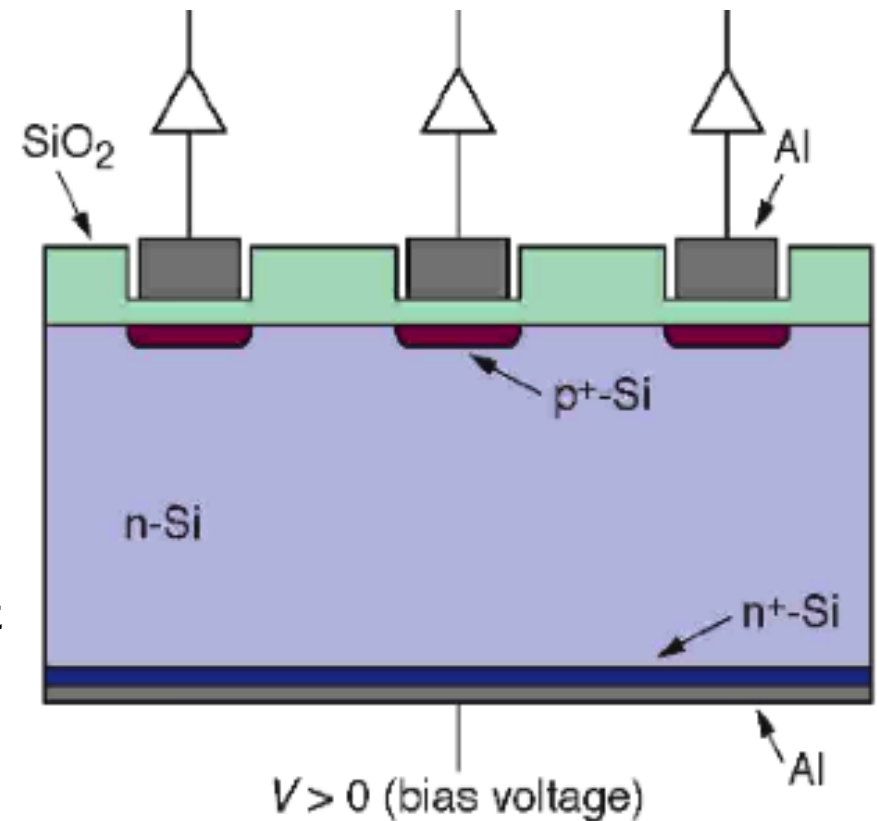
Position resolution (DC coupled)

59

- Segmentation of the implants determines precision in position reconstruction

- Typical configuration

- p implants in strips
- n-doped substrate $\sim 300\mu\text{m}$ ($2\text{-}10\text{k}\Omega\text{cm}$)
- depletion voltage $< 200\text{V}$
- backside P implant establishes ohmic contact
- Al metallisation

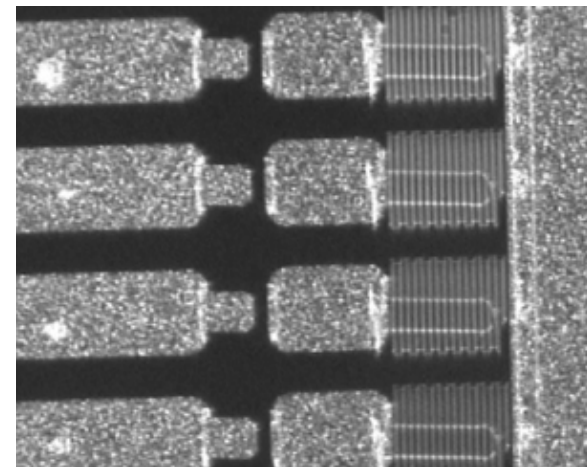
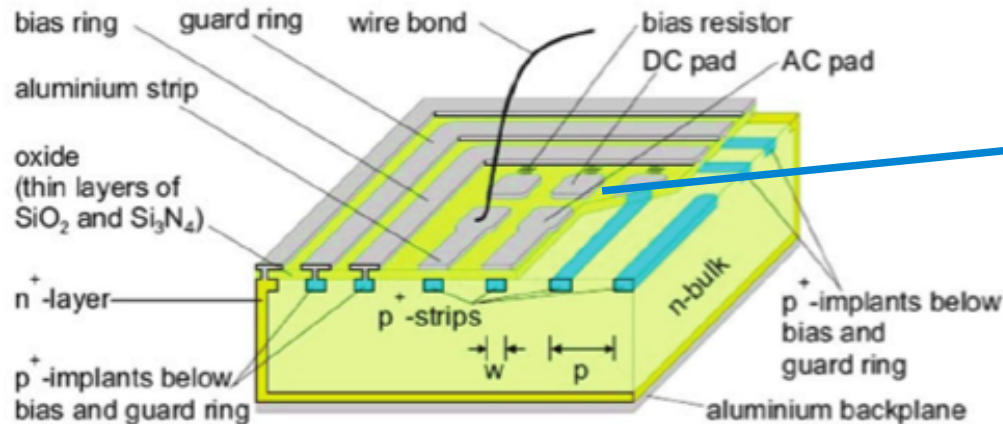
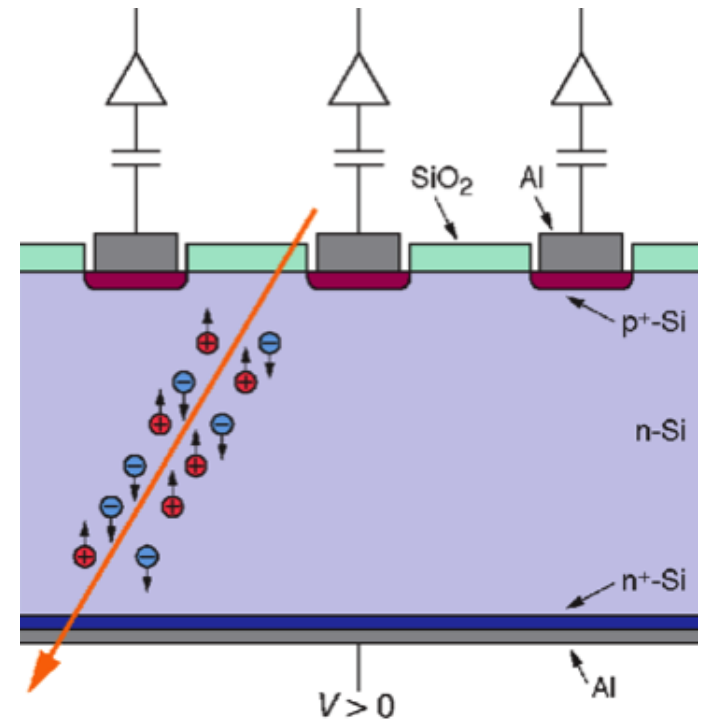


- Field is closest to the collecting electrodes (where most of the signal is)

Position resolution (AC coupled)

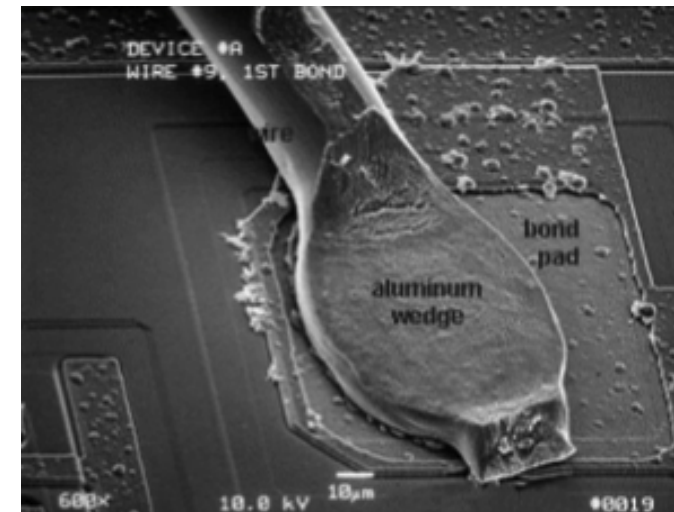
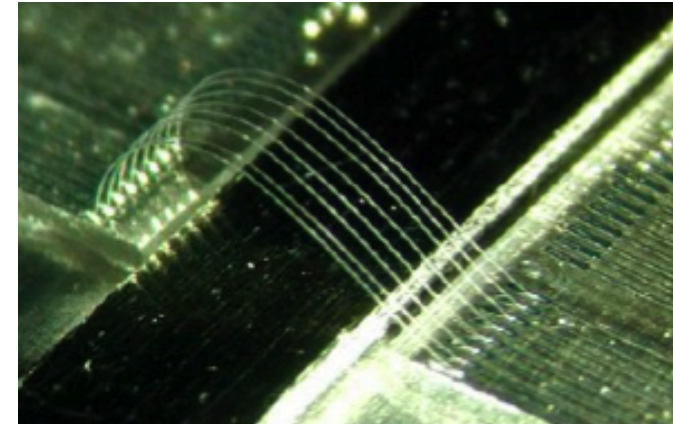
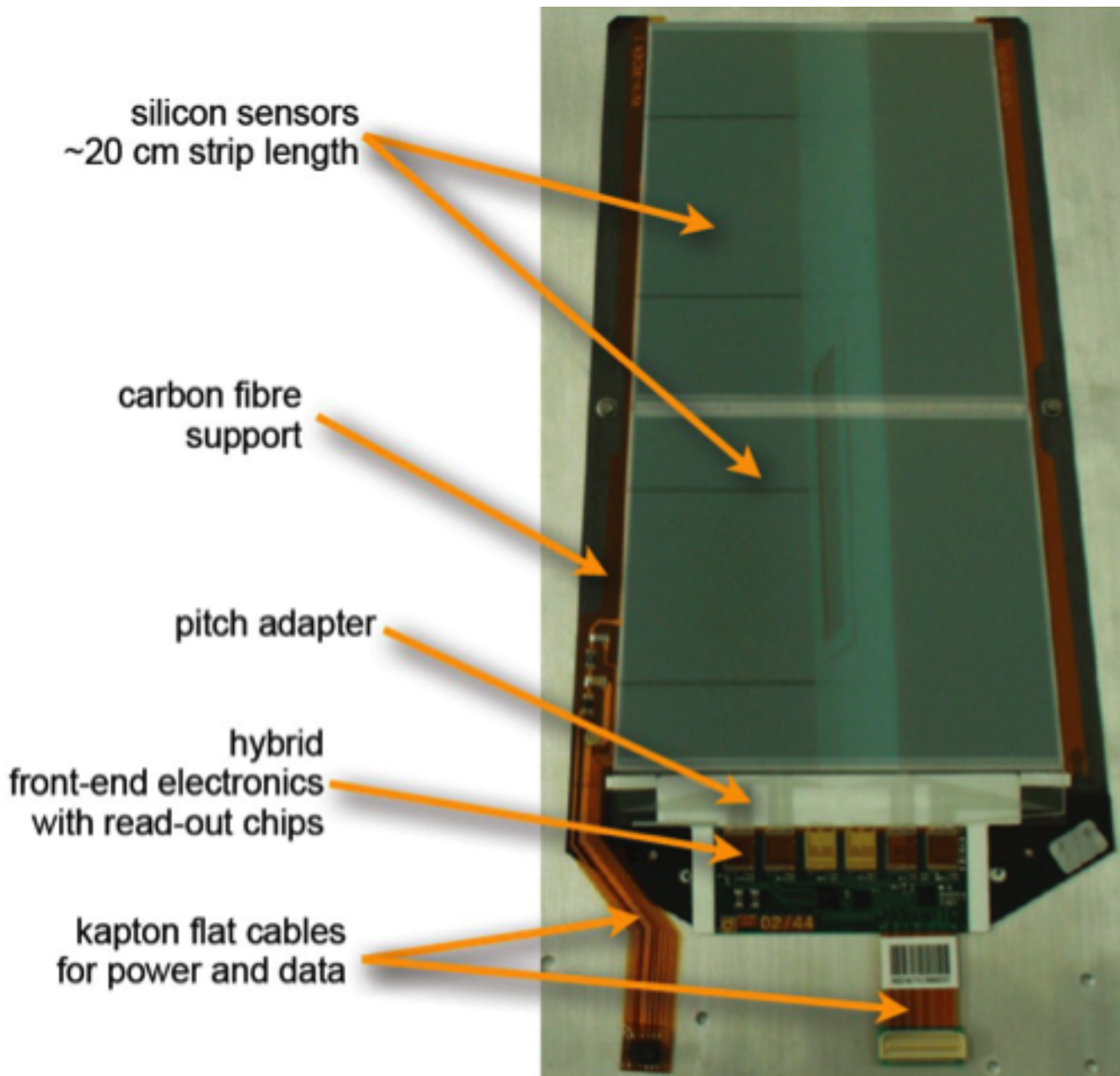
60

- AC coupling blocks leakage current from amplifier
- Deposit SiO_2 between p^+ and Al strip
 - Capacitance $\sim 32 \text{ pF/cm}$
 - Shorts through pinholes may be reduced with a second layer of Si_3N_4
- Use large poly silicon resistor ($R > 1 \text{ M}\Omega$) connecting the bias voltages to the strips



CMS module

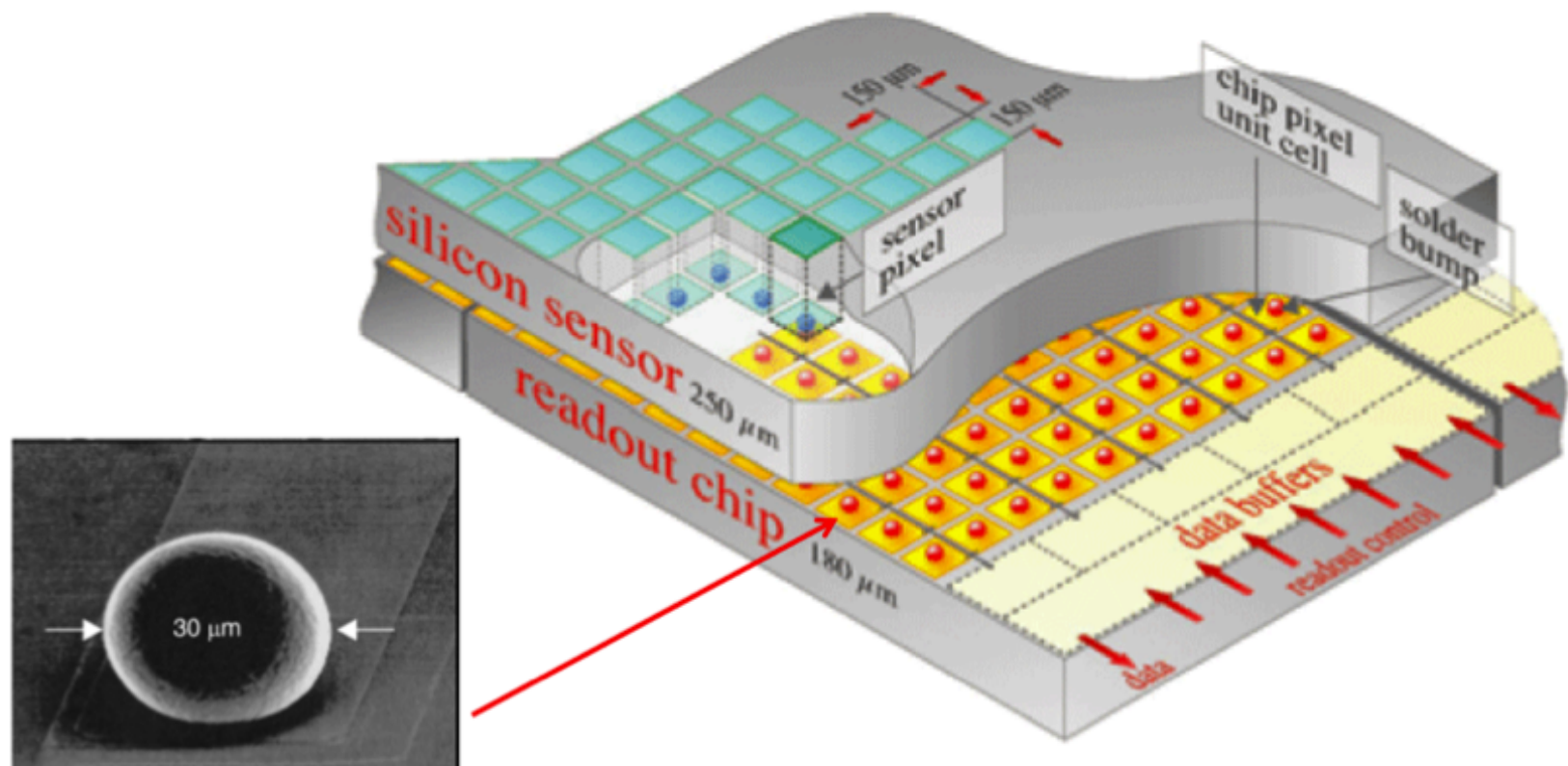
61



Pixel sensors

62

- High track density better resolved with 2D position information
 - back-to-back strips for 2D position information → yields “ghost” hits
- Hybrid pixel detectors with sensors and bump-bonded readout chips



one sensor, 16 front-end chips and 1 master controller chip

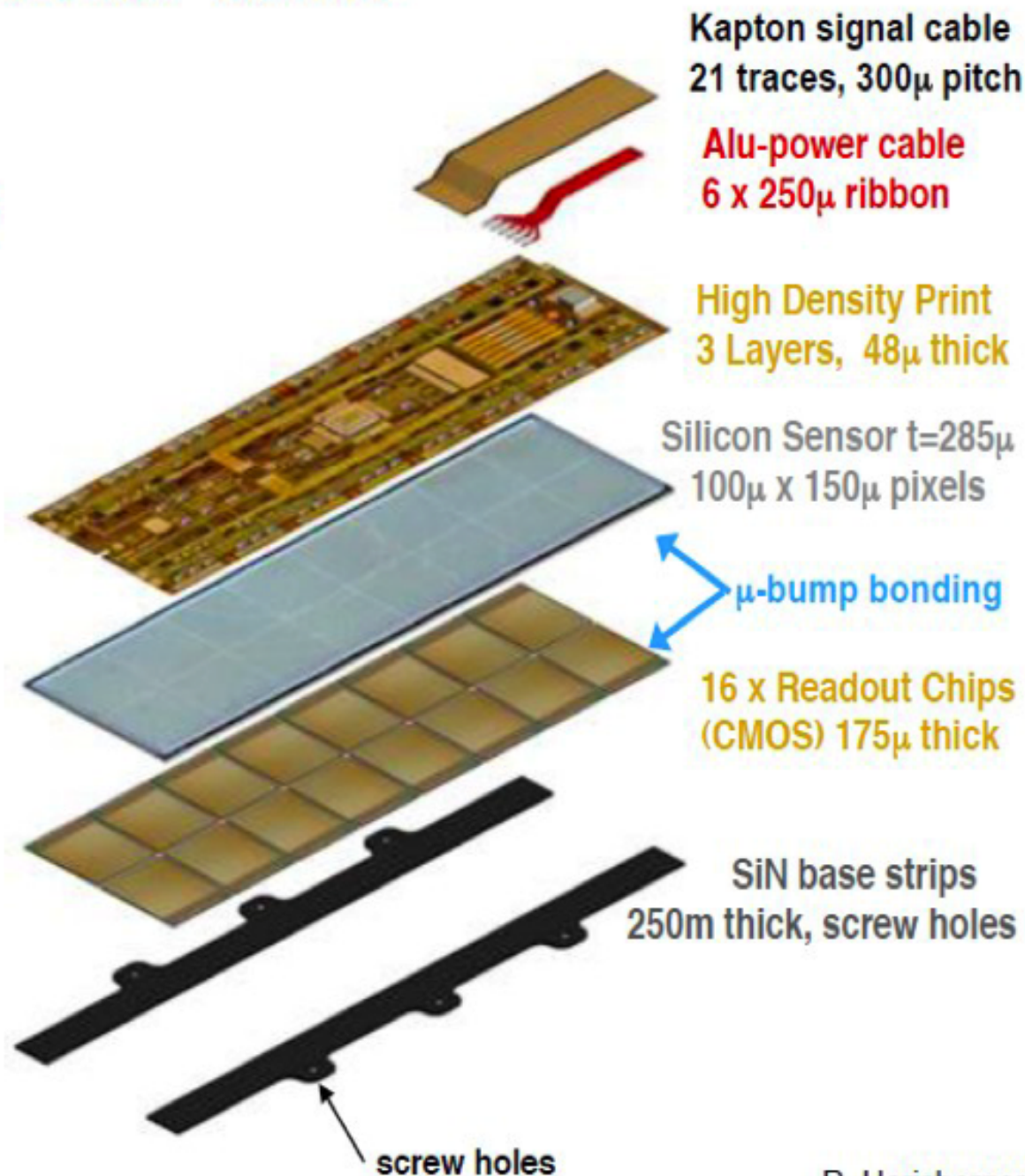
Hybrid Pixel Module for CMS

Sensor:

- Pixel Size: 150mm x 100mm
 - Resolution $\sigma_{r-\phi} \sim 15\mu\text{m}$
 - Resolution $\sigma_z \sim 20\mu\text{m}$
- n+-pixel on n-silicon design
 - Moderated p-spray \rightarrow HV robustness

Readout Chip:

- Thinned to 175 μm
- 250nm CMOS IBM Process
- 8" Wafer



Performance: S/N

64

- **Signal** depends on the thickness of the depletion zone and on dE/dx of the particle

- **Noise** suffers contributions from:

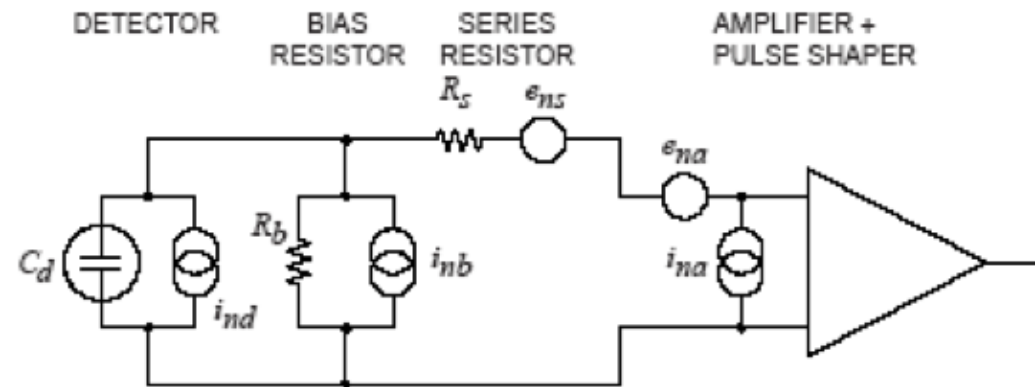
$$ENC = \sqrt{ENC_C^2 + ENC_I^2 + ENC_{R_{\parallel}}^2 + ENC_{R_{series}}^2}$$

capacitance

leakage
current

parallel
resistor

series
resistor



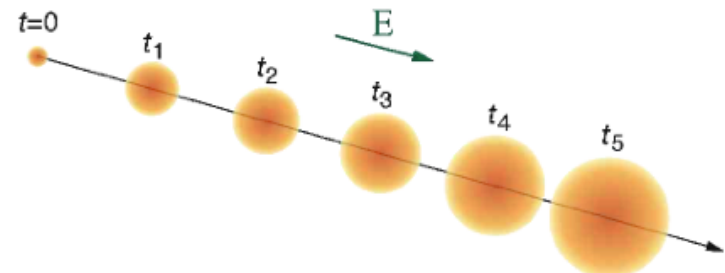
$$ENC_{peak} = (36.6 \pm 1.9) e^- / \text{cm} \cdot L + (405 \pm 27) e^-$$

$$ENC_{dec} = (49.9 \pm 3.2) e^- / \text{cm} \cdot L + (590 \pm 47) e^-$$

CMS strips

- **Optimizing S/N**

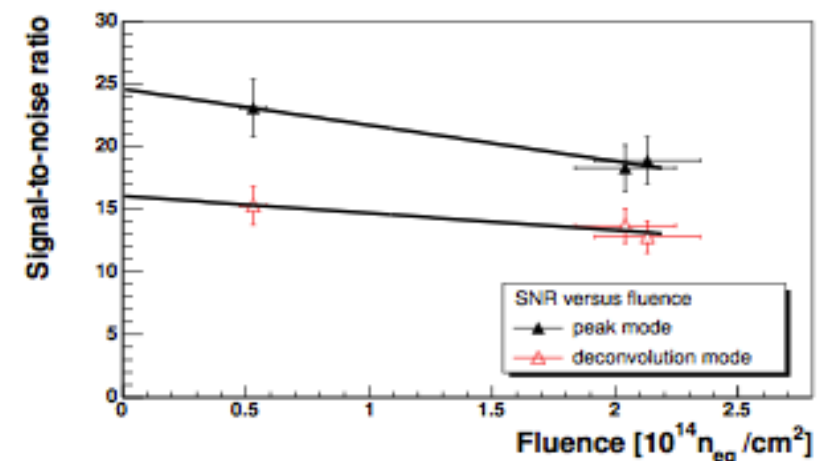
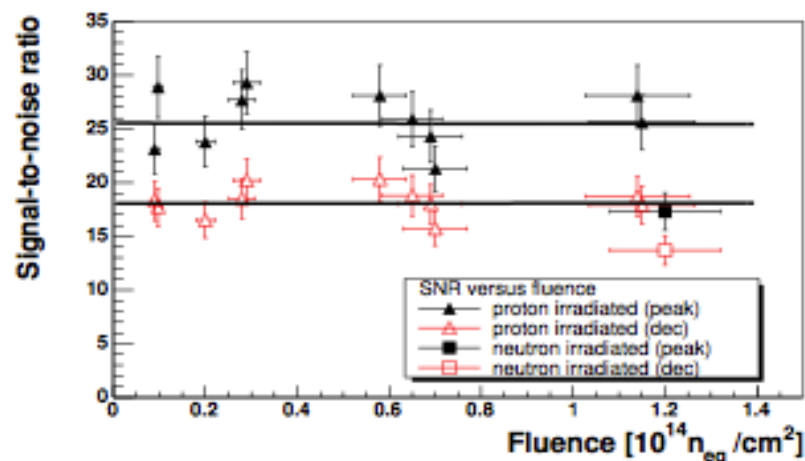
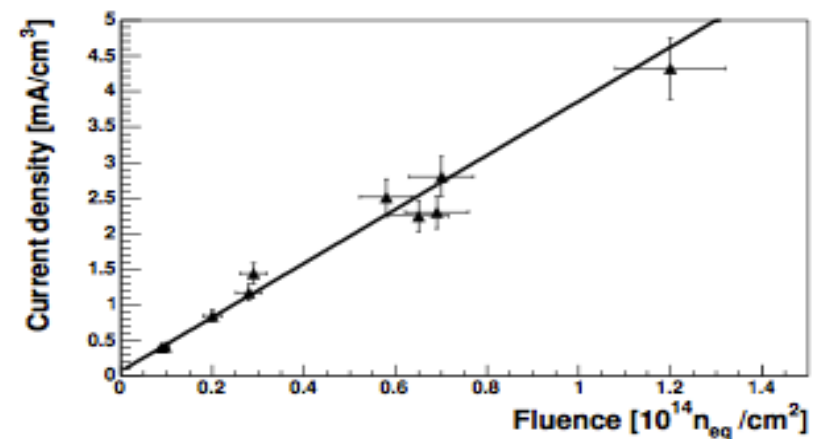
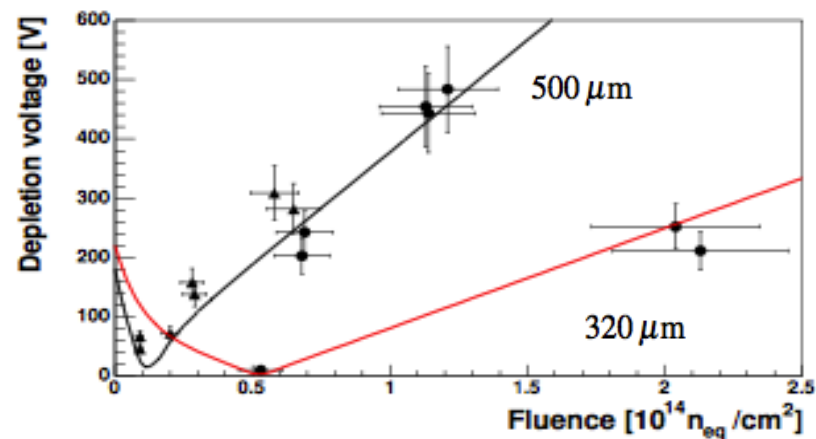
- $N_{ADC} > \text{thr}$, given high granularity most channels are empty
- decrease noise terms (see above)
- minimize diffusion of charge cloud after thermal mot
- (typically $\sim 8\mu\text{m}$ for $300\mu\text{m}$ drift)
- radiation damage severely affects S/N (next slide)

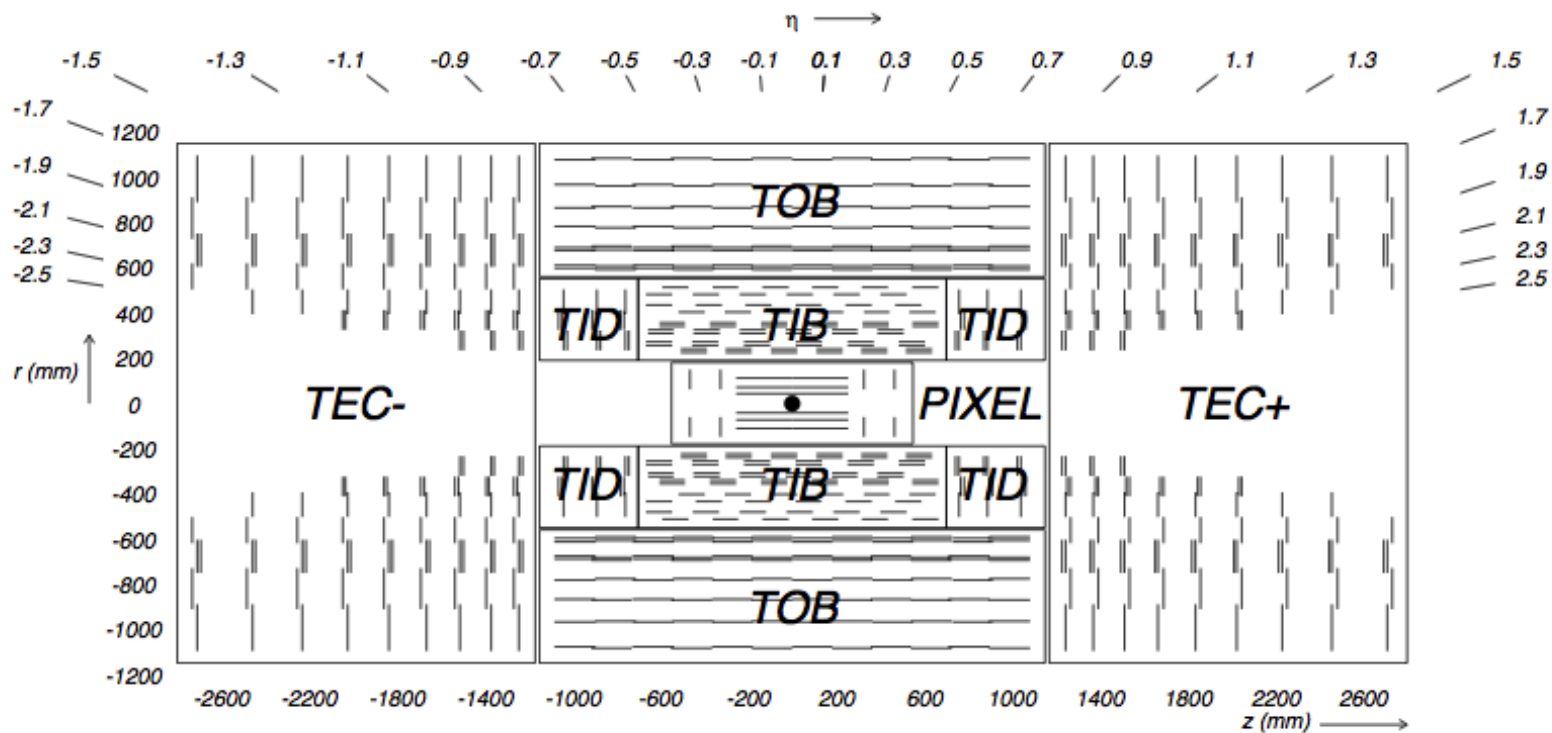


Influence of radiation

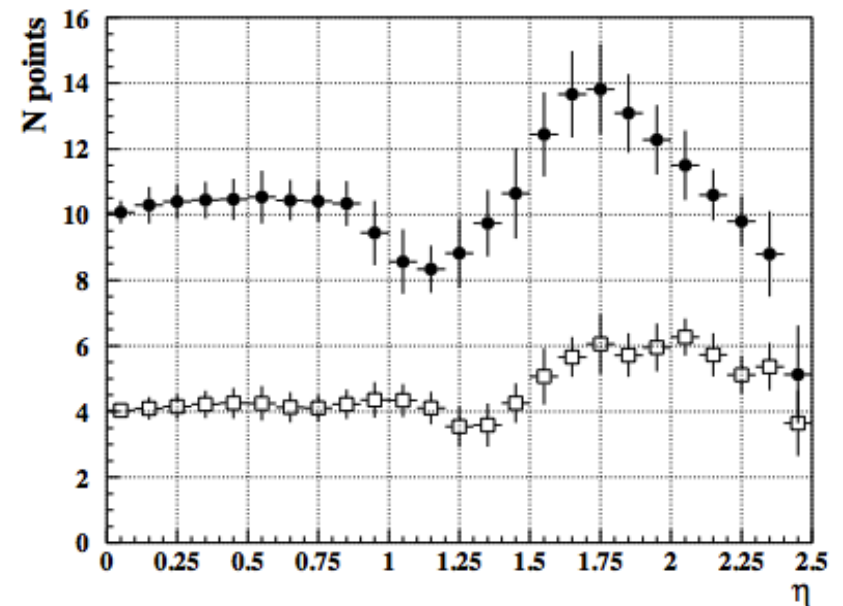
65

- Si is not fully robust against radiation
 - induced defects result in noise, inefficiency, leakage,...
 - need to increase depletion voltage at higher fluences
 - expected hit finding efficiency after 10 years of LHC operation: 95%





- **Pixel detector:** $\sim 1\text{m}^2$ area
 - 1.4k modules \Rightarrow 66M pixels
- **Strips:** $\sim 200\text{m}^2$ area
 - 24k single sensors, 15k modules
 - 9.6M strips = electronics channels
 - 75k readout chips

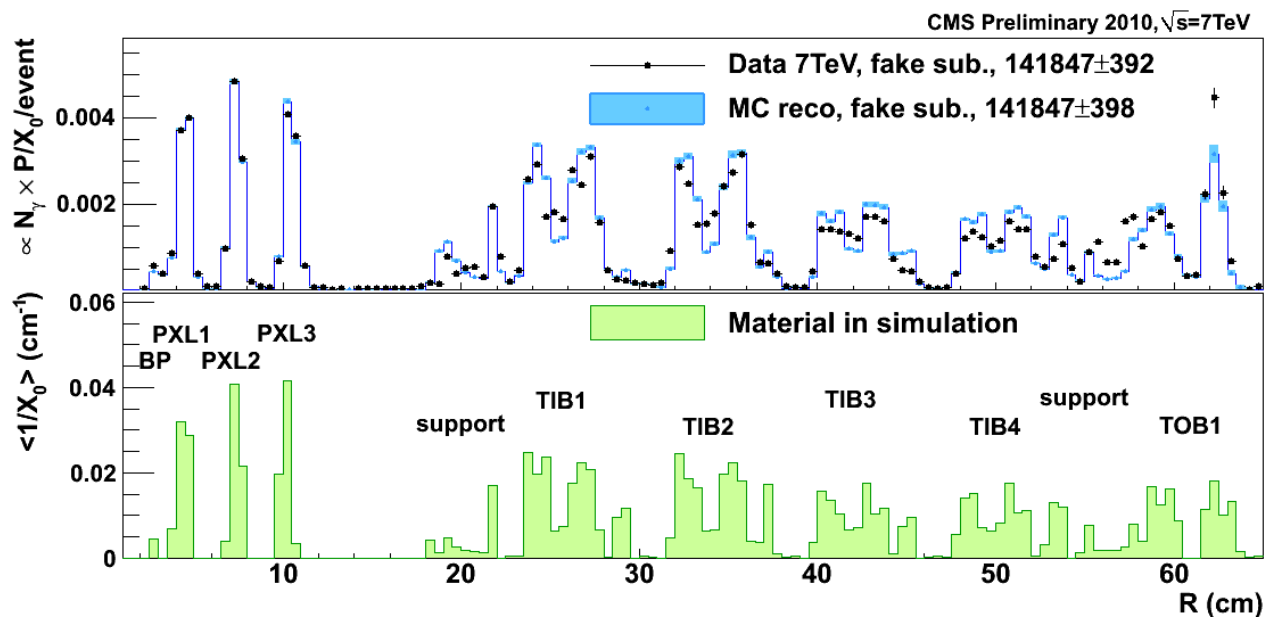
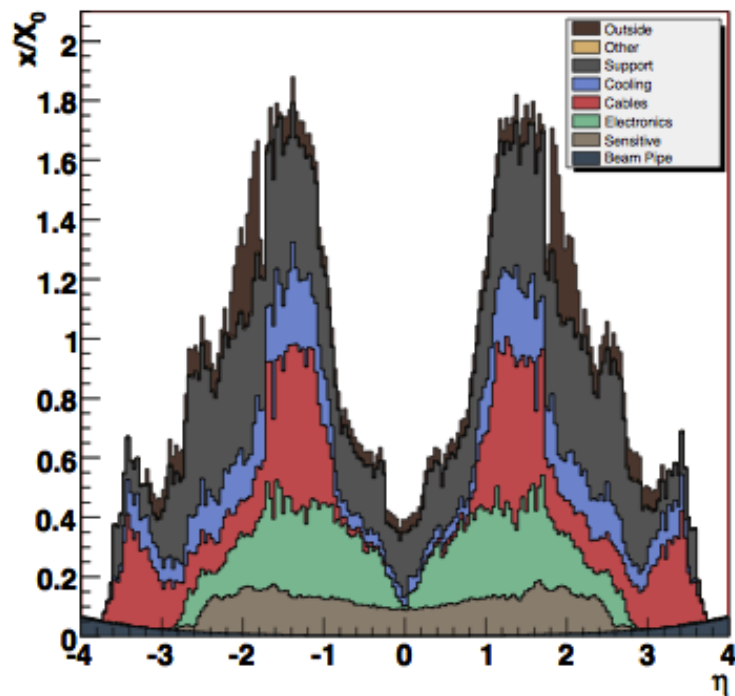


CMS tracker budget

67

- In some regions can attain $1.8X_0$
 - often photons will convert, electrons will radiate :(
 - use for alignment and material budget estimation :)
- Precise knowledge is crucial, e.g. for Higgs with γ and electrons in the final state

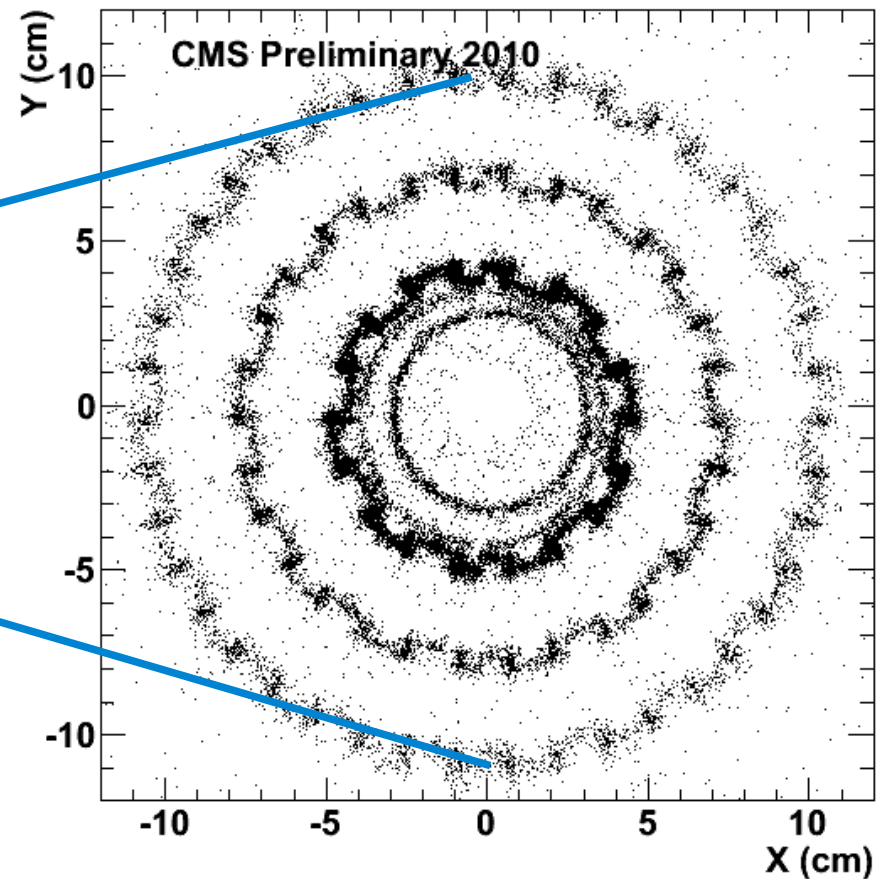
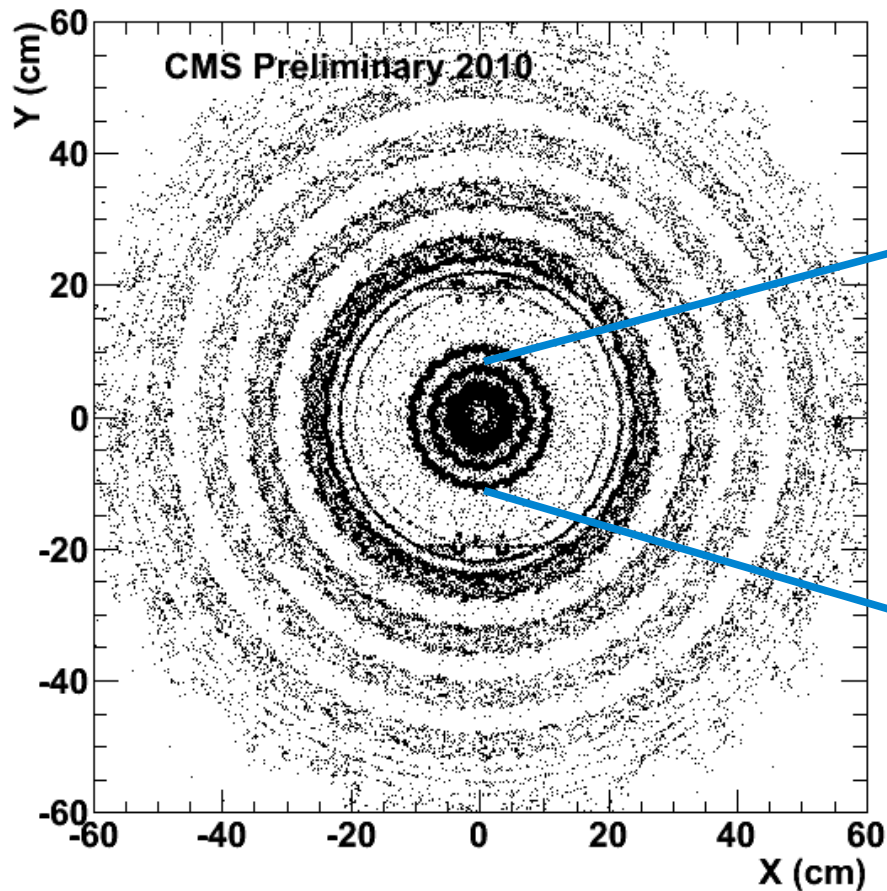
Tracker Material Budget



X-ray of the CMS tracker

68

- Use photon conversions ($\gamma \rightarrow e^+e^-$)
 - probability of interaction depends on the transversed material ($1 - e^{-x/X_0}$)
 - 54% of the $H \rightarrow \gamma\gamma$ events have are expected to have at least one conversion



Electrons

69

```
-- iSpy -- http://iguana.cern.ch/ispy
Data recorded 1970-Jan-01 00:13:55 GMT
Run number    1
Event number   667
Lumi section   666868
Orbit number    1
Beam crossing   1
```

L1 Triggers:

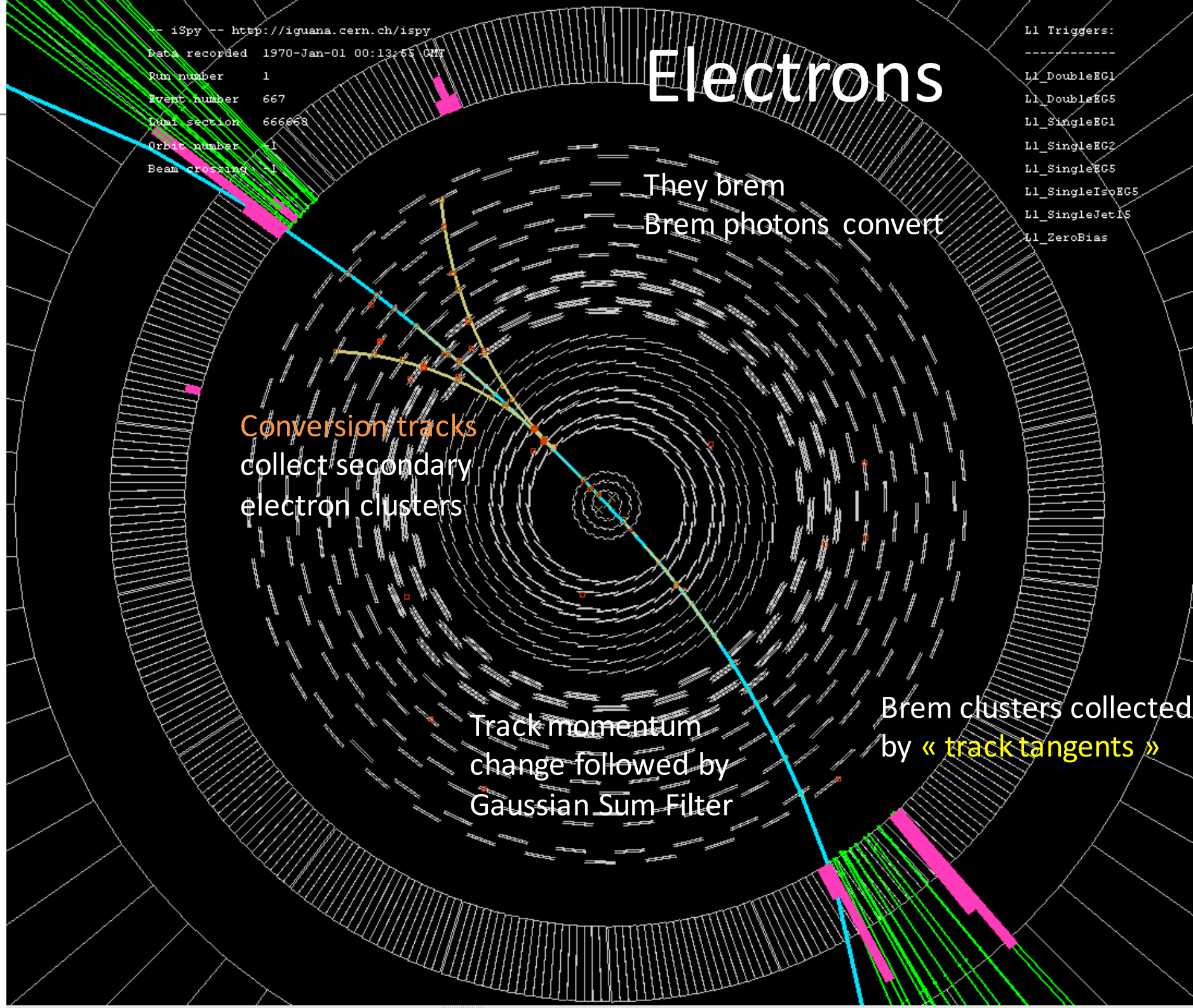
L1_DoubleEG1
L1_DoubleEG5
L1_SingleEG1
L1_SingleEG2
L1_SingleEG5
L1_SingleIsoEG5
L1_SingleJet15
L1_ZeroBias

They brems
Brems photons convert

Conversion tracks
collect secondary
electron clusters

Track momentum
change followed by
Gaussian Sum Filter

Brems clusters collected
by « track tangents »



...to be continued

- Hunting for new physics: wide variety of final states vs underlying event/pileup
 - general purpose detectors attempt to cover all possible signatures while rejecting background
 - choice of technology: trade-off between particle identification, resolution and budget
- Particle flow as a paradigm
 - use the best out of the detectors for optimal performance
 - yields a close 1:1 physics reconstruction of the hard process final state
- Magnetic field and tracking play a crucial role and set the base
 - B field is at the heart of the experiment
 - tracking detectors are at the base of the reconstruction

tomorrow: calorimetry, performance, and trigger

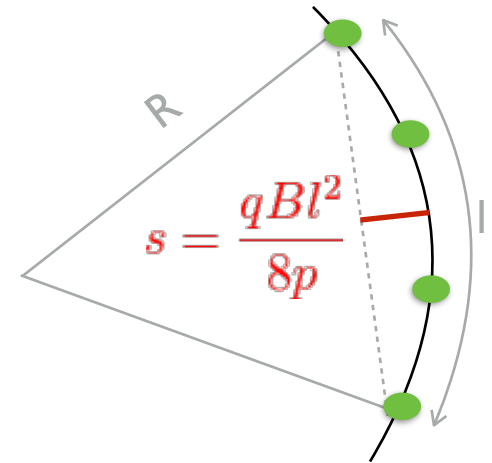
Backup

The magnet is the heart of an experiment I

73

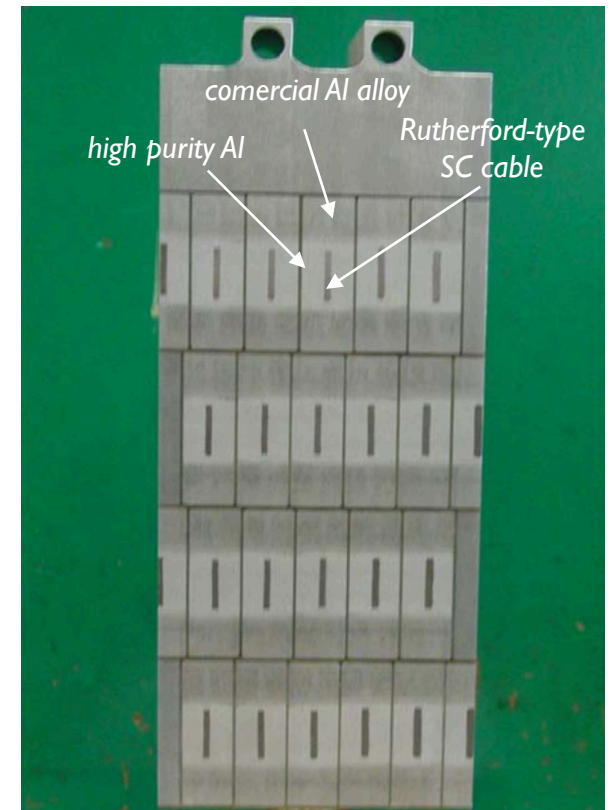
- Goal: measure 1 TeV muons with $\delta p_T/p_T = 10\%$ without charge error

- $\frac{\sigma_{p_T}}{p_T} = \frac{8p_T}{0.3Bl^2} \sigma_s$ this implies $\sim 50\mu\text{m}$ uncertainty in measuring s
- either use “continuous tracking” or “extreme field”



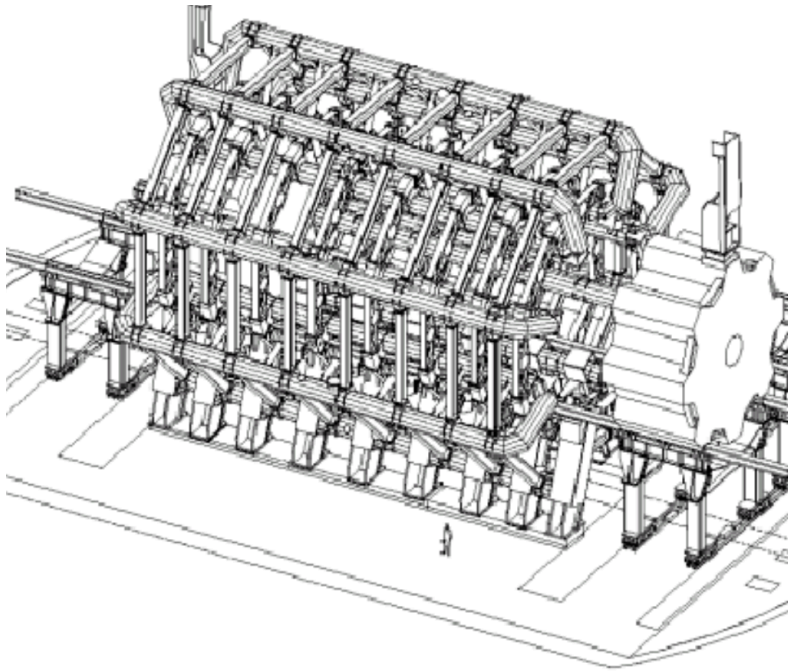
- From Ampere's theorem: $\oint \vec{B} \cdot d\vec{s} = \mu_0 I \Rightarrow B = \mu_0 n I$
 $\Rightarrow n = 2168$ (120) turns per coil in CMS (ATLAS)

- special design needed for superconducting cable in CMS
- size limited by magnetic pressure ($P \approx 6.4 \text{ MPa}$)

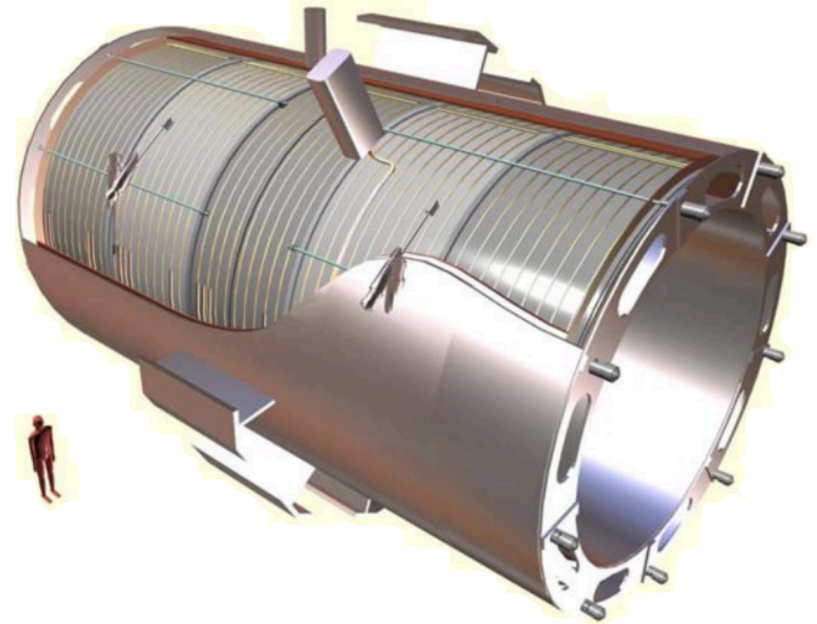


The magnet is the heart of an experiment II

74



ATLAS



CMS

B

0.6T (8 coils, 2x2x30 turns)

4T (1 coil, 2168 turns/m)

Challenges

- spatial/alignment precision over large surface
- 1.5GJ energy stored

- design and winding of the cable
- 2.7GJ energy stored

Drawbacks

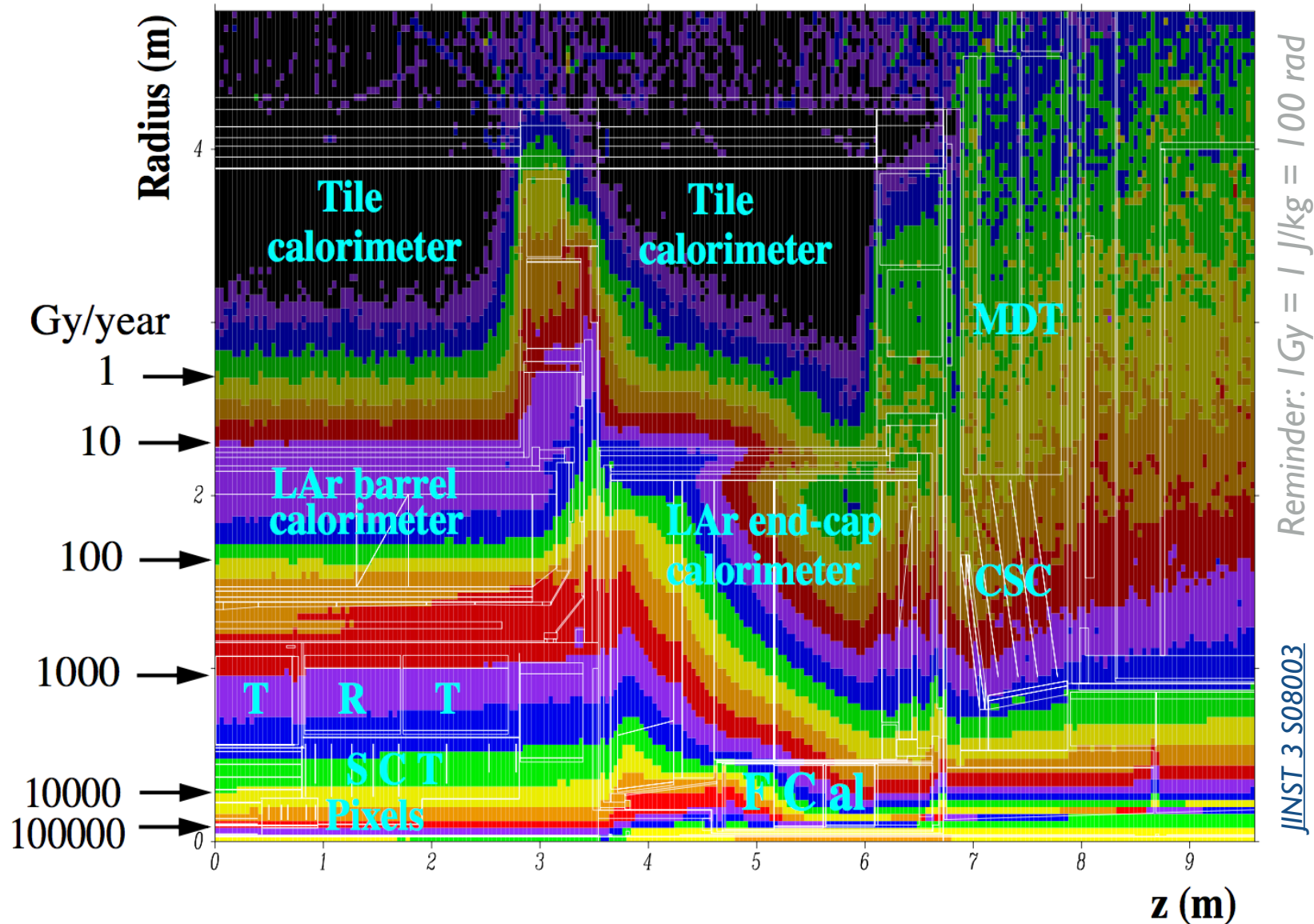
- limited pointing capabilities
- non-trivial B
- additional solenoid (2T) needed for tracking
- space needed

- limits space available for calorimetry
- no photomultipliers for calorimeters
- multiple scattering in iron core
- poor bending at large angles

Radiation levels: a challenge for detectors and electronics

75

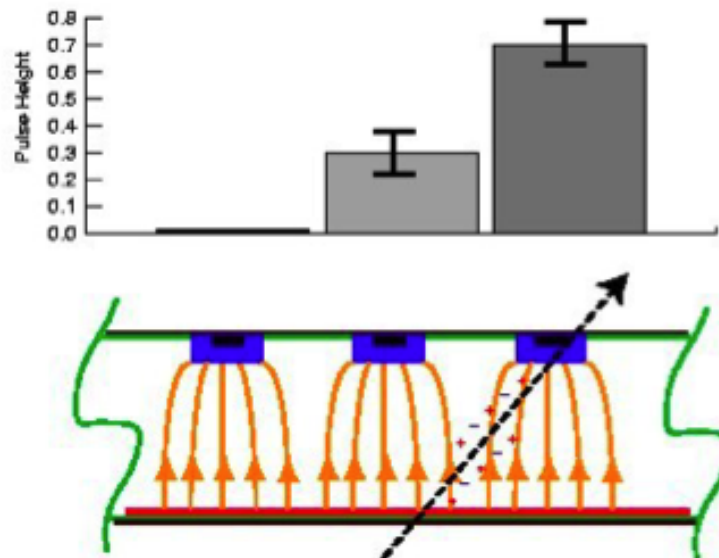
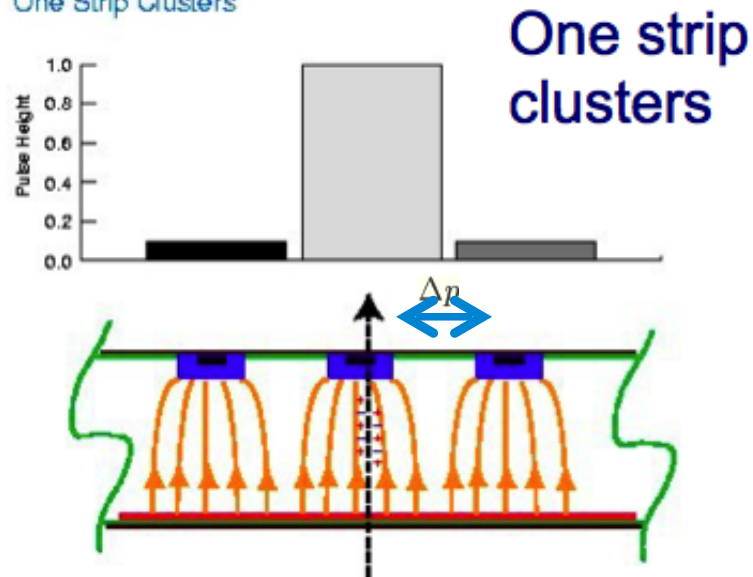
- Activation of materials, impurities, loss of transparency/response, spurious hits ...
 - additional shielding/moderators needed to limit radiation impact in the detectors



Position resolution

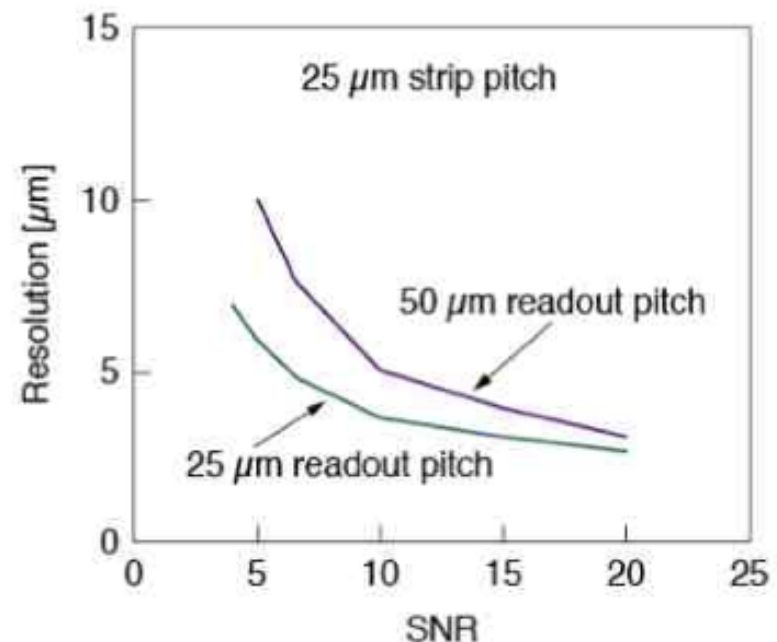
76

One Strip Clusters



- Affected by different factors
 - transverse drift of electrons to track
 - strip pitch to diffusion width relationship
 - statistical fluctuations on energy deposition

$$\sigma_x \propto \frac{\Delta p}{S/N}$$



A. Peisert, *Silicon Microstrip Detectors*,
DELPHI 92-143 MVX 2, CERN, 1992